Budapest University of Technology and Economics
Faculty of Civil Engineering
Department of Structural Engineering

Numerical analysis of composite columns under axial and torsional loads

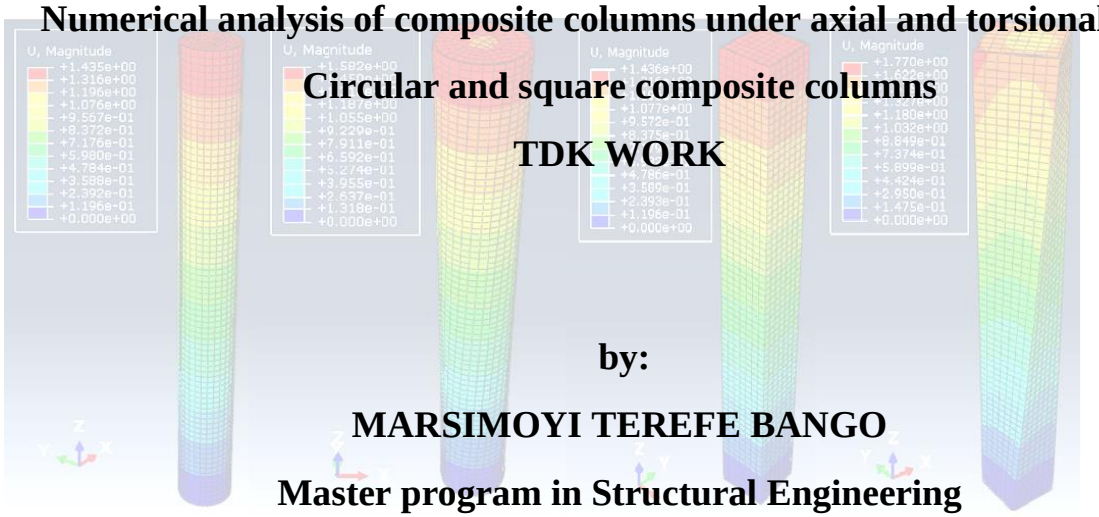

Circular and square composite columns

TDK WORK

by:

MARSIMOYI TEREFE BANGO

Master program in Structural Engineering

Supervisor:

Dr. KOVÁCS NAUZIKA -Associate Professor

Department of Structural Engineering

October-2019

Budapest

TABLE OF CONTENTS

ABSTRACT

In the recent world, different structural systems are used in combination to meet performance and functional requirements in structures. In this case, composite structures used to fulfill construction structure purposes. Most of the composite structures in construction are steel and concrete. So, when they used in the composite, give more advantageous and preferable rather than using them separately. Mainly composite structures use for High rise buildings, long-span bridge or slab, warehouse buildings, etc. Composite structures provide additional load-bearing strength, lateral stiffness, easy construction formwork and easy to place. Steel has high ductility and high strength-to-weight and stiffness-to-weight ratios. When steel and concrete properly combined, can produce synergetic high load carrying capacity, admirable structural integrity, and excellent structural and dimensional stability and can fit structures purpose as needed.

The main aim of composite column construction is to achieve a higher level of performance than would have been the case that two materials functioned separately. The flexural capacity and ductility of composite columns decreased when a constant torsion was simultaneously applied. The torsional moment may reduce the shear capacity of the columns. Un-Symmetrical building structures are almost unavoidable in modern construction due to various types of functional and architectural requirements. Torsion in buildings during earthquake shaking may be caused by the non-symmetrical distribution of mass and stiffness. Therefore, in an un-symmetrical building, it is necessary to design the beam and column for a torsional moment. This paper presents a numerical analysis of different sections of circular and square composite columns under axial and torsional loads to determine the suitable section of composite columns under different purposes of construction.

In order to achieve the goal of the study, a parametric investigation procedure was undertaken. Twelve different section types of composite columns were investigated. A circular composite column(CCC) with concrete-filled, CCC with reinforcement bars, CCC with embedded steel profile, Square composite column (SCC) with concrete-filled, SCC with reinforcement bars and SCC with steel profile embedded were investigated in detail under axial load only and combined effect of axial and torsional loads separately. The material quality used for the composite column of the same grade was used. The composite column is made to be subjected to 40%, 50% and 60% of its ultimate axial capacity (P) with a constant Torsion of about 60 KN-m. In this work, specimens of composite columns are taken for analysis with making bottom end restrained against all degrees of freedom and The nodes at the top are kept free in rotational degrees of freedom in all directions and translation in the direction where the concentrated load and torsion are applied. while the other two directions are restrained.

The analysis of composite column is performed by the finite element method using the software package Abaqus in Finite Element modeling. A three-dimensional model is defined using solid elements for both materials and paying special attention to the steel to concrete contact and constraint considered as an embedded section for reinforcement and steel profile in concrete fill as host region. Concentrated load and Torsion will be applied on the top end of the composite column at the referred point constraint at top-end by coupling. The FEM output was then examined to determine the effect of different levels of axial loads on the behavior of columns under axial and torsion loading and validated with reference experimental results. Assessing and identifying the high stress and strain zones as the axial load is applied with and without torsion and evaluating the effects of the level of axial load on deflection/compression, rotation and twisting of the column by keeping torsion constant while axial load applied is increasing investigated.

Keywords: Axial load, Circular and Square, Composite column, Finite element method, torsion.

LIST OF TABLES

LIST OF FIGURES

LIST OF NOTATIONS

A- Cross-sectional area

Aa- Cross-sectional area of the structural steel section

Ac- Cross-sectional area of concrete

AISC- American Institute of Steel Construction

CCC-circular composite column

CC-composite column

CCFST-Circular Concrete Filled Steel Tube

CCST-Circular column steel tube

CFCC- concrete-filled composite column

CFST- Concrete Filled Steel Tubes

CFT- concrete-filled tubes

FEA- Finite Element Analysis

FEM- Finite Element Method

LRFD- Load and Resistance Factor Design

N_o- Applied axial load

N_u- Axial compressive strength

P-load bearing capacity of the section

RI-rigidity index

S- Von Mises stress

SCC-square composite column

SI-strength index

SRC-steel-reinforced concrete sections

T-torsion

U- magnitude of displacement under axial or torsional loads

α_1- Longitudinal reinforcement ratio

α_{cfst}- the ratio of the cross-sectional area of the all inner of the composite column to the whole composite cross-section.

1 INTRODUCTION

1.1 Background

In the recent world, different structural systems are used in combination to meet performance and functional requirements in structures. In this case, composite structures used to fulfill construction structure purposes. Most of the composite structures in construction are steel and concrete. So, when they used in the composite, give more advantageous and preferable rather than using them separately. Mainly composite structures used for high rise buildings, long-span bridge or slab, warehouse buildings, etc. Composite structures provide additional load-bearing strength, lateral stiffness, easy construction formwork and easy to place. Steel has high ductility and high strength-to-weight and stiffness-to-weight ratios. When steel and concrete properly combined, can produce synergetic high load carrying capacity, admirable structural integrity, and excellent structural and dimensional stability and can fit structures purpose as needed.

In high rise buildings, complex multi-purpose storey building, structural steelwork is typically used together with concrete. Example; thin-walled steel tube infilled by concrete and steel beams with concrete floor slabs. The clear purpose of structures can be selected by considering different construction circumstances. In this case, composite structures are widely used to solve the problem that may arise if used only one element of the structure. It is a fact, however, that engineers are increasingly designing composite and mixed building systems of structural steel and reinforced concrete to produce more efficient structures when compared to designs using either material alone.

Most of the composite structures consist of structural steel frames with steel-concrete composite columns to satisfy the requirements of strength and serviceability under all probable conditions of loading. Composite frames, composite columns, steel beams and concrete slab together were an effective option for use as the primary lateral force resistance system of building structures; and in many cases offer significant advantages over other lateral force resistance systems [1].

Steel structural hollow sections are the most efficient of all the structural sections in resisting compression load and filling these sections with plain concrete significantly increases loadbearing capacity. CFST columns have several advantages as follows:

a) It combines tension properties of steel and compression properties of concrete and provides the hollow steel sections with greater strength and stiffness.
b) The confinement of concrete by steel enhances the failure strength of concrete.
c) Column size may be reduced more than necessary for pure steel or reinforced concrete columns and provide greater floor area for use.
d) The steel tube provides permanent formwork for concrete.
e) The steel tube column can be erected rapidly for several story heights, allowing to add floors before filling tubes with concrete.

f) Good seismic resistance because of good ductility and high energy absorbing properties.
g) In encased sections, the concrete delays failure by local buckling and acts as fireproofing while the steel provides substantial residual gravity load-carrying capacity after the concrete fails.

The use of composite structures has become widespread in recent decades and housing some of the highest buildings in the world. Also, there are extensive interests in using composite systems for seismic resistance design. The current design provisions for composite columns come primarily from the Manual of Steel Construction - Load and Resistance Factor Design (LRFD) [AISC 1999][2]. These provisions are based on rules developed in the 1960s and 1970s (SSRC TG20, 1979) [3] and utilize an approach in which the composite column is turned into an equivalent steel one. This approach has been shown to yield very low-reliability indices (Leon and Aho, 2000), and a complete reassessment of the design for composite columns have been made in the 2005 AISC Specification [4]. BS EN 1994-1-1 Euro code 4 presents the latest design recommendations for all types of composite columns [5].

In this paper, the main attention is paid to the numerical and behavior analysis of the infilled composite column considering different tubular steel shape under axial and torsion loads taking in to account the loading at different level of plastic resistance of section. Composite Column section of circular and square steel tube was investigated. Circular composite column with the outer diameter D, the inner diameter d and the height h, the circular concrete core with the diameter d and the height h, and the two thick steel plates make up the geometry of the circular composite column (CCC) and Square Composite column(SCC) with height h, width h, and depth d, is model described more in detail. The test parameters included the cross-sectional shape, the axial load level, the cross-sectional area of the section and the specimen type. The prediction accuracy of the cross-section is verified by comparing it with the test results with Abaqus software outputs in this paper.

1.2 Statement of the problem

The main aim of composite column construction is to achieve a higher level of performance than would have been the case that two materials functioned separately. The flexural capacity and ductility of composite columns decreased when a constant torsion was simultaneously applied [6]. Torsional behavior of asymmetric building is one of the most frequent causes of structural damage and failure during strong ground motions. The torsional moment may reduce the shear capacity of the columns. Un-Symmetrical building structures are almost unavoidable in modern construction due to various types of functional and architectural requirements. Torsion in buildings during earthquake shaking may be caused by the non-symmetrical distribution of mass and stiffness. Therefore, in an un-symmetrical building, it is necessary to design the beam and column for a torsional moment. In this study, the researcher investigates numerical analysis and behavior of different sections of composite columns under axial and torsional loads to determine suitable section of composite columns under different structural purposes.

1.3 Research questions

The research questions that this study goes to investigate are as follows:

1. What are the possible effects of composite column sections subjected to axial and torsional loads?
2. Which type of steel section and composite column are preferable under axial and torsional loads for different external and internal stresses of structures?
3. Which high stress and strain zones can be formed on the composite column section when it is subjected to axial and torsional loads for steel section, concrete section, and composite?
4. What is an optimal solution to resist torsional moments and axial forces applied in the infilled composite column?
5. Which infilled composite column shape is preferable under different structural purpose?

1.4 Objective

1.4.1 General Objective

The main objective of the study is to investigate the behavior and numerical analysis response of different composite column sections under axial and torsional loads.

1.4.2 Specific Objectives

1. To evaluate and analyze the effect of combined action of axial and torsional loads on the infilled composite column.
2. To evaluates the infilled composite column section under compression of axial loads.
3. To identify possible steel section type and column section suitable for composite subjected to axial and torsional loads from different kinds of literature and experimental results.
4. To identify the high stress and strain zones of composite column subjected to axial and torsional loads by using Abaqus software.

1.5 Significance of the study

1. The study evaluates the torsional strength of different infilled composite column section.
2. The study evaluates the compressive strength of different infilled composite column sections under axial loads.
3. This study compares the torsional strength of reinforced concrete column section to that of composite column.
4. The study provides/determines appropriate sections of the composite column to be used in under different construction circumstances i.e. seismic areas, based on structural purpose.

1.6 Scope

The scope of this project covers layout, modeling, analysis, and design of concrete infilled composite column which is subjected to axial and torsional loads. For modeling and analysis, ABAQUS software was used. This study also covers the comparison with experimental results with ABAQUS software output inaction of the composite column under applied axial and

torsional loads with the aim to verify the numerical model. The loads first applied separately in software and in the second case, the load applied both due to axial and torsion to check the action on cross-section and twisting effect under lateral loads.

2 REVIEW OF RELATED LITERATURES

2.1 Theoretical Review

Composite columns are structural members, which are subjected mainly to axial compressive forces and torsional loads. The general term ‘composite column’ refers to any compression member in which the steel element and concrete act together to contribute to structural strength and performance together. These composite columns have been used widely as they speed up construction by eliminating formwork, easy for placing and the need for tying of longitudinal reinforcement. Composite columns have recently undergone increased usage throughout the world, which has been influenced by the development of high strength concrete permitting these columns to be considerably economized. Columns designed to resist the majority of axial force by concrete alone can be further economized using thin-walled steel columns. Both steel and concrete materials are completely compatible and complementary to each other; they have almost the same thermal expansion, they have an ideal combination of strengths with the concrete efficient in compression and the steel in tension, concrete also gives corrosion protection and thermal insulation to the steel at elevated temperatures and additionally can restrain slender steel sections from local or lateral-torsional buckling. New developments, including the use of high strength concrete and the credit of the enhanced local buckling capacity of the steel, have allowed much more economical designs to evolve. Concrete filled steel tubes (CFST) are widely used in recent real-world construction.

CFSTs have shown better structural performance such as strength, stiffness, and ductility than that of bare steel or reinforced concrete members. Conventionally, CFSTs are designated by the shape of the steel tube which includes rectangular, square, circular, I-section and elliptical hollow sections. For CFST columns of circular section (CCFST) in particular, the steel tube provides significant confinement to the concrete core, which leads to an increase in both strength and ductility of the concrete, while the steel tube also acts as permanent formwork as well as reinforcement for the concrete. The concrete core, in turn, restricts inward local buckling of the steel tube. Comprehensive experimental and analytical researches on concrete-filled tubular steel columns have been ongoing throughout the world for many years. Most of these experiments, however, have been on moderate scale specimens (CCFST for example, less than 200 mm in diameter) using normal and high-strength concrete. The experimental study also showed (Han and Yao 2003) [7] that the concrete compaction would affect the interaction between the steel tube and the concrete core, and thus the behavior of the composite column. Codes and design specifications have been evaluated and developed, in an enormous dissimilarity in the analytical models for evaluating the strength of a CFST composite column and the effect of confinement.

Specifically, the ACI provisions (ACI Committee 318 2011) [8] assume that the capacity of a CFST column can be predicted by treating the column as an ordinary reinforced concrete column, while in AISC provisions (American Institute of Steel Construction 2010), the design philosophy is to create modified cross-sectional properties from the composite column and then design the composite column as an equivalent steel column using the modified properties in place of the steel properties. For calculating the axial capacity, codes such as ACI and Japanese

Standards (Architectural Institute of Japan 1997) do not take into consideration the concrete confinement, while some such as Eurocode 4 (European Committee for Standardization. 2004) take the strong contribution from the concrete confinement.

Most researches carried out to date on concrete-filled steel tubes are assumed that there is inherent perfect interaction between the concrete and the steel tube (Liang and Fragomeni 2010, Uwe et al. 2010, Xu et al. 2010, Bahrami et al. 2011). In construction practice, however, defects like concrete inanity or debonding of the concrete from steel tube have been found at the steel-concrete interface of the concrete-filled steel tubes. Debonding separation at the steel-concrete interface of a CFST composite member could be induced by plastic shrinkage, and long-term effect of concrete-like shrinkage and creep as well as improper concrete casting. These concrete defects would penalize the structural performance of the composite columns. Besides, some defects of inanity between the steel plate and the concrete are identified being inherent shortcomings of concrete casting owing to substantial plastic shrinkage in concrete.

The negative influences of the debonding on the axial loading capacity of the CFST columns were investigated experimentally by Jun-Qing Xue, Bruno Briseghella and Bao-Chun Chen [9]. The defects of inanity between the steel tube, steel plate, and the concrete were found to affect the structural behavior and performance of the concrete-filled steel tubes. The ultimate load capacity and the ductility of the CFSTs were also found significantly decreased with an increase of the debonding separation gap. In the CFST column construction practice, using low shrinkage concrete or even self-compact concrete is one way to improve the construction quality. But, the defects of inanity still occur between the steel and concrete in the concrete-filled steel tubes. As far as the defects are inspected, the essential retrofit and repair are required which are normally expensive and time-consuming.

A lot of experiments have been carried out to investigate the parameters that affect the axial capacity of composite columns. It was found that there are various parameters, including the shape of steel section, longitudinal steel reinforcement, material properties of the concrete, the confinement effect of the concrete, slenderness ratio of the column, and concrete and steel strength. (Ellobody & Young, 2011) [10].

Ellobody et al. (2010) [10] studied the responses of concrete-encased steel composite columns to eccentrically load acting along the major axis. Many variables that influence this response such as the concrete strength, the steel section yield stress, eccentricities, column dimensions, and structural steel sizes were investigated. A three-dimensional finite element analysis using ABAQUS has been developed and it has been validated against experimental results. Eccentric load–concrete strength curves, axial load-moment curves, and ultimate capacity were obtained. The results showed that the increase in steel section yield stress has a significant effect on the strength of the eccentrically load composite column with small eccentricity with concrete lower than 70 MPa compressive strength. A conclusion was drawn after compared the results with Eurocode 4 (Eurocode 4, 2004) that the eccentric load was predicted correctly but the moment values were overestimated.

Han LH (2002) [11], has done a research on the behavior of composite CFT columns under pure torsion. Han in this research examined the performance of square steel tubular columns

filled with concrete under pure torsion using the ABAQUS software. The finite element method (FEA) was used to assess the impact of important parameters that determine the ultimate tensional strength of composite sections. Han found that steel pipe plays an important role in the tensional resistance of composite columns which are square or circular, and the composite columns show good stability and plastic behavior under torsion.

M.A. Dabaon, M.H. El-Boghdadi, and M.F. Hassanein, (2009) [12] performed research on composite columns under earthquake loads. He found that CFT columns under seismic loads, show very high levels of ductility and energy dissipation. It was also observed that the test samples maintained the flexural capacity until the test to be concluded.

2.2 Types of Composite Columns

2.2.1 Overview of composite column cross-sections

There are several basic types of composite columns mostly used in buildings:

a. Steel sections encased in concrete (steel-reinforced concrete sections). Figure 2.1
b. Steel sections filled with concrete (concrete-filled tubes or CFT). Figure 2.2
c. Partially encased cross-section. Figure 2.3
d. Concrete filled section with reinforcement. Figure 2.4
e. Concrete filled section with a steel section. Figure 2.5

Basic composite columns pictures are listed below for all types for those discussed above.

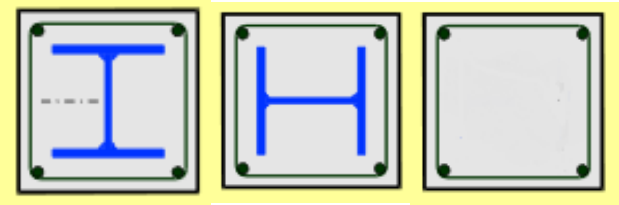

Figure 2.1: Steel-reinforced concrete sections or SRC. Source: G. Hansille: Eurocode 4 composite columns. [14].

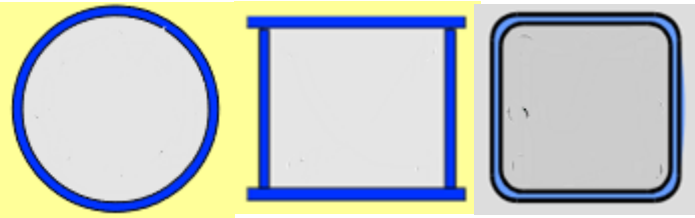

Figure 2.2: Steel sections filled with concrete only. Source: G. Hansville: Eurocode 4 composite columns. [14].

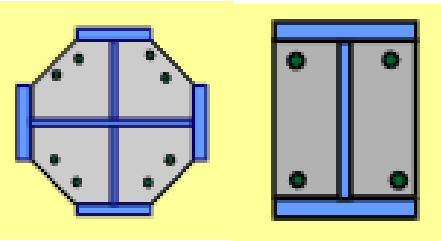

Figure 2.3: Partially encased cross-section Source: G. Hansville: Eurocode 4 composite columns. [14].

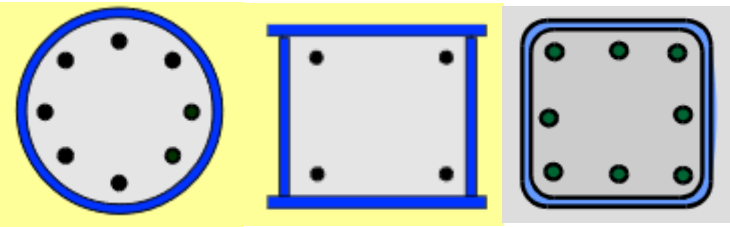

Figure 2.4: Concrete filled section with reinforcement. (Source: G. Hansville: Eurocode 4 composite columns. [14].)

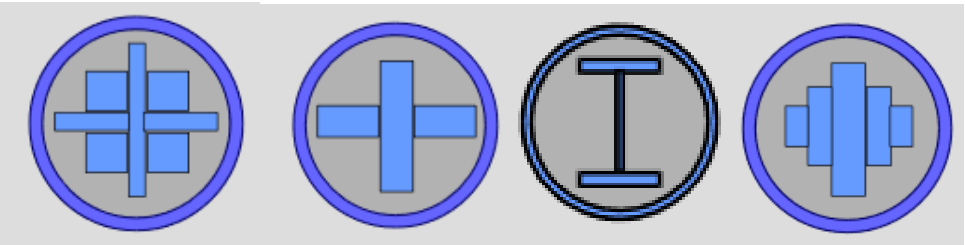

Figure 2.5: Concrete filled section with steel section (Source: G. Hansville: Eurocode 4 composite columns. [14].)

The steel or concrete cover can be different shapes in cross-section like Circular (CCFT) or square/rectangular (RCFT), encased I or H-section, octagon, etc. Some examples can be seen also below in Figure 2.6 and Figure27

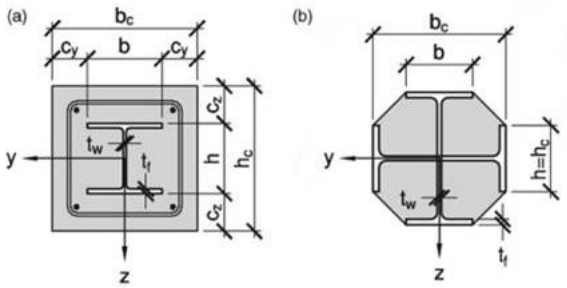

Figure 2.6: Typical cross-section of composite columns with fully or partially concrete-encased H or I-sections. (Source: Buick Davison, 2012. [13]).

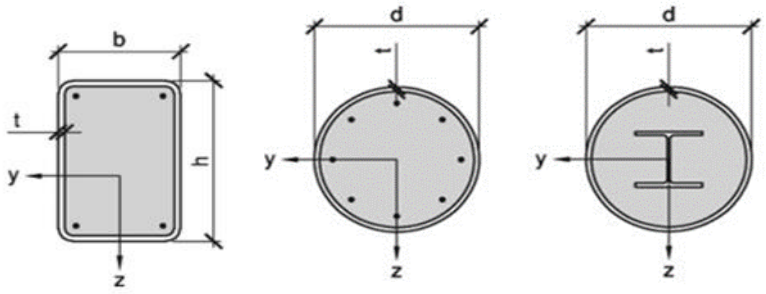

Figure 2.7: Typical cross-section of composite columns with the CFCC with reinforcement and steel profile embedded. (Source: Buick Davison, 2012. [13]).

This paper presents detail investigation on composite column Stainless steel sections filled with concrete only (concrete-filled tubes or CFT) and Stainless steel tube circular or square in which reinforcement or steel profile embedded in filled concrete, as can be seen in Figure28:b,e and Figure 2.8: a, c, d, and f respectively.

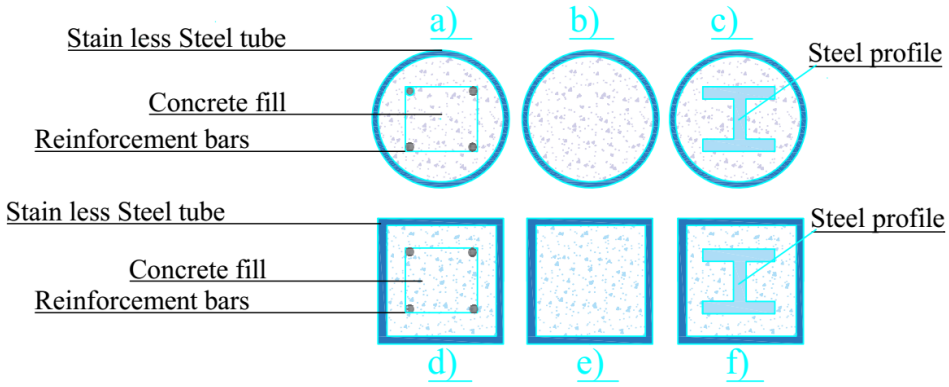

Figure 2.8: Circular and square concrete infilled composite column section.

2.2.2 Concrete encased composite column

One of the common and popular columns is the encased steel profile (Figure.2.1), where a steel H-section is encased in concrete. Sometimes, a structural pipe, tube, or built-up section is placed instead of the H or I-section. In addition to upholding a proportion of the load acting on the column, the concrete encasement enhances the behavior of the structural steel core by horizontal bar reinforcement, and so making it more effective against both local and overall buckling.

In encased sections, the concrete delays failure by local buckling and acts as fireproofing while the steel provides substantial residual gravity load-carrying capacity after the concrete fails. The cross-sections, which normally are square or rectangular, must have one or extra longitudinal bars placed in every single corner and these must be tied by lateral ties (stirrup) at regular vertical intervals in the manner of a reinforced concrete column. Ties are effective in rising column strength, confinement, and ductility. Furthermore, they stop the longitudinal bars from being displaced during construction and they resist the tendency of these same bars to buckle outward under load, which would cause spelling of the outer concrete cover even at low load

levels, remarkably in the case of eccentrically loaded columns. It will be noted that these ties will be open and U-shaped. Otherwise, they might not be installed, because the steel column shapes will have always been erected at an earlier time.

2.2.3 Concrete-filled composite column

In this type of composite column, a steel pipe, steel tubing, or built-up section is filled with concrete (Figure.2.2). The most common steel sections used are the hollow rectangular, square, circular tubes and I-section. Filled composite columns may be the most efficient application of materials for column cross-sections. It provides forms for the inexpensive concrete core and increases the strength and stiffness of the column In addition, because of its relatively high stiffness and tensile resistance, the steel shell provides transverse confinement to the concrete, making the filled composite column very ductile with remarkable toughness to survive local overloads. In concrete-filled tubes, the steel increases the strength of the concrete because of its confining effect, the concrete inhibits local buckling of the steel, and the concrete formwork can be omitted.

2.2.4 Composite column concrete-filled section with reinforcement

In this type of composite column tubular section provided and infilled with concrete in which reinforcement encased in concrete. In this case, reinforcement provided to increase ability to increase fire resistance and durability.

2.3 Composite column design via the Eurocode 4

2.3.1 General concept

For satisfaction of the main aim of this study; investigate the behavior of composite columns subjected to axial and torsional loads by comparing the capacity of different section of steel of composite column and reinforced concrete column section, it is first necessary to review the design procedures that will be used for composite and reinforced concrete columns to be able to used them in preliminary design.

In fact, Eurocode presents the most recent rules and comprehensive review among other design codes and specifications. As a result, Eurocode 2 and 4 were chosen for design of reinforced concrete and composite columns respectively. This section will be elucidated on the design procedure of composite columns according to Eurocode 4 (EN 1994) to resist axial loads and torsion moments. Whereas the design procedures of reinforced concrete columns, which will be used for comparison purposes.

To begin with, there are two design methods mentioned in Eurocode 4 for composite columns design; the general method (without application rules) which appropriate for non-symmetrical or nonuniform columns and the simplified method for members of doubly symmetrical and uniform over the member length. In this research, the simplified is applied to evaluate the resistance of the composite columns.

For the design of the composite column, Eurocode has mentioned some limitations which shall satisfy; slenderness parameter of the column should be less than 2%, the longitudinal reinforcement which can be used should be no more than 6% and not less than 0.3% of the concrete area, 0.2 and 0.5 are given as limits for the depth to width ratio of the composite cross-section used in this paper for purpose of parametrization. However, there are several other rules for column cross-section geometry as well.

2.3.2 Composite column section design for concentric compression

The plastic resistance to compression *($N_{pl,Rd}$)* of a composite cross-section should be calculated by adding the plastic resistances of its components; the structural steel, the concrete, and the reinforcement should be added. The plastic resistance equation for encased-composite column is:

$$N_{plRd}=A_a f_{yd} + 0.85A_c f_{cd} + A_s f_{sd} \quad (2.1)$$

Where:

A_a - the cross-sectional area of the structural steel,

A_c - the cross-sectional area of the concrete,

A_s - the cross-sectional area of the reinforcement,

f_{cd} - Design value of the cylinder compressive strength of concrete,

f_{sd}- Design value of the yield strength of reinforcing steel,

f_{yd} - Design value of the cylinder compressive strength of concrete.

For the filled-composite column, the coefficient 0.85 may be replaced by 1.0. The plastic resistance of circular cross-section equation is:

$$N_{pl,Rd} = \eta_{aA_a} f_{yd} + A_{cf_{cd}} [1 + \eta_c \frac{tf_y}{df_{ck}}] + A_s f_{sd} \quad (2.2)$$

Where:

f_y - nominal value of the yield strength of structural steel,

f_{ck} - characteristic compressive cylinder strength of concrete at 28 days,

d - outside diameter of the steel tube,

t - wall thickness of the steel tube.

When the eccentricity of loading, e, equal to 0, the values of $\eta a = \eta ao$ and $\eta c = \eta co$ are given by the following expressions.

$$\eta_{ao} = 0.25(3 + 2\lambda) \quad (2.3)$$

$$\eta_{co} = 4.9 - 18.5\lambda + 17\lambda^2 \quad (2.4)$$

Where: $\eta_{ao} \leq 1$ and $\eta_{co} \geq 0$

$\eta a0$, $\eta c0$ -are factors related to the confinement of concrete and λ-general slenderness parameter.

When eccentricity to outside diameter ratio, e/d, falls between 0 and 0.1, the values ηa and ηc should be determined from (Equation 2.5) and (Equation 2.6), where η_{ao} and η_{co} are given by (Equation 2.3) and (Equation 2.4):

$$\eta_a = \eta_{a0} + (1 - \eta_{a0})(10e/d) \quad (2.5)$$

$$\eta_c = \eta_{co} \ (1 - 10\frac{e}{d}) \quad (2.6)$$

When, $e/d > 0.1$, $\eta_a = 1{,}0$ and $\eta c = 0$

The eccentricity of loading, e, is defined as:

$$e = \frac{M_{ED}}{N_{ED}} \quad (2.7)$$

Where:

M_{Ed} - Design bending moment

N_{Ed} - Design value of the compressive normal force.

The steel contribution ratio δ is defined as:

$$\delta = \frac{Aafyd}{Npl,rd} \quad (2.8)$$

Where:

Npl, Rd -is the plastic resistance to compression

The relative slenderness, λ, is defined by: □

$$\lambda = \sqrt{(Npl}, Rk/Ncr) \quad (2.9)$$

Where:

$N_{pl,Rk}$ - the characteristic value of the plastic resistance to compression given by Equation-2.1

Ncr - the elastic critical normal force for the relevant buckling mode, calculated with the effective flexural stiffness *(EI)eff*

$$N_{cr} = \frac{(EI)_{eff}\pi^2}{(KL)^2} \quad (2.10)$$

Where:

L - buckling length of the column (effective length)

(*EI)eff* - Effective flexural stiffness given by (Equation 2.11)

$$(EI)_{eff} = E_a I_a + E_s I_s + K_e E_{cm} I_c \quad (2.11)$$

Where:

K_e-correction factor that should be taken as 0.6
I_a -the second moment of area of the structural steel section
I_c -the second moment of area of the un-cracked concrete section
I_s -the second moment of area of the reinforcing steel
E_a -Modulus of elasticity of structural steel
E_{cm} -The secant modulus of concrete, (Equation 2.12)
E_s-Design value of modulus of elasticity of reinforcing steel

$$f_{cm}=f_{ck}+8 \quad (2.12)$$

$$E_{cm}=22[f_{cm}/10]^{0.3} \quad (2.13)$$

For simplification for members in axial compression, the design value of the normal force N_{ed} ought to satisfy:

$$\frac{N_{ED}}{\chi N_{Pl,Rd}} \leq 1.0$$

Where:

- ✓ $N_{pl,Rd}$ -The plastic resistance of the composite section but with f_{yd} determined using the partial factor $\gamma M1$ which is equal 1 for buildings.
- ✓ χ -The reduction factor for column slenderness.

$$\phi = 0.5[1+\alpha(\lambda-0.2)+\lambda^2] \quad (2.14)$$

$$\chi = \frac{1}{\phi+\sqrt{(\phi^2-\lambda^2)}} \quad (2.15)$$

Where:

α - imperfection factor which can be considered as 0.21 for concrete-filled circular and rectangular hollow sections, 0.34 for completely or partly concrete-encased I-section with bending about the major axis of the profile, and 0.49 for completely or partly concrete-encased I-section with bending about the minor axis of the profile.

2.3.3 Torsion

There is no clearly specified design procedure for the composite column subjected to the torsional load in Eurocode 4(EC4) to design section for torsion. However, there are other standards like the American Institute of Steel Construction (AISC) Specification for Structural Steel Buildings in which the Composite column section can be designed for torsion. [19].Here is below discussed in detail According to this standard. In most cases, the nominal torsion strengths are calculated for closed sections such as Filled Boxes and Filled Pipes only. Torsion is ignored in design for all other section types. Concrete is ignored while calculating the torsional strength.

a. Round and Rectangular HSS Subject to Torsion

The design torsional strength, $\phi_T T_n$, and the allowable torsional strength, T_n/Ω_T, for round and rectangular HSS according to the limit states of torsional yielding and torsional buckling shall be determined as follows.

$$T_n = F_{cr} C \quad (2.16)$$

ϕ_T= 0.90 (LRFD) Ω_T =*1.67*(ASD)

Where:

C = HSS torsional constant, (mm^3)

The torsional constant, C, maybe conservatively taken as:

For round HSS:

$$C = \frac{\pi(D-t)^2}{2} t \quad (2.17)$$

For rectangular HSS:

$$C = 2(B-t)(H-t)t - 4.5(4-\pi)t^3 \quad (2.18)$$

The critical stress, *Fcr*, shall be determined as follows:

i. For round HSS, Fcr shall be the larger of:

$$F_{cr} = \frac{123E}{\sqrt{\frac{L}{D}(\frac{D}{t})^{\frac{5}{4}}}} \quad (2.19)$$

And

$$F_{cr} = \frac{0.60E}{(\frac{D}{t})^{\frac{3}{2}}} \quad (2.20)$$

but shall not exceed 0.6*Fy*,

where:

D = outside diameter, in. (mm)

L = length of the member, in. (mm)

t = design wall thickness(mm)

ii. For rectangular HSS

1. When $h/t<2.45\sqrt{\frac{E}{Fy}}$

$$F_{cr} = 0.6F_y \quad (2.21)$$

2. When $2.45\sqrt{\frac{E}{Fy}}<h/t\leq 3.07\sqrt{\frac{E}{Fy}}$

$$F_{cr} = 0.6F_y \frac{2.45\sqrt{\frac{E}{Fy}}}{\sqrt{\frac{h}{t}}} \quad (2.22)$$

3. When $3.07\sqrt{\frac{E}{Fy}} < h/t < 260$

$$F_{cr} = \frac{0.458\pi^2 E}{\left(\frac{h}{t}\right)^2} \quad (2.23)$$

Where:

h = flat width of the longer side, as defined in mm.

This paper aims to investigate the incremental level of the axial load 40%, 50%, 60% at constant Torsional load value.

2.4 Experimental reviews literature

2.4.1 Introduction

To investigate the strength and behavior of CFST columns, many researchers have carried out experimental and theoretical studies. There are below some experimental investigation that conducted on composite columns by citing the source of references to validate Abaqus software result.

2.4.2 Experimental programme-1 [15]

In the experimental investigation of Qing-Xin Ren, Lin-Hai Han, Chao Hou, Zhong Tao, and Shuai Li on Concrete-encased CFST columns under combined compression and torsion, there are 2 square concrete-filled composite columns and 4 circular concrete-filled composite column samples were investigated in their paper from all 26 specimen.

a. Material properties and samples

The test parameters included the cross-sectional shape, the axial load level, the cross-sectional area of the inner CFST and the specimen type are proposed. Simple design formulae are proposed to predict the ultimate strength of composite columns, and the prediction accuracy is verified by comparing with the test results with the software outputs in this experiment which is used as one of the reference experiment for this study.

The result from this experiment is summarized below in Table 2.3.

In Table 2.3. they used the following nomenclature to name the test specimens:

- the initial character “s” or “c” stands for a square or circular cross-section respectively;
- the second character “c” refers to column specimens;
- the last character “o” or “i” (if any) stands for a hollow outer RC without an inner CFST or an inner CFST without an outer RC respectively;
- the first number in the specimen label stands for a group of the same type of specimens,
- the second number is used to distinguish duplicate specimens.

From those 26 specimens, specimen numbers 11,12,23,24,25 and 26 are part of the concrete-filled or steel composite column. For validation of the Abaqus software result, those specimen material properties were used in this paper.

Table 2.3: Reference Experimental Summary of concrete-encased CFST column specimens and concrete-filled composite column [15].

Specimen type	No.	Specimen label	Cross-section $B(D) \times H$ (mm)	Steel tube $d_i \times t$ (mm)	N_o (kN)	n	α_{cfst}	α_l (%)	K_t (kN·m^2)		T_{ue} (kN·m)		T_{uc} (kN·m) calculated	T_{uc}/T_{ue}
									Measured	Average	Measured	Average		
	1	sc1-1	200 × 600	120 × 2.98	0	0	0.28	2.95	481.5	484.8	24.2	24.3	21.6	0.893
	2	sc1-2	200 × 600	120 × 2.98	0	0	0.28	2.95	488.1		24.3		21.6	0.889
	3	sc2-1	200 × 600	120 × 2.98	664.2	0.3	0.28	2.95	506.8	509.3	25.1	25.4	22.5	0.896
	4	sc2-2	200 × 600	120 × 2.98	664.2	0.3	0.28	2.95	511.7		25.6		22.5	0.879
	5	sc3-1	200 × 600	120 × 2.98	1328.4	0.6	0.28	2.95	471.0	473.0	26.2	26.3	20.4	0.779
	6	sc3-2	200 × 600	120 × 2.98	1328.4	0.6	0.28	2.95	474.9		26.3		20.4	0.776
	7	sc4-1	200 × 600	100 × 2.98	0	0	0.20	2.63	426.4	427.8	18.4	18.5	16.5	0.897
	8	sc4-2	200 × 600	100 × 2.98	0	0	0.20	2.63	429.2		18.5		16.5	0.892
	9	sc5-1	200 × 600	80 × 2.98	0	0	0.13	2.42	372.6	368.1	14.3	14.3	12.5	0.874
	10	sc5-2	200 × 600	80 × 2.98	0	0	0.13	2.42	363.5		14.2		12.5	0.880
	11	sco1-1	200 × 600	–	0	0	–	2.95	239.1	236.4	6.8	7.0	–	–
	12	sco1-2	200 × 600	–	0	0	–	2.95	233.7		7.1		–	–
	13	cc1-1	200 × 600	120 × 2.98	0	0	0.36	4.21	421.0	425.4	20.9	21.0	20.5	0.981
	14	cc1-2	200 × 600	120 × 2.98	0	0	0.36	4.21	429.7		21.1		20.5	0.972
	15	cc2-1	200 × 600	120 × 2.98	587.7	0.3	0.36	4.21	427.9	433.0	21.4	21.5	21.0	0.981
	16	cc2-2	200 × 600	120 × 2.98	587.7	0.3	0.36	4.21	438.1		21.5		21.0	0.977
	17	cc3-1	200 × 600	120 × 2.98	1175.4	0.6	0.36	4.21	400.2	409.7	21.7	21.9	18.8	0.866
	18	cc3-2	200 × 600	120 × 2.98	1175.4	0.6	0.36	4.21	419.2		22.0		18.8	0.855
	19	cc4-1	200 × 600	100 × 2.98	0	0	0.25	3.59	348.0	351.5	15.8	15.9	15.4	0.975
	20	cc4-2	200 × 600	100 × 2.98	0	0	0.25	3.59	355.0		15.9		15.4	0.969
	21	cc5-1	200 × 600	80 × 2.98	0	0	0.16	3.20	306.7	303.1	11.9	12.2	11.1	0.933
	22	cc5-2	200 × 600	80 × 2.98	0	0	0.16	3.20	299.4		12.4		11.1	0.895
	23	cco1-1	200 × 600	–	0	0	–	4.21	196.4	192.0	5.2	5.4	–	–
	24	cco1-2	200 × 600	–	0	0	–	4.21	187.5		5.5		–	–
	25	cci1-1	–	120 × 2.98	0	0	–	–	187.2	186.0	15.3	15.2	–	–
	26	cci1-2	–	120 × 2.98	0	0	–	–	184.8		15.1		–	–

b. Test set up

A specially designed experimental setup was used to apply the combined compression and torsion to the column specimen as shown in Figure 2.9. The left end of the specimen was fixed to a reaction wall through 8 high-strength bolts. A jack with a capacity of 2000 KN was mounted on the right reaction block and used to apply a constant axial compressive force to the specimen through a tapered roller bearing. The use of the tapered roller bearing enabled the transfer of the axial compressive force. but allowed the specimen to rotate freely around its longitudinal axis. A grooved disk was installed between the specimen and the tapered roller bearing for applying a torsional moment to the specimen. A jack with a capacity of 600 KN was connected to the strong floor, and the jack was used to apply a tensile force to the edge of the grooved disk through a steel cable. Since the grooved disk was firmly connected to the specimen through bolts, the applied tensile force by the jack induced torsion in the column specimen.

They applied two load cells to measure the applied axial compressive force and tensile force, respectively. The torsional angle (θ) of the specimen during testing was measured using two displacement transducers. Strain rosettes installed on the external surfaces of the specimen and the embedded steel tube were used t measure the shear strains (γ) at the mid-height of the specimen. Prior to testing, the axial load (No) was applied to the right end of the specimen and kept constant during the whole process of testing. In their experiment, the highest axial load level n was selected as 0.6, which generally covers the actual range of load levels in engineering practice. [15]

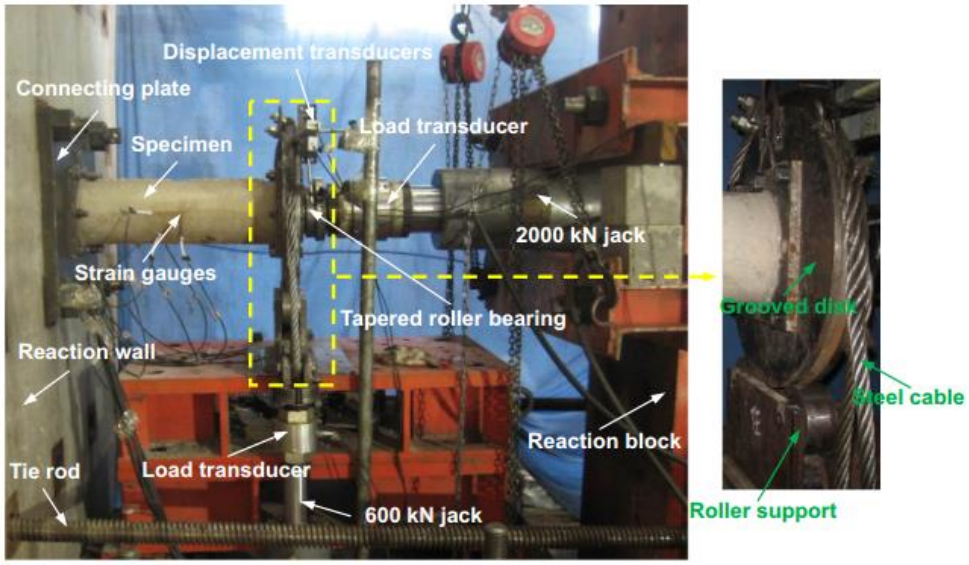

Figure 2.9: Test set up (Source: [15])

c. Failure modes

From this experimental program, it was found some failure modes of specimens shows the composite columns after testing, and a schematic of the failure modes of the outer concrete is shown in Figure 2.10. In the initial loading stage, all specimens remained in good condition without any cracking of the outer concrete. Upon further loading to about 45% of the torsional strength, the first tiny diagonal crack with an approximately 45° inclination to the member axis was detected on the surface of the outer concrete. The crack width and number of cracks increased with increasing torsional moment. After the yield load, only a few main cracks continued to propagate whereas the width of other cracks was generally stable and small.

From this experiment, it was found that, in the initial loading stage, all specimens remained in good condition without any cracking of the outer concrete. Upon further loading to about 45% of the torsional strength, the first tiny diagonal crack with an approximately 45° inclination to the member axis was detected on the surface of the outer concrete. The crack width and number of cracks increased with increasing torsional moment. After the yield load, only a few main cracks continued to propagate whereas the width of other cracks was generally stable and small. Additionally, from the result, it was observed that the cross-sectional shape, axial load level, and CFST ratio had little influence on the failure mode of concrete-encased CFST columns. However, the specimen type indeed affected the failure mode.

For Concrete filled CFST columns, the specimens demonstrated little sign of damage, except the minor local diagonal buckling of the steel tube near the mid-height of the specimens. Because of the presence of the inner CFST, the outer concrete in a concrete-encased CFST column showed relatively good integrity with a maximum crack width of about 7 mm at the end of testing. However, without an inner CFST, the hollow RC columns experienced severe damage and the corresponding maximum crack width reached 10 mm at the end of testing. The comparison indicates that the presence of the inner CFSTs helped maintain the integrity of concrete-encased CFST columns under combined compression and torsion.

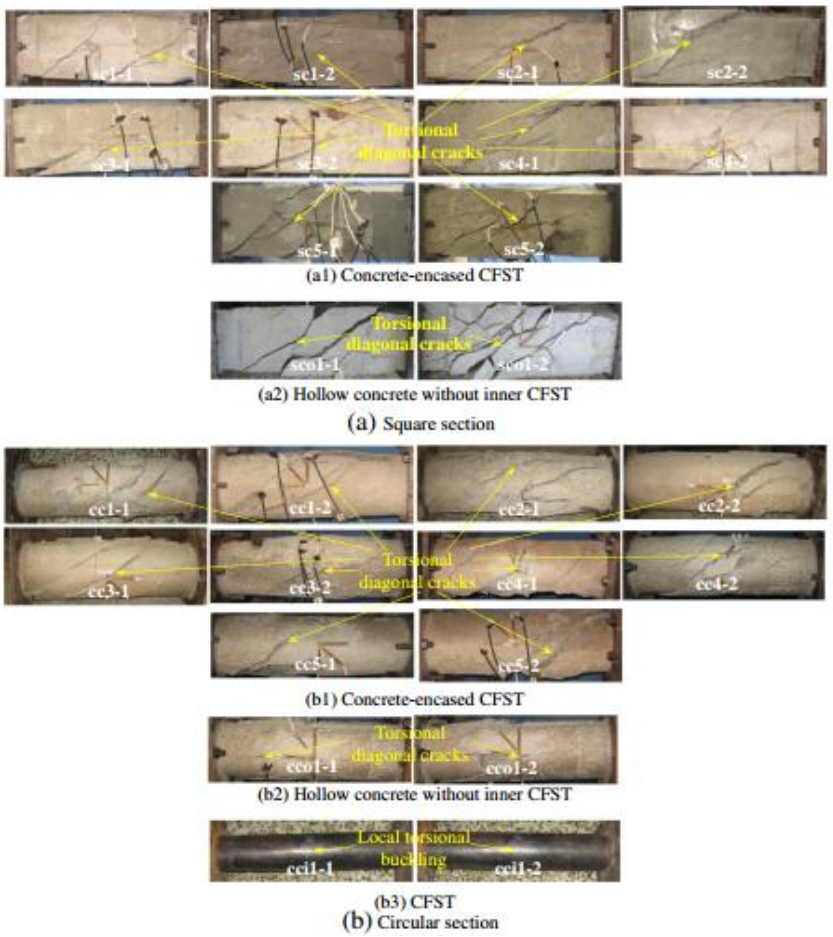

Figure 2.10: Specimens After testing, Failure mode. (Source: [15])

d. Conclusions

From this experiment, it was investigated that, the behavior of concrete-encased CFST and concrete-filled columns under combined compression and torsion. Based on the experimental results, the following conclusions can be drawn.

1. The tested CFST columns under combined compression and torsion behaved in a ductile manner owing to the existence of the inner CFST component. The typical failure mode of these composite columns was the development of diagonal cracks in the outer concrete with an approximately 45° inclination to the member axis.

2. The axial load level has slight effects on the rigidity and strength of the concrete-encased CFST columns under combined compression and torsion, whilst the effects of CFST ratio, the existence of inner CFST and outer RC are significant. For both types of column cross-sections, more than 20% decrease of the rigidity index RI and strength index SI was detected when the CFST ratio decreased by about 30%. These two indexes of CFST increase significantly compared to the individual CFST or RC components.

Where:

RI-Implies to quantify the torsional rigidity variation, a relative rigidity index and

SI- implies to quantify the torsional strength variation.

3. It was advised simple superposition method to predict the torsional strength of CFST columns under combined compression and torsion.

2.4.3 Experimental programme-2 [16]

David Hernández-Figueirido, Carmen Ibañez, Ana Piquer, and Óscar Martínez-Ramos were studied Experimental study of cross-section shape and infill influence on CFST stub columns subjected to axial loads. In their paper, a total of 12 composite columns were tested with the objective of evaluating the effect of the concrete infill and cross-sectional shape(Circular, Square).

a. Test set up

They tested all column specimens in a horizontal testing frame with a capacity of 5000 KN. The figure below shows the set-up of an experiment. As can be seen in Figure below, a steel plate with dimensions 300x300x15 mm was welded at both ends of each specimen to assure a buckling length of 300 mm for all the columns with pinned pinned (PP) boundary conditions during the tests. For the sake of accuracy of the measurements, the corresponding displacement control test was performed after the correct collocation of the column.

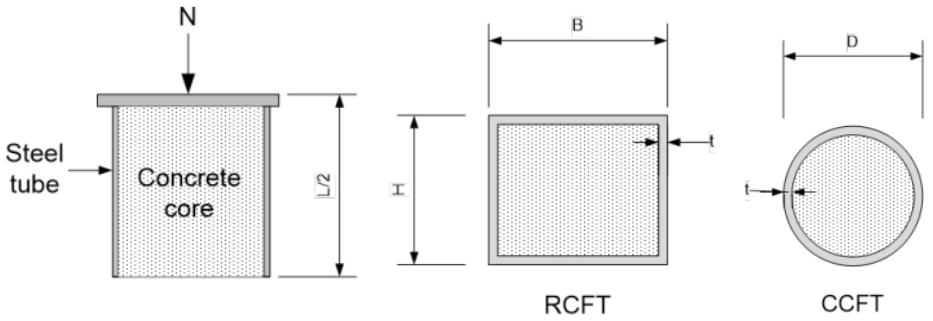

Figure 2.11: Samples and Test set up [16]

In this experimental program, the material properties used were the nominal yield strength of all the steel tubes was S275, circular hollow sections of diameter 108 mm and thickness 2 mm, which had a yield strength of S355. The nominal compressive strength of concrete used is 30 MPa which used as a reference for this paper. Material properties used in this reference are summarized in the following Table 2.4.

Table 2.4: Details of reference specimens [16]

No	Name	D(mm)	t(mm)	A(mm^2)	Concrete in fill	N_{exp}(KN)	SI	CCR
1	C108.2_30	108,0	2	666	C30	694,20	1,41	2,94
2	C168,3.2,8_30	168,3	2,8	1456	C30	1282,50	1,25	3.2
3	C159.3_30	159	3	1470	C30	1185,70	1,24	2,93
4	S125.125.3_30	125	3	1464	C30	824,50	1,00	2,05
5	S125.125.4_30	125	4	1936	C30	1159,20	1,23	2,18

Where: C-stands for specimen with Circular shape and S-square shapes, R-rectangular shape.

SI-Strength Index and can be calculated using equation -(2.24)

b. Strength Index, SI

The Strength index, the ratio between the theoretical cross-sectional capacity and the actual ultimate load was calculated for each column by means of Equation (2.16).

$$SI = \frac{N_{exp}}{A_S F_Y + A_C F_C} \quad (2.24)$$

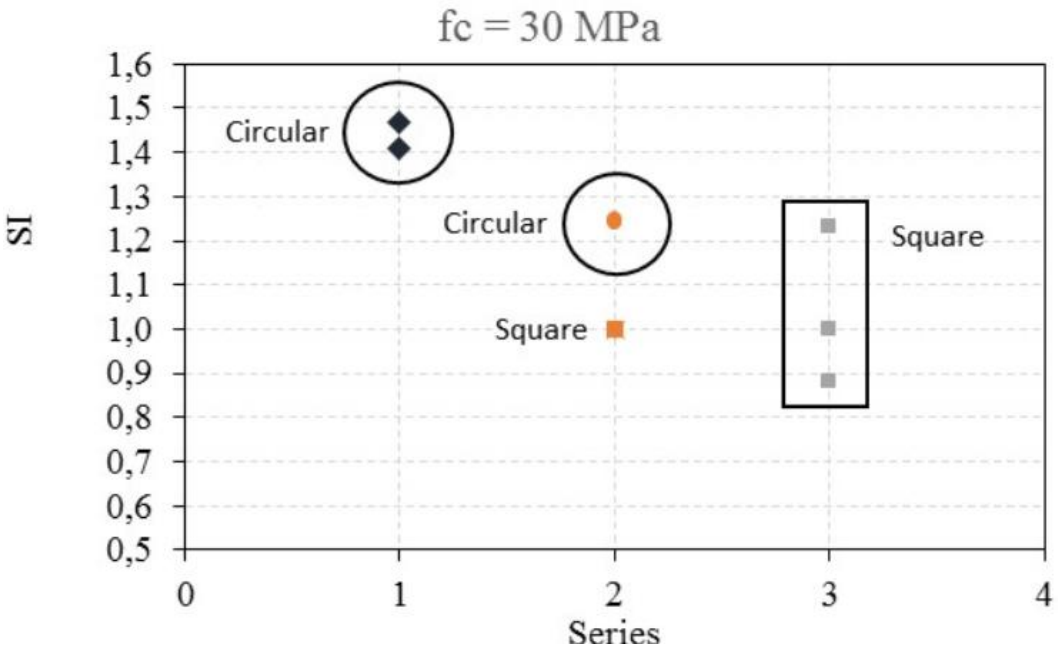

Figure 2.12: Strength index (SI) variation with the steel cross-sectional area [16]

From this chart, it is observed that, In the case of High strength concrete (HSC) and circular sections, the value of SI is in general like the unity for all the cases. In the case of Normal strength concrete (NSC) and circular sections the values are higher than the unity, it is said, the sectional capacity is higher than the sum of all the components. For rectangular/square sections and HSC, the SI is less than the unit, which means that the sectional capacity calculated as the sum of all the components overestimate the ultimate load of the members.

c. Concrete Contribution Ratio

In this program, it's calculated, the contribution of the concrete infill was analyzed for each member by means of the Concrete Contribution Ratio which can be calculated by means of Equation (2.25)

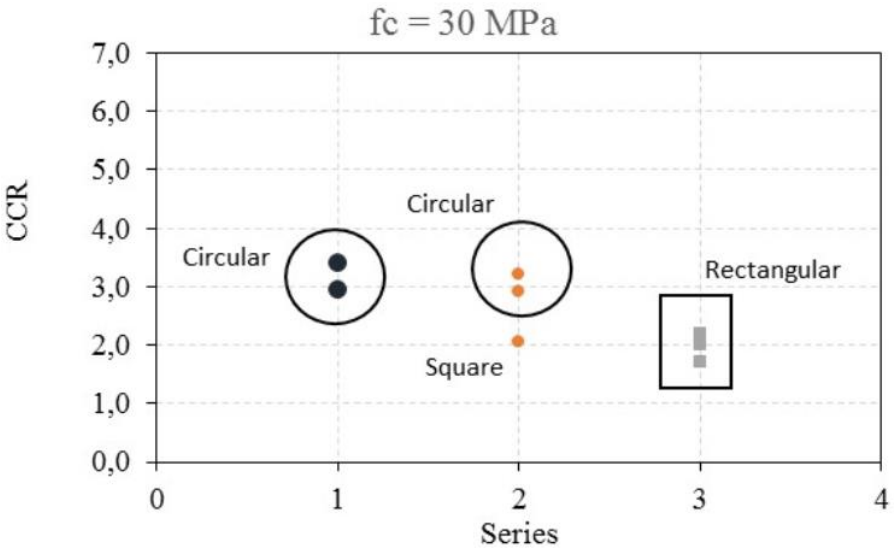

Figure 2.13: Concrete contribution ratio (CCR) variation with the steel cross-sectional area and shape [16]

CCR- Concrete Contribution Ratio can be calculated using equation-(2.25)

$$CCR = \frac{N_{exp}}{A_{S,eff}F_Y} \quad (2.25)$$

From Figure 2.12 it can be observed that the variation of the CCR with the steel cross-sectional area and shape applied to the columns. The results obtained corroborate that observed for the ultimate load. The effect of the concrete infill is much higher when HSC is employed and, again, this effect is less important with rectangular/square sections. The concrete core delays the local buckling effect and the confinement of the concrete by the steel tube explains the results obtained.

From this experiment program, it was summarized by three aspects that are analyzed to draw conclusions about the most efficient combination of geometries: ultimate load, strength index, and concrete contribution ratio. As though, the use of high strength concrete results in an increment in the ultimate load and in the concrete contribution ratio of the CFST columns. As regards to the shape effect, the configuration with circular steel tubes provides to be the most efficient, contrarily to the square sections, which presents the poorest ultimate load and indexes values.

2.4.4 Experimental programme-3 [17]

Schneider studied the effects of geometric shapes of concrete-filled steel tubes (CFST) columns subjected to concentric loads on his paper 'Axially Loaded Concrete-Filled Steel Tubes'. Fourteen specimens (three circular, five square and six rectangular) were tested to investigate the how tube shape and steel tube thickness affect column strength. The results showed that the circular specimens achieved hardening-type post-yield behavior, whereas most of the square and rectangular specimens underwent softening post-yield behavior.

a. **Test Specimens**

For convenience, circular tubes were designated with C, S for square, and R for rectangular. For each tube profile, specimens were arranged in order of increasing wall thickness. As

shown by the table below, D/t ratios in this study ranged from 17 to -50, and the steel to total composite area ratio As/A_{ttal} ranged from 8 to 22%. For the rectangular shapes, D/t was listed for the broad face. Although the nominal dimension of each tube was given, outside dimensions and wall thickness were measured at several locations. These measured values were used in determining the cross-sectional properties listed. Since it was desired to keep tube depths approximately the same, the L/D ratios ranged between 4 and 5.

Table 2.1: Properties for concrete-filled Steel Tube Components [17]

Shape (1)	Outer nominal diameter (mm) (2)	Actual dimensions (mm) (3)	Actual wall thickness (mm) (4)	D/t ratio (5)	L/D ratio (6)	A_s/A_{total} (%) (7)	Steel Properties			Concrete Properties		
							A_s (mm^2) (8)	F_y (MPa) (9)	E_s (MPa) (10)	A_c (mm^2) (11)	f'_c (kPa) (12)	E_c (MPa) (13)
C1	140	140.8	3.00	47.0	4.3	8.3	1,297	285	189,475	14,258	28,180	25,599
C2	140	141.4	6.50	21.7	4.3	17.5	2,755	313	206,011	12,968	23,805	23,528
C3	140	140.0	6.68	21.0	4.4	18.2	2,794	537	205,322	12,581	28,180	25,599
S1	127 × 127	127.3 × 127.3	3.15	40.4	4.8	9.5	1,535	356	180,518	14,645	30,454	26,611
S2	127 × 127	126.9 × 126.9	4.34	29.2	4.8	13.0	2,077	357	190,164	13,935	26,044	24,609
S3	127 × 127	126.9 × 127.0	4.55	27.9	4.8	13.6	2,174	322	205,322	13,871	23,805	23,528
S4	127 × 127	125.3 × 126.5	5.67	22.3	4.8	17.0	2,684	312	203,944	13,097	23,805	23,528
S5	127 × 127	126.8 × 127.2	7.47	17.0	4.8	21.5	3,426	347	204,633	12,516	23,805	23,528
R1	76 × 152	76.6 × 152.3	3.00	50.8	4.0	11.3	1,316	430	190,164	10,323	30,454	26,611
R2	76 × 152	76.5 × 152.8	4.47	34.2	4.0	16.6	1,923	383	213,590	9,677	26,044	24,609
R3	102 × 152	101.8 × 152.4	4.32	35.3	4.0	13.5	2,077	413	214,968	13,355	26,044	24,609
R4	102 × 152	102.8 × 152.7	4.57	33.4	4.0	14.1	2,200	365	206,011	13,419	23,805	23,528
R5	102 × 152	101.3 × 151.4	5.72	26.5	4.0	17.5	2,671	324	204,633	12,581	23,805	23,528
R6	102 × 152	102.13 × 152.37	7.34	20.8	4.0	22.0	3,381	358	205,322	12,000	23,805	23,528

b. **Founded results from this experiment by Schneider** [17]

From Schneider's paper, test results have been separated by tube shape and analyzed by graphs showing behavior for the circular, square, and rectangular steel tubes separately. For this paper, only circular and square columns are investigated in detail and the result from this experimental program used for validation of Abaqus software results.

From Figure 2.14, it can be observed the post-yield behavior of each tube shape. In general, circular tube shapes exhibited strain-hardening characteristics long after the CFT reached yield. Square tube shape exhibited various post-yield behavior depending on the tube wall thickness. Specimen S5 was classified as strain-hardening signs of modest strain-hardening. Specimen S4 was classified as elastic, perfectly plastic, and Specimen R5 appeared to be in transition between elastic-plastic and degrading stiffness. The behavior of the remaining cross-sections was classified as degrading stiffness type, or strain-softening, behavior.

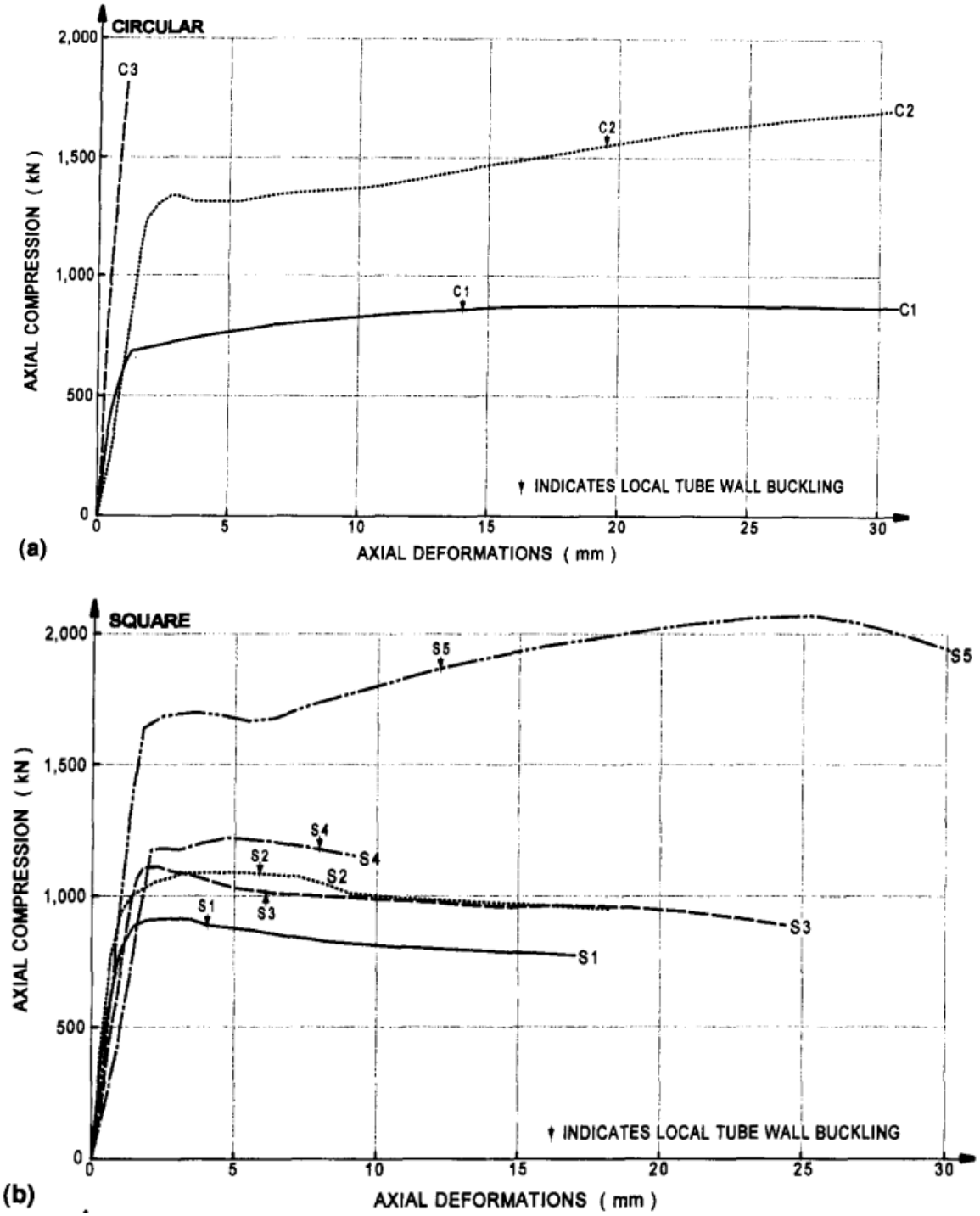

Figure 2.14: Comparison of CFT Behaviour with Respect to Tube Shape: (a) Circular Tubes; (b) Square Tubes [17]

c. **Conclusion**

From this experimental program, it was investigated, Circular steel tubes offer much more post-yield axial ductility than the square or rectangular tube sections. All circular tubes in this experimental study were classified as strain hardening, while only the small D/t ratios, approximately D/t < 20 for this study, exhibited strain-hardening characteristics for the square or rectangular tubes. Local wall buckling for the circular tubes occurred at an axial

ductility of 10 or more, while most local wall buckling of the square and rectangular tubes occurred at a ductility between 2 and 8.

2.5 Summary of Experimental Program [15] [16] [17]

Different Experimental programs conducted by different researchers converge to a similar general conclusion about the action of Concrete filled steel tube columns under Axial and torsional loads. The results of tests convey important information about the physical behavior of concrete-filled steel tube (CFST) columns and present the opportunity to assess the contribution of steel and concrete properties to column axial capacity. Based on the above experimental program the following conclusions can be drawn:

- The use of high strength concrete results in an increment in the ultimate load and in the concrete contribution ratio of the CFST columns. As regards to the shape effect, the configuration with circular steel tubes provides to be the most efficient, contrarily to the square sections, which presents the poorest ultimate load and indexes values.
- The tested CFST columns under combined compression and torsion behaved in a ductile manner owing to the existence of the inner CFST component. The typical failure mode of these composite columns was the development of diagonal cracks in the outer concrete with an approximately 45° inclination to the member axis.
- The axial load level has slight effects on the rigidity and strength of the concrete-encased CFST columns under combined compression and torsion, whilst the effects of CFST ratio, the existence of inner CFST and outer RC are significant. For both types of column cross-sections, more than 20% decrease of the rigidity index RI and strength index SI was detected when the CFST ratio decreased by about 30%. These two indexes of CFST increase significantly compared to the individual CFST or RC components.
- It was advised simple superposition method to predict the torsional strength of CFST columns under combined compression and torsion.
- The axial load level has slight effects on the rigidity and strength of the concrete
- The behavior of CFCSTs in this study subjected to axial compression is slightly better than that of circular tube confined concrete columns and performed much better than RC specimens.
- The larger variation for slender CFTs between the experimental values and the values predicted from the codes indicates that more studies are needed, and the code provisions should be refined.
- The circular specimens achieved hardening-type post-yield behavior, whereas most of the square and rectangular specimens underwent softening post-yield behavior.
- Circular steel tubes offer much more post-yield axial ductility than the square or rectangular tube sections. All circular tubes in this experimental study were classified as strain hardening, while only the small D/t ratios, approximately $D/t < 20$ for this study, exhibited strain-hardening characteristics for the square or rectangular tubes.

- Local wall buckling for the circular tubes occurred at an axial ductility of 10 or more, while most local wall buckling of the square and rectangular tubes occurred at a ductility between 2 and 8.

3 RESEARCH METHODOLOGY

3.1 Solution strategy and specimen for analytical study

The main purpose of this study was to determine the effects of torsion on different levels of axial loads on the load-bearing capacity of the different sections of the composite column. To achieve this, a finite element analysis was conducted with all appropriate parameters considered.

This study focused on the following composite columns sections:

1. [Circular, square] concrete-filled composite column (Figure *3.1*).
2. [Circular, square] concrete-filled composite column with longitudinal reinforcement (Figure *3.2*).
3. [Circular, square] concrete-filled composite column with I or H- section steel profile embedded (Figure *3.3*).

Totally 6 specimens investigated under different levels of axial loads and constant torsion will be carried out. The behavior of circular/square concrete-filled steel tube column under the action of axial and torsional loads is discussed by comparing the result from Abaqus software with an Experimental program that was discussed under the referenced Experimental program in Chapter-2. The result from software also checked with an actual design according to Eurocode-4.

First, for all specimens of the composite column are subjected to 40%, 50% and 60% of its respective axial load capacity without applying torsion moment and under different axial load level conducted using Abaqus software. From software result output the compression or deflection in the direction of load, stress distribution is evaluated for each case of loading.

In the second case keeping all conditions of composite column and axial loading the same to the previous one but applying a constant torsion with increasing axial load, the results again evaluated in terms of compression/deflection, rotation, stress distribution and compared with the first case.

In the third case, analysis is done by providing longitudinal reinforcement in the composite column. The result also compared to other cases which are analyzed without providing longitudinal reinforcement in terms of rotation, compression and stress distribution. The cross-section of the composite column taken is as shown in Figure 3.1 and Figure 3.2.

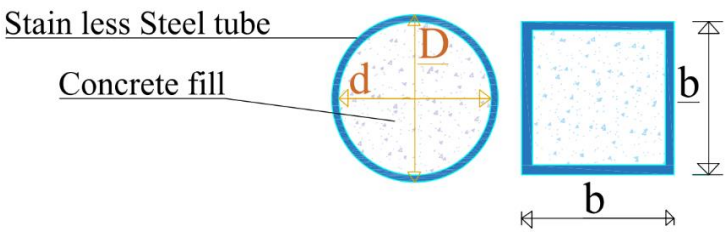

Figure 3.1: Circular and square cross-section layout without reinforcement.

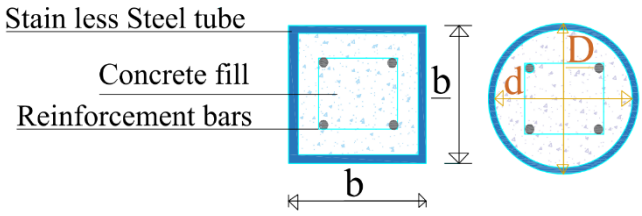

Figure 3.2: Circular and square cross-section layout with reinforcement.

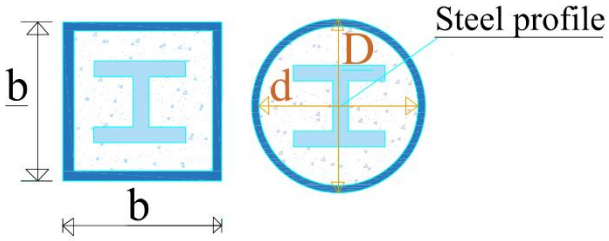

Figure 3.3: Circular and square cross-section layout with steel profile embedded.

The analysis is conducted on the three-dimensional numerical model, the details of the models can be found in Chapter **Error! Reference source not found.**. **Error! Reference source not found.**. The first model consists of two or more independent components which are later related to each other by interaction model and constraints. The geometry of composite column is:

- The circular steel tube, with the outer diameter D, the inner diameter d and the height h, the circular concrete core with the diameter d and the height h, and the two thick steel plates make up the geometry of the circular composite column (CCC) model.
- The square steel tube, with width bxb and height h .make up the geometry of the square composite column (SCC) model.

3.2 Material Definition

The material definition is an important part of finite element analysis, and each component should be defined carefully, and all parts should be defined with appropriate material parameters. Detail of material properties was discussed under section 4.2.3.

3.3 Proposed Geometry of Section

To compare and analyses the effects of axial load and torsion over the different shapes of the cross-section, the cross-section area is assumed to be equal regardless of shape and infilled concrete or embedded steel profile.

- For circular steel tube, with the outer diameter D=400mm, the inner diameter d=380mm and the height h=3500mm. This parameter also used for Concrete filled circular column with reinforcement and steel profile embedded.
- The square steel tube, with width bxb=355x355 in mm and height h=3500mm. For both circular and square cross-section, the other option like with or without reinforcement and steel profile were considered from this parameter as reference. Detail of the geometrical section for all parts are discussed under section 4.2.2.

4 NUMERICAL MODELLING

4.1 Introduction

The Finite Element Method (FEM) is known nowadays as one of the well-established and convenient numerical techniques for the computer solution of complex engineering problems, such as three-dimensional problems in structural engineering. A method is a powerful tool for the approximate solution of the differential equations that describe the physical phenomena. Before analyzing any mechanical problem, there is the need for idealizing reality into analytical formulation first. In order to make the FEM applicable to a given structure, it should be split into smaller solid finite elements assigned with material properties, boundary conditions, and imposed loads or displacements. These elements are assembled at their nodes to form the structure's geometry, composing the finite element mesh, which is the domain of analysis. The equilibrium equations are then solved through an approximate integration on the finite element domain, usually achieved by defining polynomial approximation functions to describe the displacement field of each element. The number of elements in the mesh and the order of the approximation functions have a fundamental influence on the quality of the results. Aiming at reproducing the behavior of the Composite Column with relative accuracy, finite element models were built using the code from ABAQUS, based on the recommendations of its respective theory manual (Abaqus 6.11 User manual Documentation). Firstly, the properties of the materials are defined after the parts of modeling were created, followed by the basic modeling assumptions and analysis techniques. Afterward, a qualitative and comparative analysis of the results is done. Detail procedures of modeling and analysis were discussed below.

4.2 Finite Element Modelling

Introduction

In the study done by Ellobody et al. (2006) [10] in the analysis of the axially loaded circular CFT columns, the finite element method was developed by the program Abaqus using the three-dimensional eight-node elements for the concrete core and the steel tube. According to the authors of that study, the 3D solid elements were found more appropriate for the study because of the previous decision to model only the compact steel tubes, and because of the clearly defined boundaries of their elements. The efficiency of these elements was first verified by modeling the empty circular compact steel tubes and comparing the FE results with the results of the tests conducted by Giakoumelis and Lam (2004) and Sakino et al. (2004). [18] In another study done by Hu et al. (2005), both the concrete core and the steel tube were modeled by 27- node solid elements with a reduced integration rule.

In the modeling, there is no clearance exists between the concrete core and the steel tube. The rigid plate is placed at the two ends of the column. The purpose of placing the thick steel plates on the top and the bottom is to simulate the real conditions of the column in an integral overall section. As can been seen here, the geometry of the steel tube is introduced as the three dimensional solid. This can present certain advantages and disadvantages. Among the advantages are the clear separation of the steel-concrete boundaries, and the possibility to mesh the steel tube with several layers of the finite elements which provide more data for results analysis. One of the main disadvantages is the increased computing time, and a possibility to get slightly wrong results in case of using only one layer of finite elements in the steel tube as it was discussed in the previous study of (Ellobody et al. 2006,

Hu et al. 2005, Johansson 2002, Huang et al. 2002) [10] and those stainless steel tube was modeled as a three dimensional solid element.

In this study, the Abaqus /CAE was used to prepare the simulations while the Abaqus/Explicit was used to run the nonlinear analysis of the models. To make a valid simulation of the behavior of the composite columns, the modeling must be done properly. The main elements which must be modeled are the steel tube, the concrete which must be confined, and the interaction between the steel and the concrete. Apart from these parameters, it is also important to choose the appropriate type of finite elements and the size of the mesh in order to obtain as accurate results as possible with reasonable computing time.

In the analysis presented in this document the finite element (FE) model developed in the context of ABAQUS software [20] is intended to simulate CFST columns with circular/square cross-section under axial compression and then under combined axial compression and constant torsion.

General Procedures in FEM modeling by using Abaqus software Package are discussed in detail in the below sections.

4.2.1 Geometry and Creating parts of Modelling

The analysis is conducted on the three-dimensional numerical model. The first model consists of three up to five independent components which are later related to each other by interaction model and constraints. The geometry of composite column is:

- The circular steel tube, with the outer diameter D, the inner diameter d and the height h, the circular concrete core with the diameter d and the height have elements of the circular composite column (CCC) model.
- The square steel tube, with width BXB and height h and Square shape concrete, fill with the same height with steel tube as elements of the square composite column bxb (SCC) model.
- For both circular and square cross-section, the other option like with or without reinforcement and steel profile were considered. The assumed height of the column is 3500mm for all.

The detailed geometry of the models can be found in Table 4.1.

Table 4.1: Geometry and dimension of Composite column sections

Column Types	Dimension		Steel section
	D(b mm)	d(mm)	Thickness, t
Circular composite column(CCC)	400	380	t=10
Square composite column(SCC)	355	355	t=10
Embedded H-Section (Steel profile) HEA 200	200	190	t_f=10, t_w=6.5
Reinforcement bars	14	-	-
Stirrup bars	8	-	-

Parts are the building blocks of an Abaqus/CAE model. In this paper, the Part module to create each part, and Assembly module to assemble instances of the parts was used. In this study four parts were created, such as steel tube, inner concrete to fill, reinforcement bar, stirrup, and steel profile were used. In this section of modeling longitudinal bar and stirrup modeled as 3D with base feature of wire as truss and assigned as beam properties. The parts are shown in Figure 4.1 - Figure 4.5.

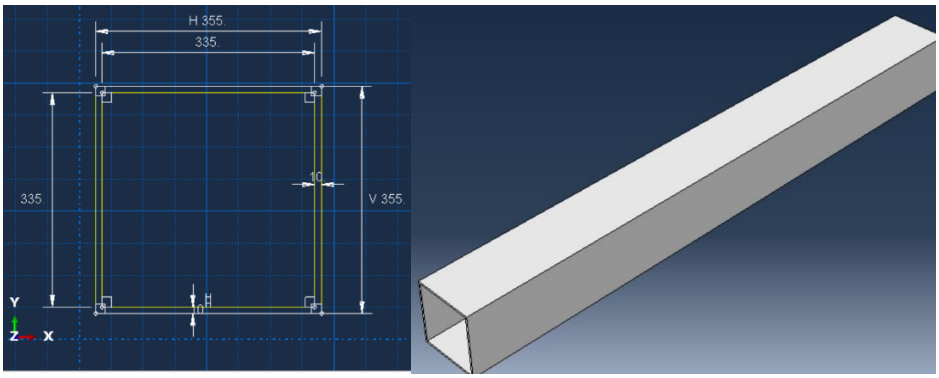

Figure 4.1: Square Stainless steel tube geometry parametrization

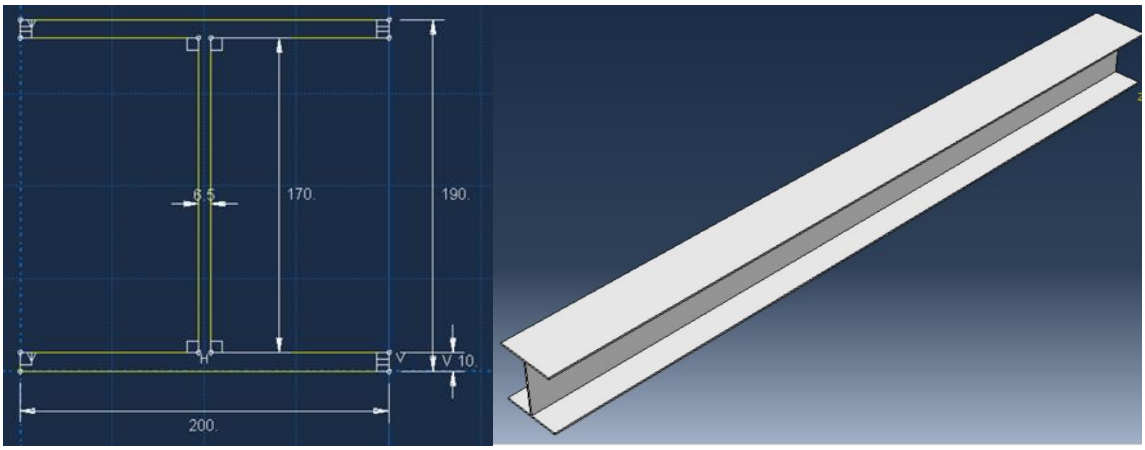

Figure 4.2: Embedded steel profile H-section geometry parametrization

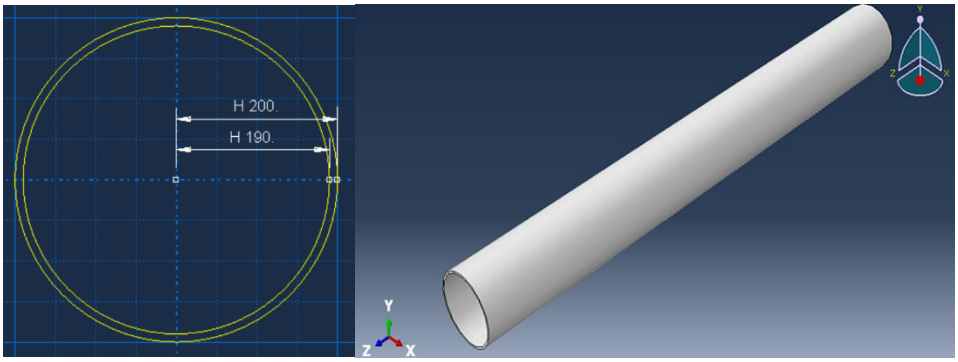

Figure 4.3: Circular stainless steel tube geometry parametrization

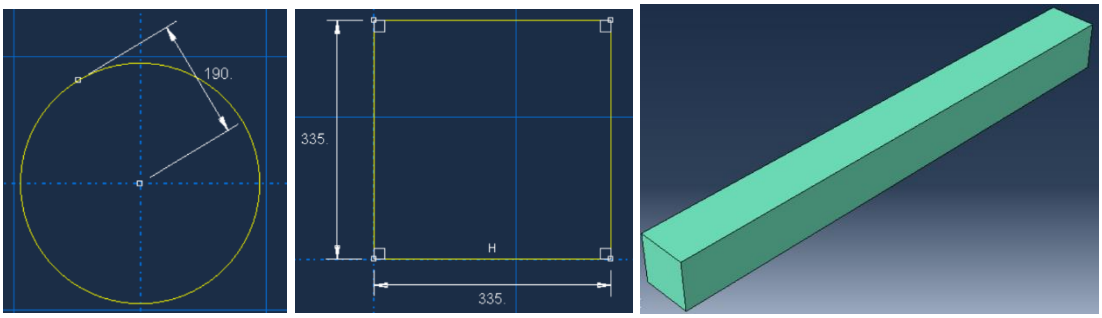

Figure 4.4: Circular and Square Concrete fill parts layout and parametrization

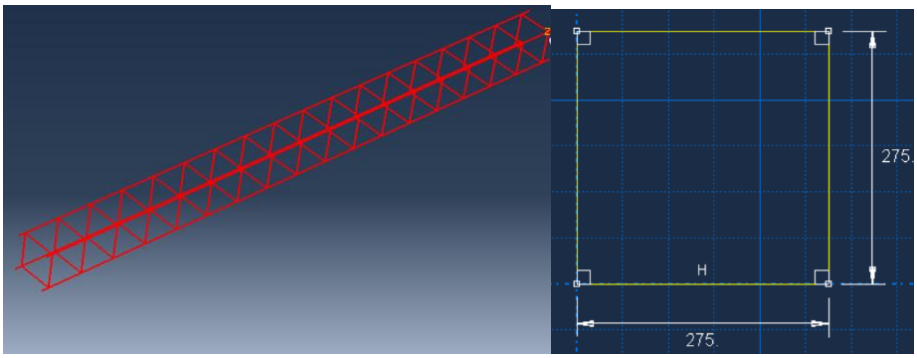

Figure 4.5: Longitudinal reinforcement and Stirrup bars parametrization

4.2.2 Material properties of created parts

Under this stage, the material behaviors were selected. The material editor contains several menus that allow us to add most of the material behaviors available in Abaqus/Standard, Abaqus/Explicit, or Abaqus/CFD to a material definition.

I. Concrete

In the case of the concrete, a nonlinear constitutive model called Concrete Damage Plasticity available in the software Abaqus 6.9 is chosen. This model is a plasticity-based continuum damage model. According to the Abaqus manual (6.9), this model assumes that the main two failure mechanisms are the compressive crushing and the tensile cracking of the concrete material. The evolution of the yield surface is controlled by two hardening variables, the tensile equivalent plastic strain (t_{pl}) the parameters which are defined for the Concrete Damage.

Plasticity model is the following:

- for the plasticity, dilatation angle: 30, eccentricity 0.1, fb0/fc0=1.16, K=0.667, Viscosity parameter = 0
- for the compressive behavior, it is taken that the material yields at the 25MPa.
- for the tensile behavior, the yield stress is taken as 2.25MPa (0.09fc').
- poisson's ratio is taken as 0.2

II. Steel section and reinforcement bar

Steel tube is modeled as elastic-perfectly plastic with von mises yield criterion. Due to steel tube is subjected to multiple stresses and therefore the stress-strain curve crosses the elastic

limit and reaches in the plastic region. The nonlinear behavior of steel tube is obtained from the uniaxial tension test and used in steel modeling. In this analysis Poisson's ratio, density and young's modulus are taken as μ=0.3, ρ=7860kg/m3 and Es=210000MPa respectively. All the specimens were analyzed with the steel yield point at 355MPa and 400Mpa for reinforcement bars. [17]. For modeling, the dimension of cross-sections is assumed to be equal under interval that investigated from the previous study by Schneider [17] Material properties are used directly the same in all section to respective element. Steel profile embedded, Number of Stirrup and longitudinal are assumed for modeling purpose and kept the same consideration for all types of the composite column in this paper.

Table 4.2: Detailed cross-section and material properties

Column Types	Dimension		Steel section	Reinfor-cement	Stirrups	Material properties (Mpa)		
	D(b) [mm]	d(mm)				f_{yc}	f_{ys}	f_{yr}
Circular composite column(CCC)	400	380	t=10	4ϕ14	Φ8	25	355	400
Square composite column(SCC)	355	355	t=10	4ϕ14	Φ8	25	355	400
Embedded H-Section (Steel profile) HEA 200	200	190	t_f=10 t_w=6.5	-	-	25	355	400

Where:

- f_{yc}, f_{ys}, f_{yd} are characteristic strength of concrete, yield strength of reinforcement bar and structural steel respectively.
- t_f and t_w are Thickness of flange and web HEA 200 steel profile respectively.

Table 4.3: Summary of the mechanical properties of materials

properties	Materials		
	steel	Reinforcement bar	concrete
Density	7860kg/m3	7860kg/m3	2400kg/m3
Poisson ratio (v)	0.3	0.3	0.2
Young's modulus (E)	210000Mpa	210,000Mpa	31,500Mpa

Steel, concrete and reinforcement properties were inputted as discussed in Table 4.2 in detail. And the considered behavior of the material is assumed as elastic behavior which is under the mechanical menu in Abaqus Software.

4.2.3 Section Assignment and Creating Profiles

Under this stage Parts of the section are assigned to respective material properties. Steel tube [Steel properties], Concrete fill [concrete properties], Bar [steel properties for reinforcement] and Steel profile with respective steel profile properties.

4.2.4 Assembling of Parts section modeling

In Abaqus Assembly module is used to create and modify the assembly. The model contains only one assembly, which is composed of instances of parts from the model. In this paper also composed of instance, assembling was used.

This stage has different main assemblies for the purpose of this paper as seen below with pictures from Abaqus software too;

- [Circular, Square] Concrete filled steel tube Column without longitudinal reinforcement. It consists of parts of the steel tube and concrete fill only which can be seen in Figure 4.6.
- [Circular, Square] Concrete filled steel tube Column with longitudinal reinforcement. It consists parts of Steel tube, Concrete fill, longitudinal reinforcement and stirrup bars which can be seen in Figure 4.7.
- [Circular, Square] Concrete filled steel tube with steel profile embedded. It consists parts of Stainless-steel tube, concrete infill and embedded H-section steel profile which can be seen in Figure 4.8.

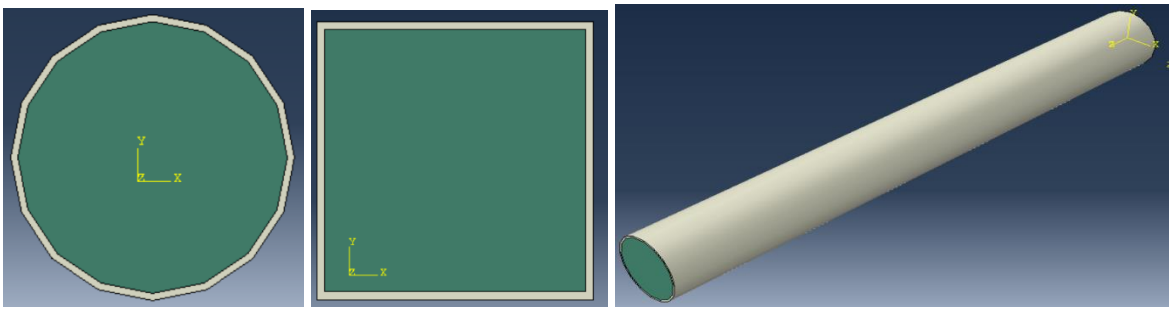

Figure 4.6: Circular and square concrete-filled steel tube column

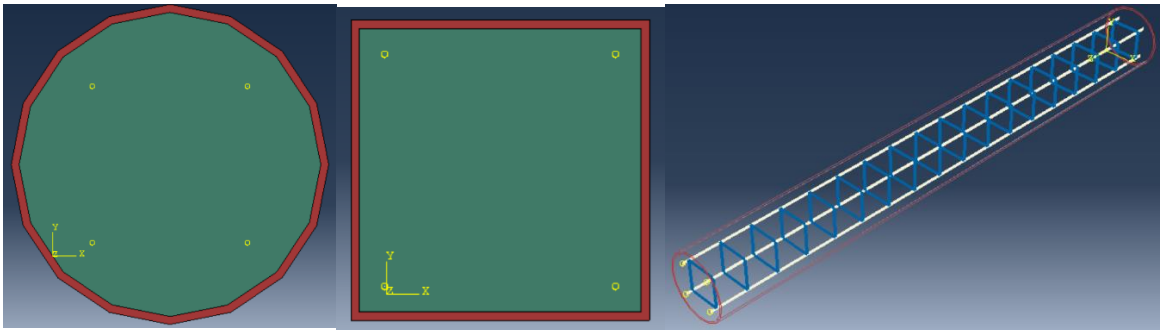

Figure 4.7: Circular and square concrete filled steel tube column longitudinal reinforcement

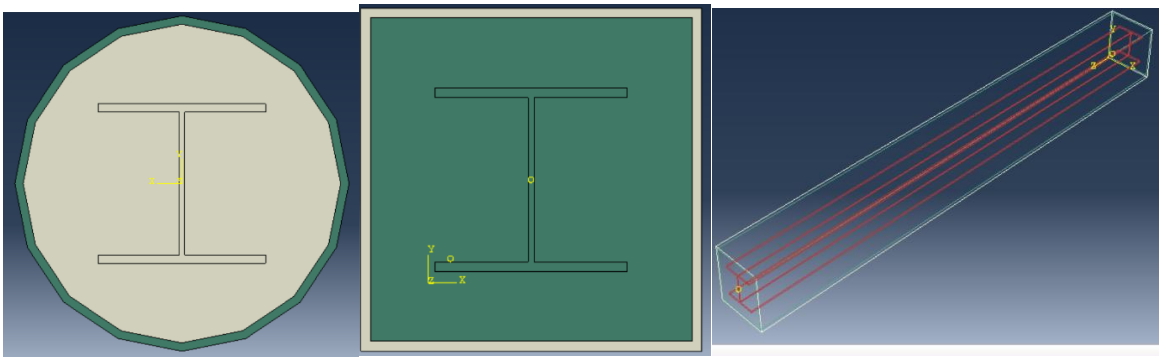

Figure 4.8: Circular and square concrete-filled steel tube with steel profile embedded

4.2.5 Steps module stage

Within a model, we define a sequence of one or more analysis steps. The step sequence provides a convenient way to capture changes in the loading and boundary conditions of the model, changes in the way parts of the model interact with each other, the removal or addition of parts, and any other changes that may occur in the model during the course of the analysis. The Step module is used to perform the following tasks: create analysis steps, specify output requests, specify adaptive meshing and Specify analysis controls.

4.2.6 The interaction Module Stage

Interactions are step-dependent objects, which means that when we define them, we must indicate in which steps of the analysis they are active. According to the Abaqus manual [20] 6.13, there are two types of contact simulations in Abaqus/Standard:

- surface-based or
- contact element based.

First, the surfaces of different components that will be in contact must be created. After that pairs of surfaces which are going to be in contact must be identified. These are called contact pairs. And finally, the constitutive models which describe the interactions between the various surfaces must be defined. In this work, a surface-based contact is chosen, and the contacting surfaces are the outer surface of the concrete core cylinder and the inner surface of the steel hollow cylinder. The discretization method chosen is surface to surface, and the sliding formulation is taken as finite sliding.

There are two components that define the interaction of contacting surfaces, one normal to the surfaces and one tangential. In Abaqus the default normal interaction between the surfaces is called the 'hard contact', meaning that the surfaces can contact each other when the clearance between them becomes zero and they can transmit between each other the unlimited magnitude of pressure but cannot penetrate each other. On the other hand, these surfaces can separate when the contact pressure between them becomes zero or negative. This type of normal contact was chosen in the work presented in this paper.

In the analysis that is presented in this document, interaction between the inner surface of the steel tube and the outer surface of the concrete core, tangential behavior is described by the penalty friction formulation, described above, and the friction coefficient is taken as 0.3. By default, the maximum elastic slip is taken as 0.005 fractions of the characteristic surface dimension as can be seen in Figure 4.9 below. Apart from the interaction between the

concrete core and embedded bars or steel profile, the constraints are also defined as it can be seen in Figure 4.10 and frictional of exterior tolerance 0.05 was used as a default for all sections.

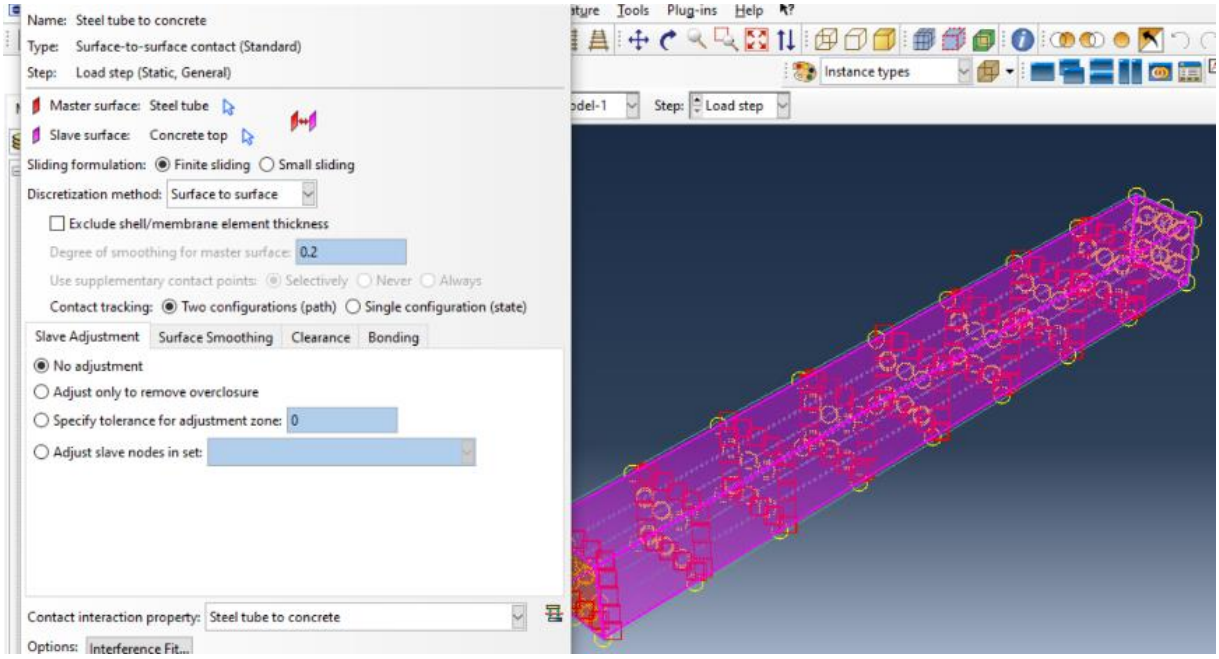

Figure 4.9: Interaction between the inner surface of the steel tube, and the outer surface of the concrete core.

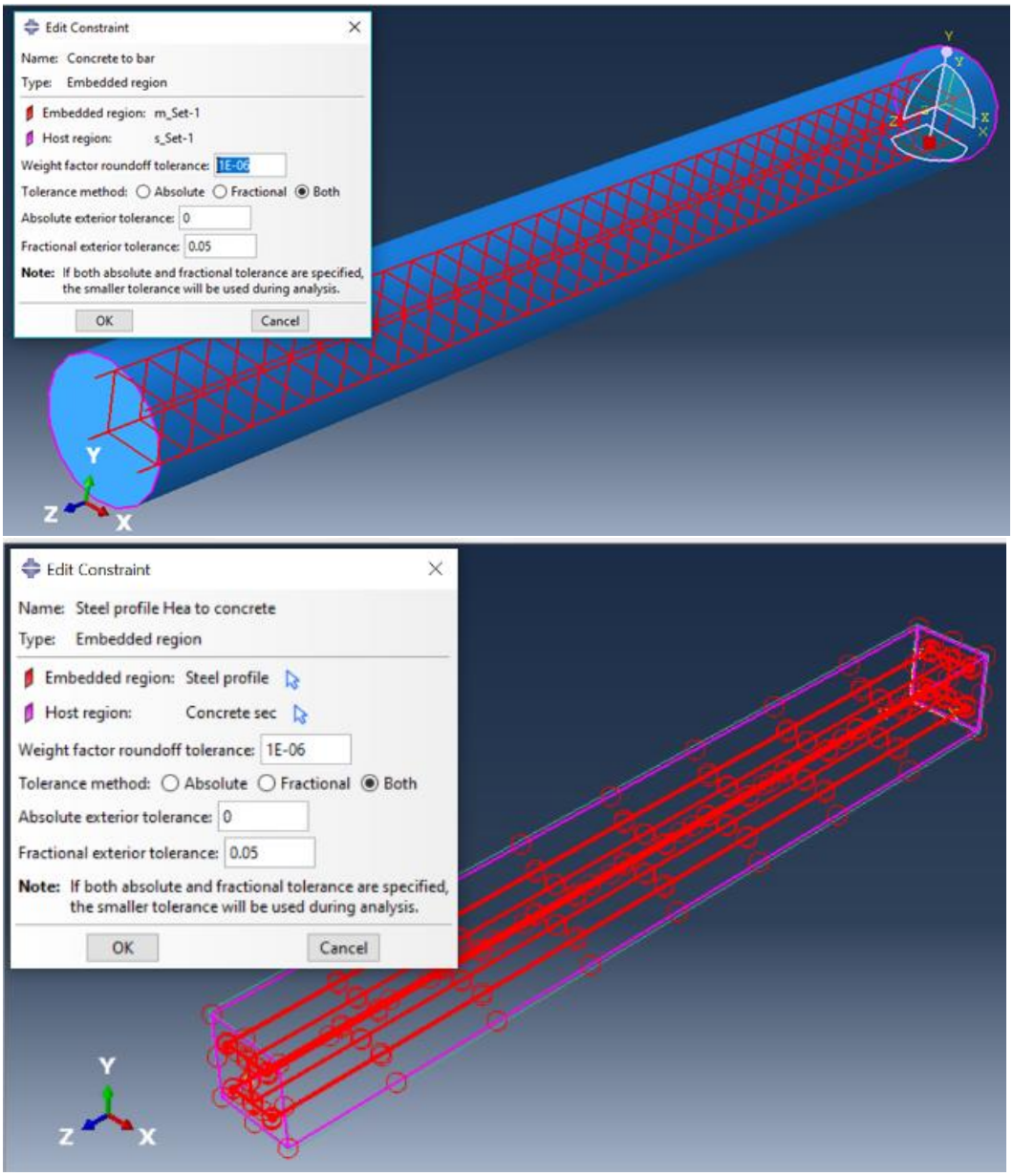

Figure 4.10: Interaction between the concrete core and bars or embedded H- section Steel profile

4.2.7 Boundary Condition and Loading

Loads and boundary conditions must be applied to the geometry of the model accurately to get the perfect result. In this analysis for each of two ends, two different types of boundary conditions were used. The nodes of the bottom end were fixed, displacement degrees of freedom in 1, 2, 3 directions (u1, u2, u3) as well as rotational degrees of freedom in 1, 2, 3 directions (Θ1, Θ2, Θ3) were restrained to zero. The nodes at the top are kept free in rotational degrees of freedom in all directions and translation in the direction where the concentrated load and torsion are applied and the other two directions are restrained.

The magnitude of axial load and torsional loads are discussed in detail under Section 4.3 and section 4.4 for circular and square composite columns respectively based on Eurocode-4 manual calculation of composite column. The load step and displacement step were solved using static and general arithmetic with geometrical and material nonlinear methods available in the ABAQUS library. The axial load level is 40%, 50% and 60% of its axial

load capacity and a constant torsion value of 60kNm which assumed scaled value from data that is used under section 2.4.2 of experimental program 1 and applied at the top end of the column.

4.2.8 Meshing of parts

In ABAQUS 6.13 meshing can be done individually on parts and then assembled or vice-versa. In this analysis, parts were individually meshed and then assembled for further process. The key in finite element analysis is the appropriate selection of element type. The ABAQUS standard modules consist of a comprehensive element library that provides different types of elements catering to different situations. Meshes are composed of tri-dimensional continuum solid elements with 8 nodes called C3D8R, 8 node linear brick elements with reduced integration and hourglass control are used for both materials, the steel tube and the concrete core. The eight-node C3D8R brick element with reduced integration is a general-purpose linear brick element with only 1 integration point. In the analysis presented in this document, C3D8R, 8 node linear brick elements with reduced integration and hourglass control are used for both materials, the steel tube and the concrete core. All parts of composite column like Stainless steel tube, concrete fill, Steel profile, stirrup, and longitudinal reinforcement meshed to the good meshing appearance and good timing for getting results from software as some parts can be seen in Figure 4.11.

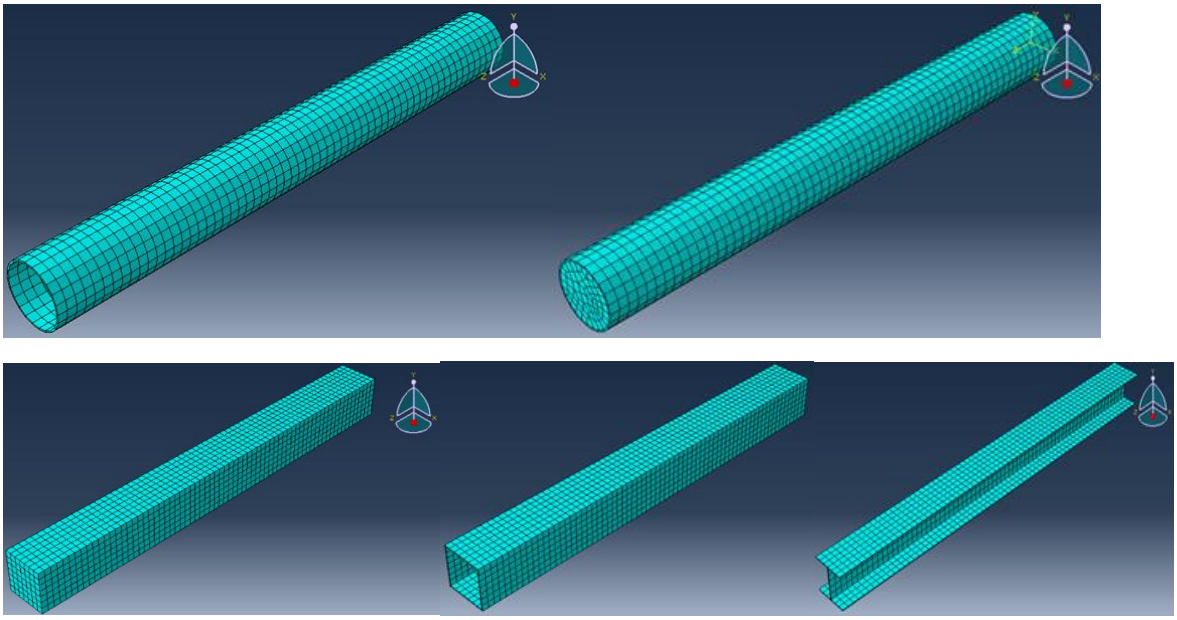

Figure 4.11: Meshing of Circular and Square section's Stainless steel tube, concrete fill and steel profile

4.2.9 Analysis and Job Creation

We can use the Job module to create and manage analysis jobs and to view a basic plot of the analysis results according to ABAQUS 6.13. We can also use the Job module to create and manage adaptively analyses and co-executions. Detail of results and discussion are discussed in detail in next, chapter 5.

4.2.10 Characteristics of the proposed model for Composite Columns

The aim is to prove that the model developed in this study using the finite element program Abaqus is valid for the analysis of the circular and Square composite columns. Finally, the

numeric result from software is validated using experimentally studied conclusion. The main characteristics of the proposed model are:

- Use of the elastic- perfectly plastic material with the Von Misses yield criterion in modeling the steel tube.
- Use of the concrete damage plasticity model offered by Abaqus/CAE in the modeling of the concrete core.
- Modeling of both the concrete and the steel with 8 node solid elements with reduced integration C3D8R brick element.
- The loads are introduced as a concentrated load and concentrated moment. The analysis is done in two steps:
  i. axial loading only and
  ii. axial load with Torsional loading.

4.3 Circular Composite Column Design according to Eurocode-4 Manual Calculation

The detail section geometry and Material properties used for design are discussed in Table 4.2 above.

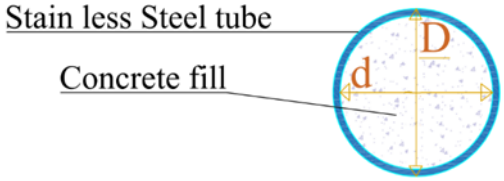

i. Section Geometry

- Height of Column [L] =3500mm
- External Width [D] = 400mm
- Internal width [d] =380mm
- Concrete Cover to longitudinal reinforcement to be used or from inner face of steel tube to outer face of reinforcement (Cc) is 40mm.

ii. Characteristics of Cross-section

a. Steel Section

- Steel grade used: S-335 and yield strength-355MPa
- Elastic modulus of steel (Ea): 210000 MPa
- Thickness of steel tube (t): 10 mm
- Area of steel tube (Aa): $\frac{\pi(D^2-d^2)}{4}=\frac{\pi(400^2-380^2)}{4}=12252.21mm^2$
- Moment of Inertia of steel tube (Ia): $\frac{\pi(D^4-d^4)}{4}=2.33098*10^8mm^4$
- Section modulus w_{pa}: $\frac{\pi(D^4-d^4)}{32D}\pi=1165491.60mm^3$
- fyd= $\frac{fsk}{1.1}$=335/1.1=304.545MPa

b. Reinforcement Bar Section

- Reinforcement bar used grade-S400
- Yield Strength of bars (fyr)=400Mpa
- Diameter of bars (Dia) is 14
- Elastic modulus of reinforcing steel (Es)=210000Mpa
- Area of Longitudinal Reinforced bar (Ab)= $\frac{\pi Dia^2}{4}=153.94mm^3$
- Total area of Longitudinal Reinforced of 4bars (As)=4*Ab=615.76mm^2

- Moment of inertial of reinforcing steel Ir: 8.79E+06mm^4
- Section modulus of reinforcement bar W_{pr}: 6.37E+04mm^3
- fsd= $\frac{fsk}{1.15}=\frac{400}{1.15}$=347.826Mpa

c. Concrete core section

- Concrete grade:c25/30
- Cylinder strength fck: 25Mpa
- Ecm=31500Mpa
- Area of concrete Ac: $\pi*190^2$=112795.735mm^2
- Moment of inertial of concrete Ic: 1021716640mm^4
- Section modulus of concrete section Wpc=5377456mm^3
- fcd=25/1.35=18.519Mpa

iii. Design Procedures

I. Plastic Resistance of Section:

N_{plRd}=Aafyd + Acfcd + Asfsd

=(11252.21*304.545)+(112795*18.519)+(615.76*347.826)=**6257.1KN**

Note: This Load applied in Abaqus software to consider the cross-section under axial load effect by having 40%, 50% and 60% of 6257.1KN respectively.

- 40%=0.4*6257.1KN =**2502.84KN**
- 50%=0.5*6257.1KN =**3128.55KN**
- 60%=0.6*6257.1KN =**3754.26KN**

Those loads once applied individually and again repeated with constant torsion 60kNm to consider the section which subjected to both axial load and torsional loads.

Summary of the applied axial load used as input for all options of sections to consider the effects.

Composite column	Axial Load(P) [KN]	P1=40%	P2=50%	P3=60%
Circular Composite column	**6257.1KN**	**2502.84KN**	**3128.55KN**	**3754.26KN**

By using the above Summary of the applied axial load, the magnitudes of loads in each step are used in Abaqus software to analysis. The load step and displacement step were solved using static and general arithmetic with geometrical and material nonlinear methods available in the ABAQUS library. The axial load level is 40%, 50% and 60% of its axial load capacity and a constant torsion value of 60kNm is applied at the top edge of the column, which is assumed scaled magnitude based on experimentally measured torsion capacity that is discussed under section 2.4.2 [15].

4.4 Square Composite Column Design according to Eurocode-4 Manual Calculation

The detail section geometry and Material properties used for design areas discussed in Table 4.2 above.

i. Section Geometry.

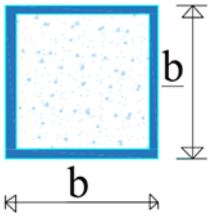

- External Length of Column [L] =355mm
- External Width [B] = 355mm
- Height of Column [L] =3500mm
- Internal width [b] =335x335mm
- Thickness of stainless-steel tube (t) is 10mm.
- Concrete Cover to longitudinal reinforcement to be used or from the inner face of steel tube to outer face of reinforcement (Cc) is 40mm.

ii. Characteristics of Cross-section

a. **Steel Section**, B=355mm and b=335mm

- Steel grade used: S-335 and yield strength-355MPa
- Elastic modulus of steel (Ea): 210000 MPa
- Thickness of steel tube (t): 10 mm
- Area of steel tube (Aa): $B^2 - b^2$=$355^2 - 335^2$=13800mm^2
- Moment of Inertia of steel tube (Ia): $\frac{B^4-b^4}{12}$ = 273987500mm^4
- Section modulus w_{pa}: $\frac{B^4-b^4}{6B}$= 1543591.549mm^3
- fyd= $\frac{fsk}{1.1}$=$\frac{335}{1.1}$=304.545MPa

b. Reinforcement Bar Section

- Reinforcement bar used grade-S400
- Yield Strength of bars (fyr)=400Mpa
- Diameter of bars (Dia) is 14
- Elastic modulus of reinforcing steel (Es)=210000Mpa
- Area of Longitudinal Reinforced bar (Ab)= $\frac{\pi Dia^2}{4}$=153.94mm^3
- Total area of Longitudinal Reinforced of 4bars (As)=4*Ab=615.76mm^2
- Moment of inertial of reinforcing steel Ir: 8.79E+06mm^4
- Section modulus of reinforcement bar W_{ps}: 6.37E+04mm^3
- fsd= $\frac{fsk}{1.15}$=$\frac{400}{1.15}$=347.826Mpa

c. Concrete core sections

- Concrete grade:c25/30
- Cylinder strength fck: 25Mpa
- Ecm=31500Mpa
- Area of concrete Ac: b^2=112225mm^2
- Moment of inertial of concrete Ic: $\frac{b*b^3}{12}$=1049537552mm^4
- Section modulus of concrete section Wpc=$\frac{b^3}{6}$= 6265895.833mm^3

- fcd=$\frac{25}{1.35}$=18.519Mpa

i. Design Procedures

I. Plastic Resistance of Section:

N_{plRd}=Aafyd + Acfcd + Asfsd

=(13800*304.545)+(112225*18.519)+(615.76*347.826)=**6495.2KN**

Note: This Load applied in Abaqus software to consider the cross-section under axial load effect by having 40%, 50% and 60% of 6257.1KN respectively.

- 40%=0.4*6495.2KN =**2598.08KN**
- 50%=0.5*6495.2KN =**3247.60KN**
- 60%=0.6*6495.2KN =**3897.12KN**

Those loads once applied individually and again repeated with constant Torsion 60KNm to consider the section which subjected to both axial load and Torsional loads.

Summary of the applied axial load used as input for all options of sections to consider the effects.

Composite column	Axial Load(P) [KN]	P1=40%	P2=50%	P3=60%
Square Composite column	**6495.2KN**	**2598.08KN**	**3247.60KN**	**3897.12KN**

By using the above Summary of the applied axial load, the magnitudes of loads in each step are used in Abaqus software to analysis. The load step and displacement step were solved using static and general arithmetic with geometrical and material nonlinear methods available in the ABAQUS library. The axial load level is 40%, 50% and 60% of its axial load capacity and a constant torsion value of 60kNm is applied at the top end of the composite column which is assumed scaled magnitude based on experimentally measured torsion capacity that is discussed under section 2.4.2 [15]. For all other composite column options, this axial load calculated is used as a reference to input axial load in ABAQUS software to consider uniformly in all cases.

5 RESULTS AND DISCUSSIONS

5.1 General introduction

Analysis of [Circular, square] section of composite column done using Abaqus software package and behavior of composite column under axial load only and under both axial and torsion load is determined. The FEM output was then examined to determine the effect of different levels of axial loads on behavior under torsion loading, high-stress zone, and the following discussion covers the results of Abaqus software.

5.2 Composite columns subjected to axial load only

Results of stress distribution (S-Mises) and displacement magnitude from Abaqus software for circular section of composite column or circular composite column (CCC) section under 40%, 50% and 60% of its axial load capacity- 6257.1KN (P) is loaded as 2502.84KN, 3128.55KN and 3754.26KN respectively as computed in detail in section 4.3

Results of stress distribution (S-Mises) and displacement magnitude from Abaqus software for the square section of the composite column or square composite column (SCC) section under 40%, 50% and 60% of its axial load capacity- 6495.2KN is loaded as 2598.08KN, 3247.6KN and 3897.12KN respectively as computed in detail in section 4.4

5.2.1 CCC with concrete-filled subjected to axial load

a. Circular composite column subjected to Axial Load at 40% [2502.84KN] of load-bearing capacity, P[6257.1KN].

When columns subjected to axial load(compression effect) and displacement under this axial load (U) will be occurred. Figure 5.1(a) shows Von Mises stress distribution, which is used to predict the yielding of materials under loading from the results of axial load. This figure showed three patterns of elements of composite column results of stress distribution from Abaqus software. The First part is indicating the stress distribution in the circular steel tube. As it can be seen from diagram stress distributed by a colorful rainbow with different values between 80.24 MPa and 89.68 MPa. at the edge support, it shows less stress and maximal stress around edge support, while the entire elements are distributed as a medium in green colors. The second part of Figure 5.1 (a) indicating the stress distribution in the concrete core element. As can be seen from this figure, stress distributed by a colorful rainbow with different values between 9.735 MPa and 13.29 MPa. at the edge support, it shows less stress, while the entire elements are distributed as the moderate medium. The third part of Figure 5.1 (a), Shows stress distribution of all parts of the composite column when sticking together. In this case from this result, it clearly understood the Mises stress magnitude is between 9.735Mpa and 89.68Mpa, which is the lower magnitude stress distributed in concrete and higher value in a steel tube element. From this figure, it concluded that stress distribute in concrete is less by 87.1 % than stress distributed in steel tube.

The magnitude of displacement distribution in member is showed in Figure 5.1 (b). This figure has two parts. The first part indicates the magnitude of Displacement distribution (U-

magnitude) of the composite column in deformed state plot only. The second part indicates the magnitude of the Displacement distribution (U-magnitude) of the composite column in the deformed state from the undeformed state plot. From Figure 5.1 (b), it is observed that the member is more displaced around section close to points of load application or at the top edge of the column. Here is the maximum magnitude of displacement under 40% of axial load that has occurred at the top which is 1.435mm. Member displacement gradually decreases from top to bottom and negligible at the bottom end of the column which is fully fixed support.

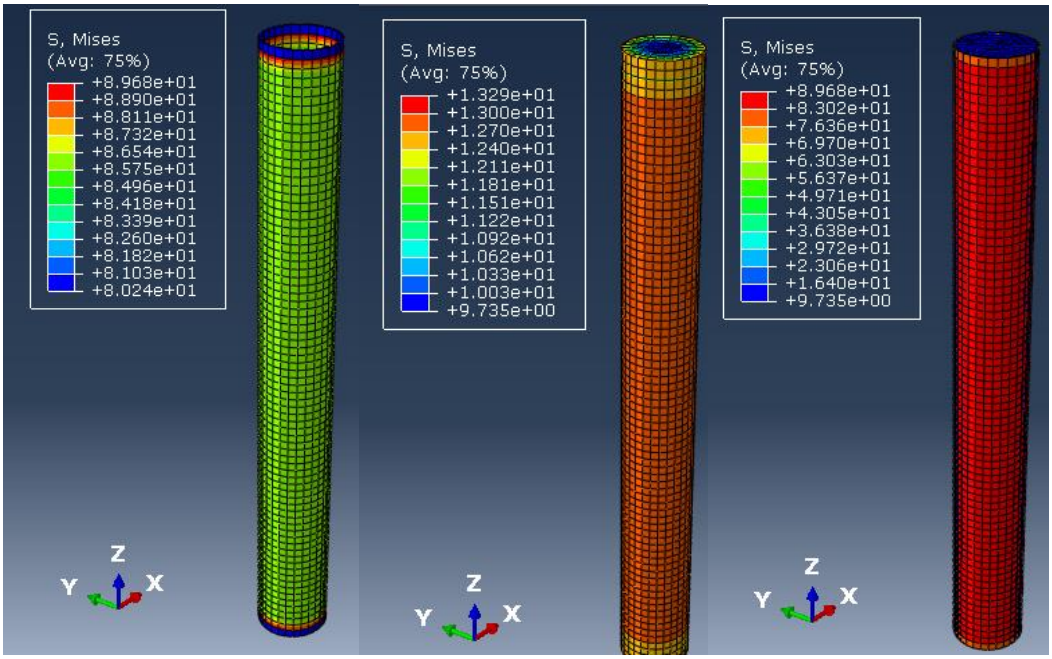

(a)

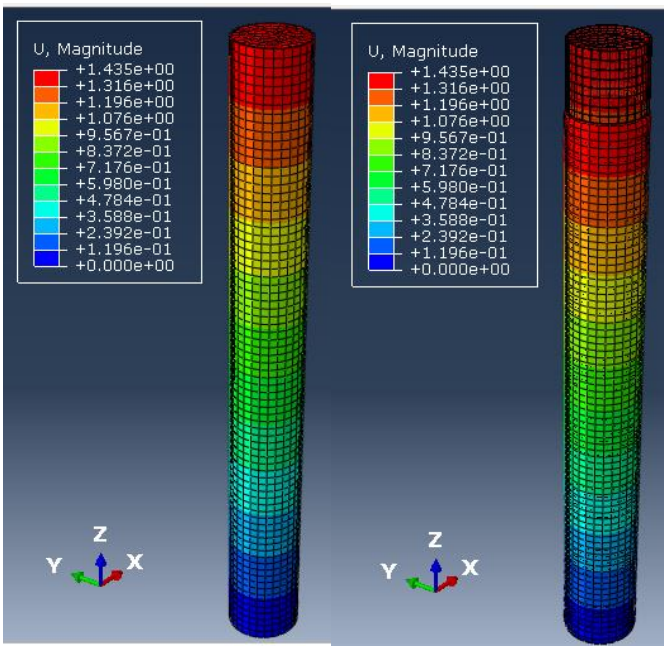

(b)

Figure 5.1: Stress and Magnitude of Displacement distribution in CCC with concrete fill at 40% of P.

b. Circular composite column subjected to Axial Load at 50% [3128.55KN] of load-bearing capacity, P[6257.1KN].

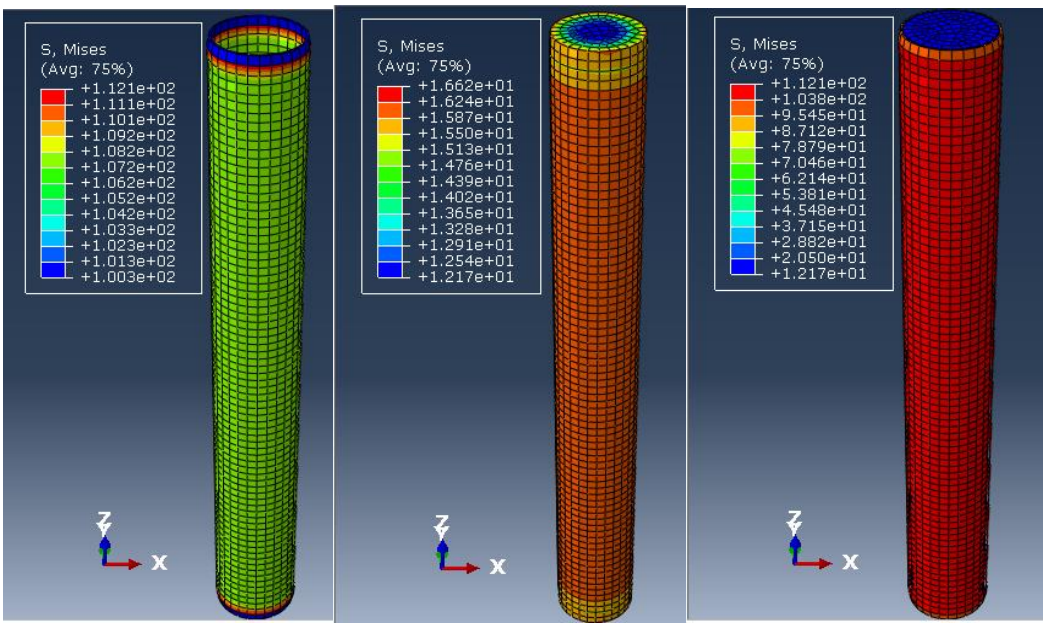

(a)

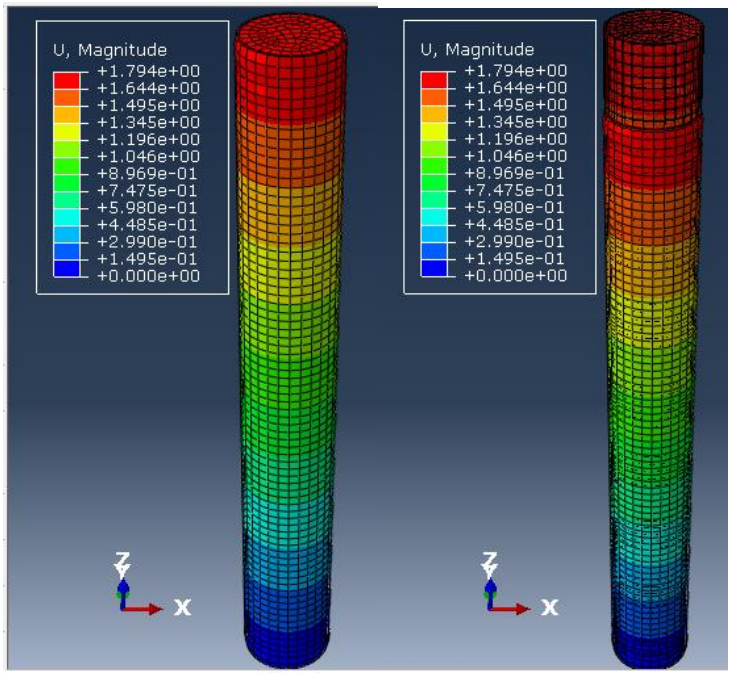

(b)

Figure 5.2 Stress and Magnitude of Displacement distribution in CCC with concrete fill at 50% of P

In Figure 5.2 (a) shows Von Mises stress distribution, which is used to predict the yielding of materials under loading from the results of the axial load. This figure showed three patterns of elements of composite column results of stress distribution from Abaqus software. The First part is indicating the stress distribution in the circular steel tube. As it can be seen from diagram stress distributed by a colorful rainbow with different values between 100.3 MPa and 112.1 MPa. at the edge support, it shows less stress and maximal stress around edge support, while the entire elements are distributed as the medium in green colors. The second part of Figure 5.2 (a) indicating the stress distribution in the concrete core element. As can be seen from this figure, stress distributed by a colorful rainbow with different values between 12.17 MPa and 16.62 MPa. at the edge support, it shows less stress, while the entire elements are distributed as a moderate medium. The third part of Figure 5.2 (a), Shows stress distribution of all parts of the composite column when sticking together. In this case from this result, it clearly understood the Mises stress magnitude is between 12.17Mpa and 112.1Mpa, which is the lower magnitude stress distributed in concrete and higher value in a steel tube element. From this figure, it concluded that stress distribute in concrete is less by 85.17 % than stress distributed in steel tube.

The magnitude of displacement distribution in members is shown in Figure 5.2 (b). This figure has two parts. The first part indicates the magnitude of Displacement distribution (U-magnitude) of the composite column in deformed state plot only. The second part indicates the magnitude of the Displacement distribution (U-magnitude) of the composite column in the deformed state from the undeformed state plot. From Figure 5.2 (b), it is observed that the member is more displaced around section close to points of load application or at the top edge of the column. Here is the maximum magnitude of displacement under 50% of the axial load has occurred at the top which is 1.794mm. Member displacement gradually decreases from top to bottom and negligible at the bottom end of the column which is fully fixed support.

c. Circular composite column subjected to Axial Load at 60% [3754.26KN] of load-bearing capacity, P[6257.1KN].

According to the result from Abaqus software as in Figure 5.3 (a) shows Von Mises stress distribution, which is used to predict yielding of materials under loading from the results of axial load. This figure showed three patterns of elements of composite column results of stress distribution from Abaqus software. The First part is indicating the stress distribution in the circular steel tube. As it can be seen from diagram stress distributed by a colorful rainbow with different values between 120.4 MPa and 134.5 MPa. at the edge support, it shows less stress and maximal stress around edge support, while the entire elements are distributed as a medium in green colors. The second part of Figure 5.3 (a) indicating the stress distribution in the concrete core element. As can be seen from this figure, stress distributed by a colorful rainbow with different values between 14.6 MPa and 19.94 MPa. at the edge support, it shows less stress, while the entire elements are distributed as the moderate medium. The third part of Figure 5.3 (a), Shows stress distribution of all parts of the composite column when sticking together. In this case from this result, it clearly understood the Mises stress magnitude is between 14.6Mpa and 134.5Mpa, which is the lower magnitude stress distributed in concrete and higher value in a steel tube element.

From this figure, it concluded that stress distribute in concrete is less by 85.2 % than stress distributed in steel tube.

The magnitude of displacement distribution in members is shown in Figure 5.3 (b). This figure has two parts. The first part indicates the magnitude of Displacement distribution (U-magnitude) of the composite column in deformed state plot only. The second part indicates the magnitude of the Displacement distribution (U-magnitude) of the composite column in the deformed state from the undeformed state plot. From Figure 5.3 (b), it is observed that the member is more displaced around section close to points of load application or at the top edge of the column. Here is the maximum magnitude of displacement under 60% of the axial load that has occurred at the top which is 2.153mm. Member displacement gradually decreases from top to bottom and negligible at the bottom end of the column which is fully fixed support.

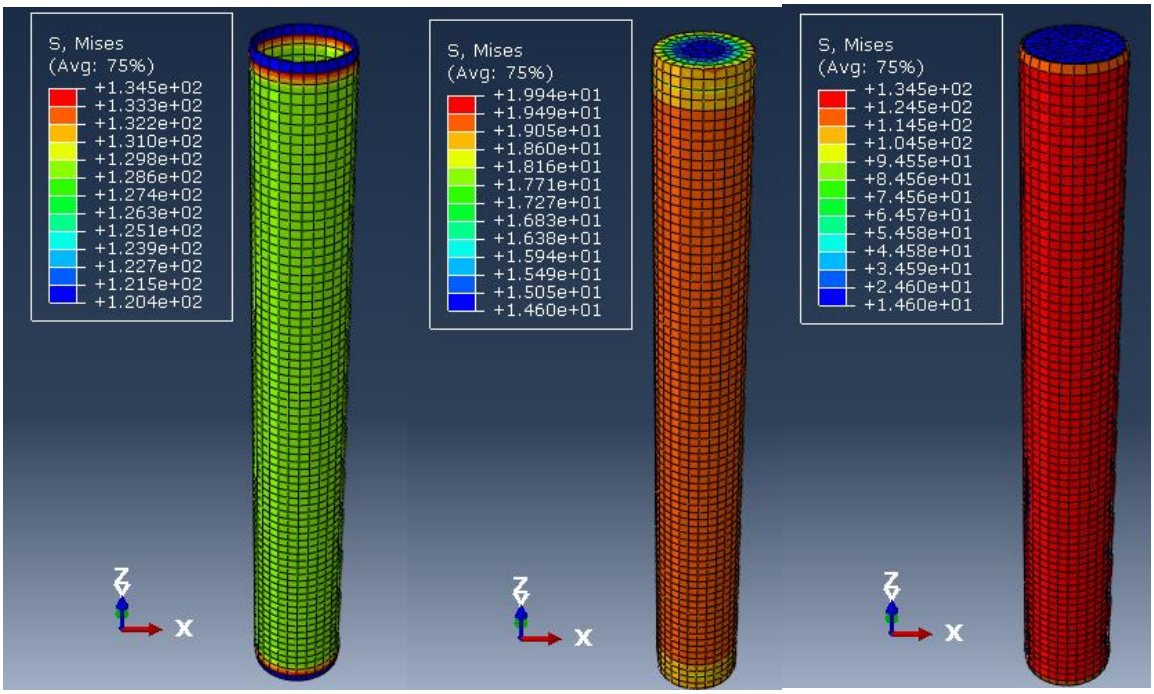

(a)

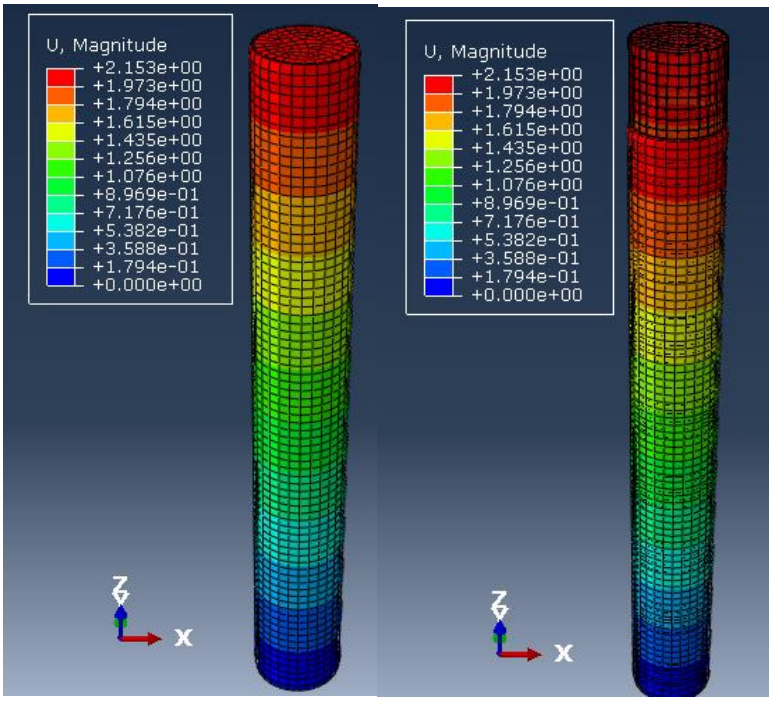

(b)

Figure 5.3: Stress and Magnitude of Displacement distribution in CCC with concrete fill at 60% of P

For summarization, When Concentrated load of 40%P, 50%P and 60%P (where P=6275.1KN is axial load capacity of circular composite column) applied on circular composite column, As it discussed before, stress of Composite column section is 89.68, 112.1, and 134.5 as axial load of 2502.84KN, 3128.55KN and 3754.26KN respectively and maximum magnitude of displacement also increased 1.345mm, 1.794mm and 2.153mm respectively.. which is summarized in Figure 5.4 below. The stress distribution of concrete is high on the outside of the concrete section where it has contact with steel and it lower at the center of steel core but the stress distribution of in steel is higher than the concrete material.

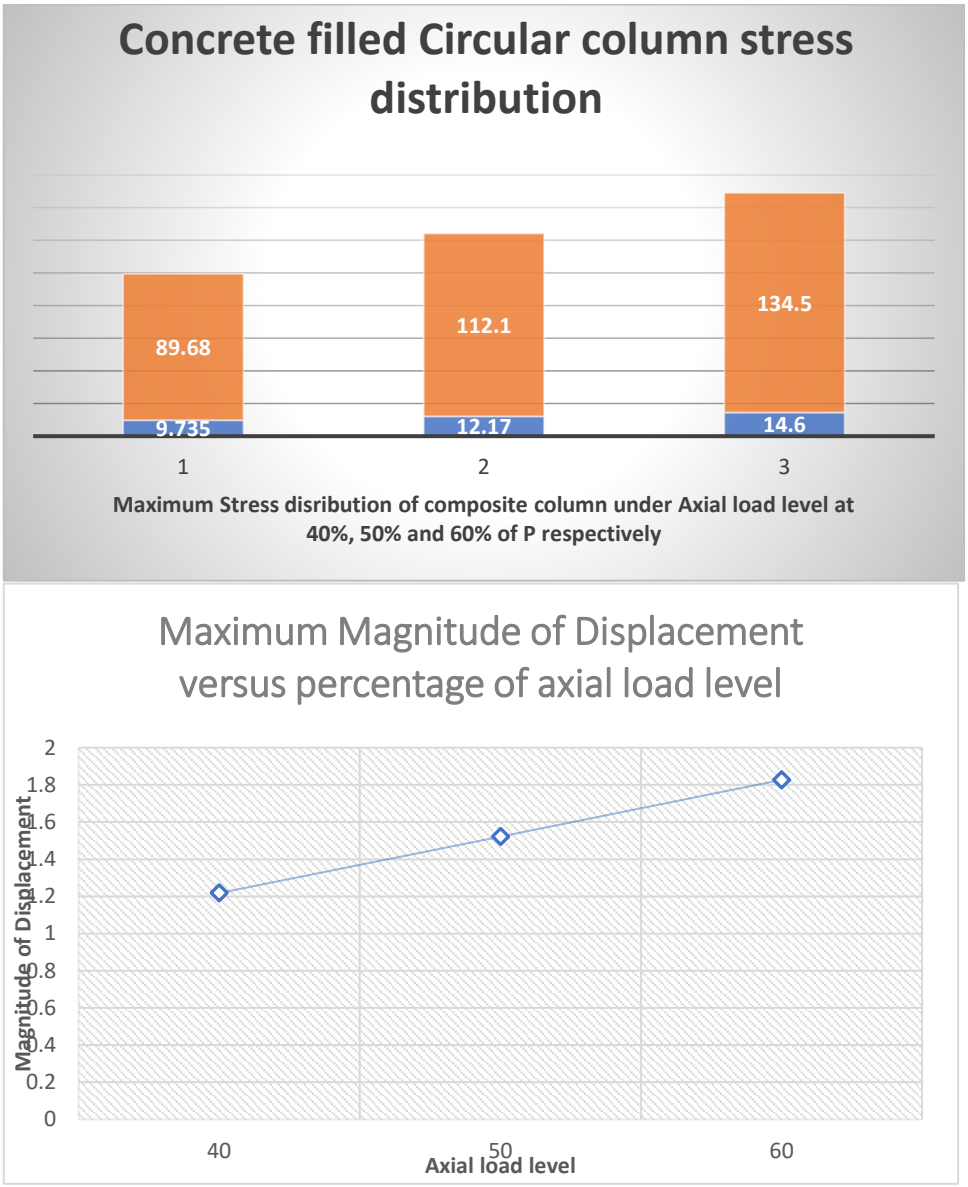

Figure 5.4: Summary of maximum Stress and displacement magnitude under different level of axial load of CCC with concrete fill only

5.2.2 CCC with reinforcement embedded under axial load

a. Circular composite column subjected to Axial Load at 40% [2502.84KN] of load-bearing capacity, P[6257.1KN].

According to the result from Abaqus software as in Figure 5.5 (a) shows Von Mises stress distribution, which is used to predict yielding of materials under loading from the results of axial load. This figure showed in four patterns of elements of composite column results of stress distribution from Abaqus software. The First part is indicating the stress distribution in a circular steel tube. As it can be seen from diagram stress distributed by a colorful rainbow with different values between 78.56MPa and 87.8MPa. at the edge support, it shows less stress and maximal stress around edge support, while the entire elements are distributed as a medium in green colors. The second part of Figure 5.5 (a) indicating the

stress distribution in the concrete core element. As can be seen from this figure, stress distributed by a colorful rainbow with different values between 9.54MPa and 13MPa. at the edge support, it shows less stress, while the entire elements are distributed as a moderate medium. The third part of Figure 5.5 (a), Shows longitudinal and stirrup bars embedded in concrete fill core stress distribution varies widely between 6.152Mpa and 86.32MPa rather than concrete and steel tube elements. The fourth part indicates, all parts of the composite column when sticking together. In this case from this result, it clearly understood the Mises stress magnitude is between 6.152Mpa and 87.8Mpa, which is the lower magnitude stress distributed in bars and higher value in a steel tube element.

The magnitude of displacement distribution in members is shown in Figure 5.5 (b). This figure has two parts. The first part indicates the magnitude of Displacement distribution (U-magnitude) of the composite column in deformed state plot only. The second part indicates the magnitude of the Displacement distribution (U-magnitude) of the composite column in the deformed state from the undeformed state plot. From Figure 5.5 (b), it is observed that the member is more displaced around section close to points of load application or at the top edge of the column. Here is the maximum magnitude of displacement under 40% of axial load that has occurred at the top which is 1.405mm. Member displacement gradually decreases from top to bottom and negligible at the bottom end of the column which is fully fixed support.

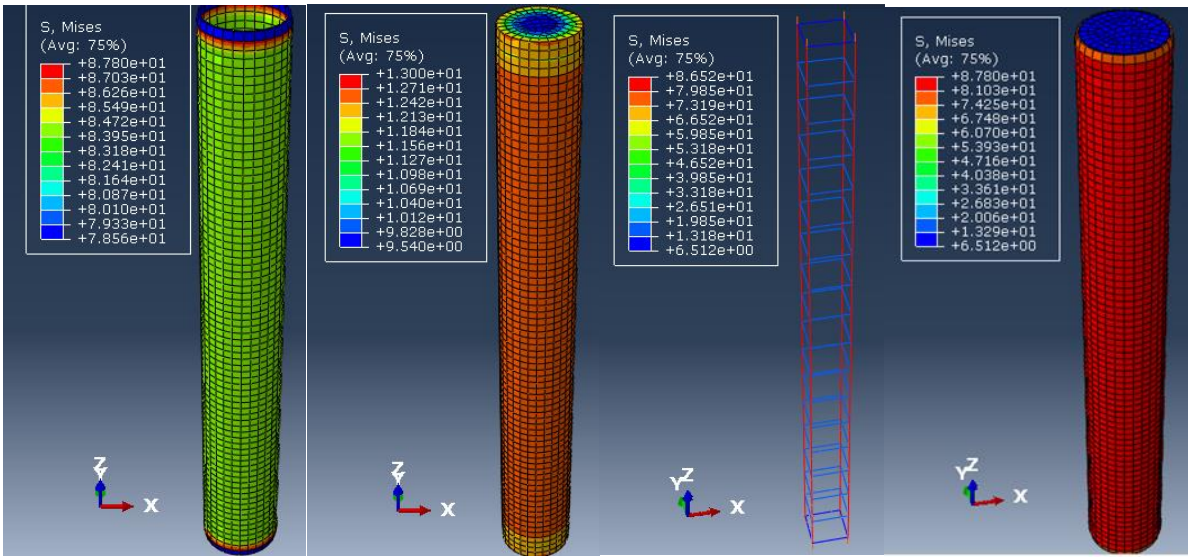

(a)

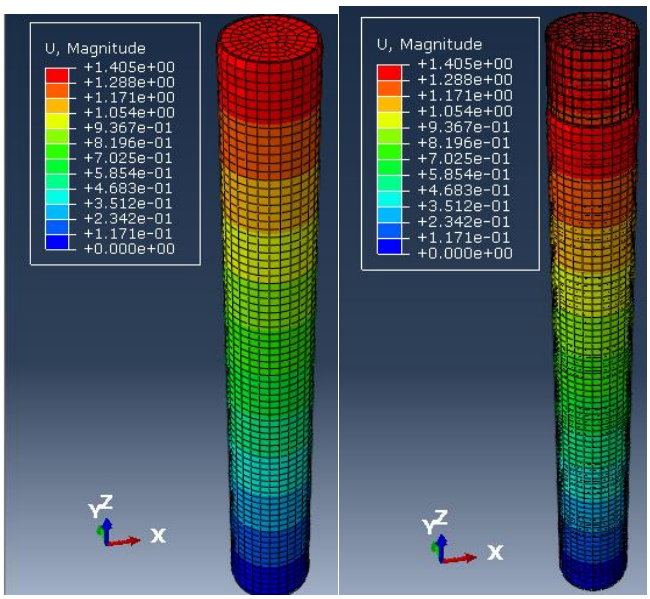

(b)

Figure 5.5: Stress and Magnitude of Displacement distribution in CCC with reinforcement at 40% of P.

b. Circular composite column subjected to Axial Load at 50% [3128.55KN] of load-bearing capacity, P[6257.1KN].

According to the result from Abaqus software as in Figure 5.6 (a) shows Von Mises stress distribution, which is used to predict yielding of materials under loading from the results of axial load. This figure showed in four patterns of elements of composite column results of stress distribution from Abaqus software. The First part is indicating the stress distribution in a circular steel tube. As it can be seen from diagram stress distributed by a colorful rainbow with different values between 98.2MPa and 109.8MPa. at the edge support, it shows less stress and maximal stress around edge support, while the entire elements are distributed as a medium in green colors. The second part of Figure 5.6 (a) indicating the stress distribution in the concrete core element. As can be seen from this figure, stress distributed by a colorful rainbow with different values between 11.92MPa and 16.25MPa. at the edge support, it shows less stress, while the entire elements are distributed as a moderate medium. The third part of Figure 5.6 (a), Shows longitudinal and stirrup bars embedded in concrete fill core stress distribution varies widely between 8.139Mpa and 108.2MPa rather than concrete and steel tube elements. The fourth part indicates, all parts of the composite column when sticking together. In this case from this result, it clearly understood the Mises stress magnitude is between 8.139Mpa and 109.8Mpa, which is the lower magnitude stress distributed in bars and higher value in a steel tube element.

The magnitude of displacement distribution in member is showed in Figure 5.6 (b). This figure has two parts. The first part indicates the magnitude of Displacement distribution (U-magnitude) of the composite column in deformed state plot only. The second part indicates the magnitude of the Displacement distribution (U-magnitude) of the composite column in the deformed state from the undeformed state plot. From Figure 5.6 (b), it is observed that the member is more displaced around section close to points of load application or at the top edge of the column. Here is the maximum magnitude of displacement under 50% of the axial load has occurred at the top which is 1.756mm. Member displacement gradually

decreases from top to bottom and negligible at the bottom end of the column which is fully fixed support.

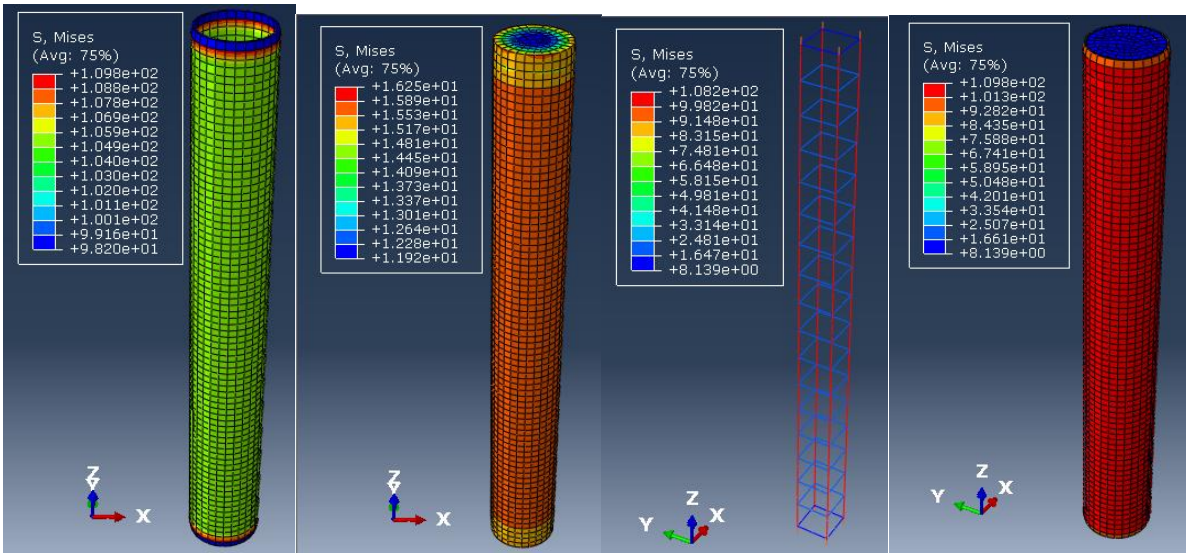

(a)

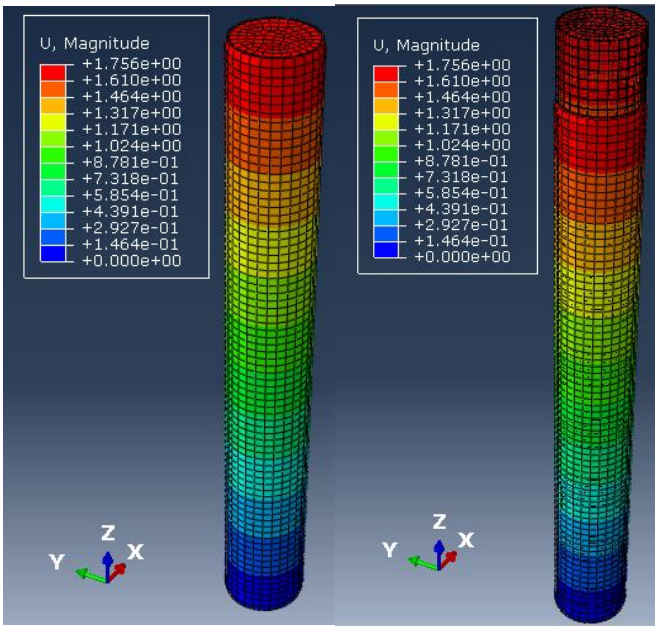

(b)

Figure 5.6: Stress and Magnitude of Displacement distribution in CCC with reinforcement at 50% of P

c. Circular composite column subjected to Axial Load at 60% [3754.26KN] of load-bearing capacity, P[6257.1KN].

According to the result from Abaqus software as in Figure 5.7 (a) shows Von Mises stress distribution, which is used to predict yielding of materials under loading from the results of axial load. This figure showed in four patterns of elements of composite column results of stress distribution from Abaqus software. The First part is indicating the stress distribution

in a circular steel tube. As it can be seen from diagram stress distributed by a colorful rainbow with different values between 117.8MPa and 131.7MPa. at the edge support, it shows less stress and maximal stress around edge support, while the entire elements are distributed as a medium in green colors. The second part of Figure 5.7 (a) indicating the stress distribution in the concrete core element. As can be seen from this figure, stress distributed by a colorful rainbow with different values between 14.31MPa and 19.3MPa. at the edge support, it shows less stress, while the entire elements are distributed as a moderate medium. The third part of Figure 5.7 (a), Shows longitudinal and stirrup bars embedded in concrete fill core stress distribution varies widely between 9.767Mpa and 129.8MPa rather than concrete and steel tube elements.

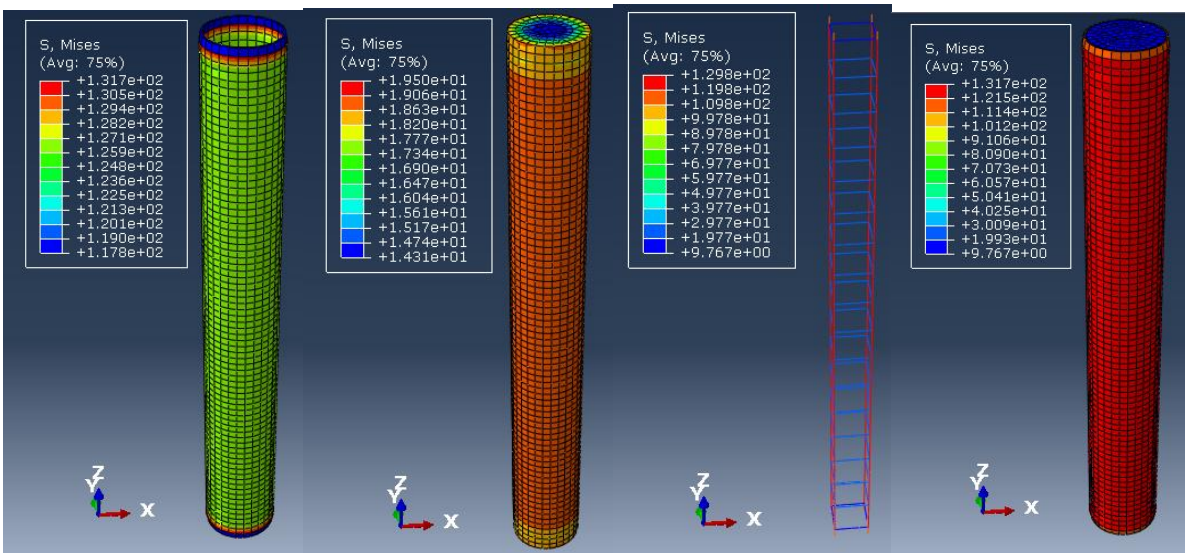

(a)

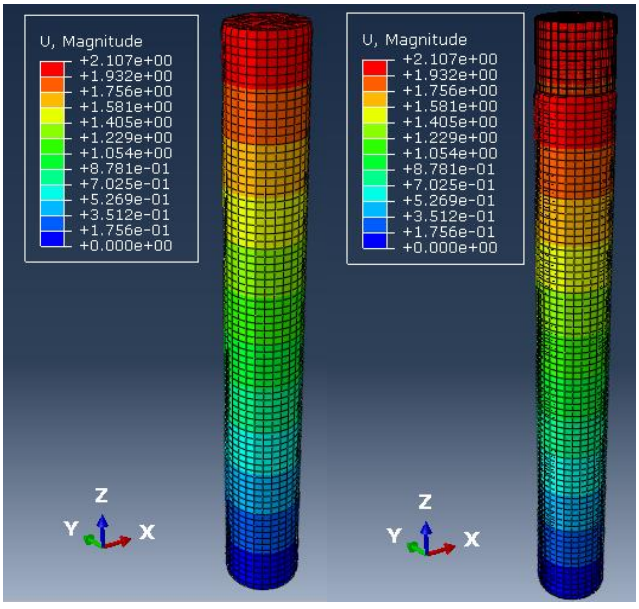

(b)

Figure 5.7: Stress and Magnitude of Displacement distribution in CCC with reinforcement at 60% of P.

The fourth part indicates, all parts of the composite column when sticking together. In this case from this result, it clearly understood the Mises stress magnitude is between 9.767Mpa and 131.7Mpa, which is the lower magnitude stress distributed in bars and higher value in a steel tube element.

The magnitude of displacement distribution in member is showed in Figure 5.7 (b). This figure has two parts. The first part indicates the magnitude of Displacement distribution (U-magnitude) of the composite column in deformed state plot only. The second part indicates the magnitude of the Displacement distribution (U-magnitude) of the composite column in the deformed state from the undeformed state plot. From Figure 5.7 (b), it is observed that the member is more displaced around section close to points of load application or at the top edge of the column. Here is the maximum magnitude of displacement under 60% of the axial load that has occurred at the top which is 2.107mm. Member displacement gradually decreases from top to bottom and negligible at the bottom end of the column which is fully fixed support.

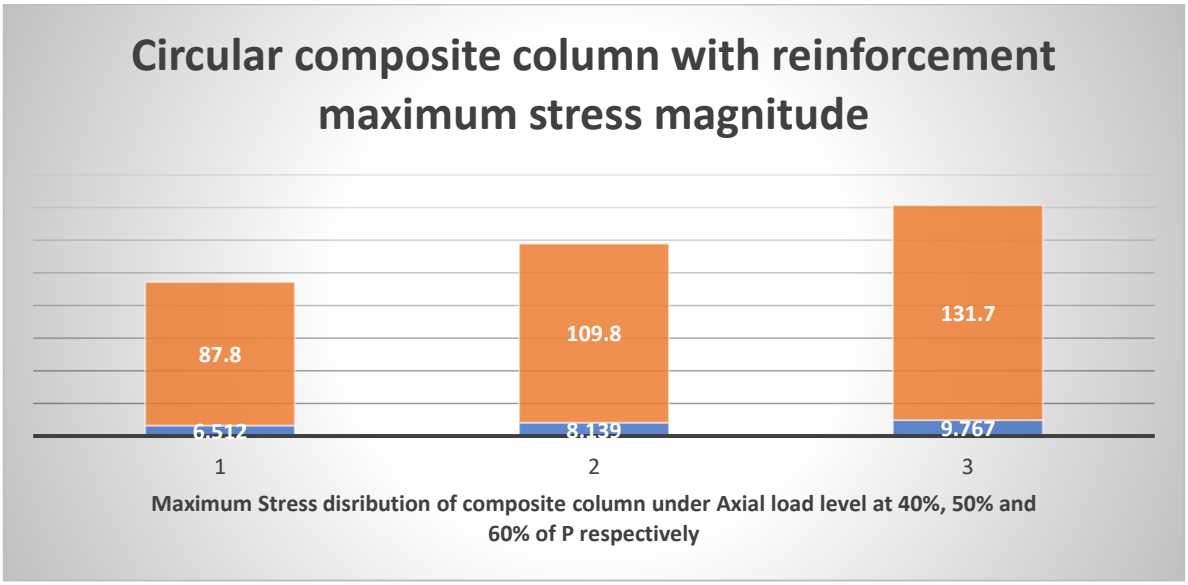

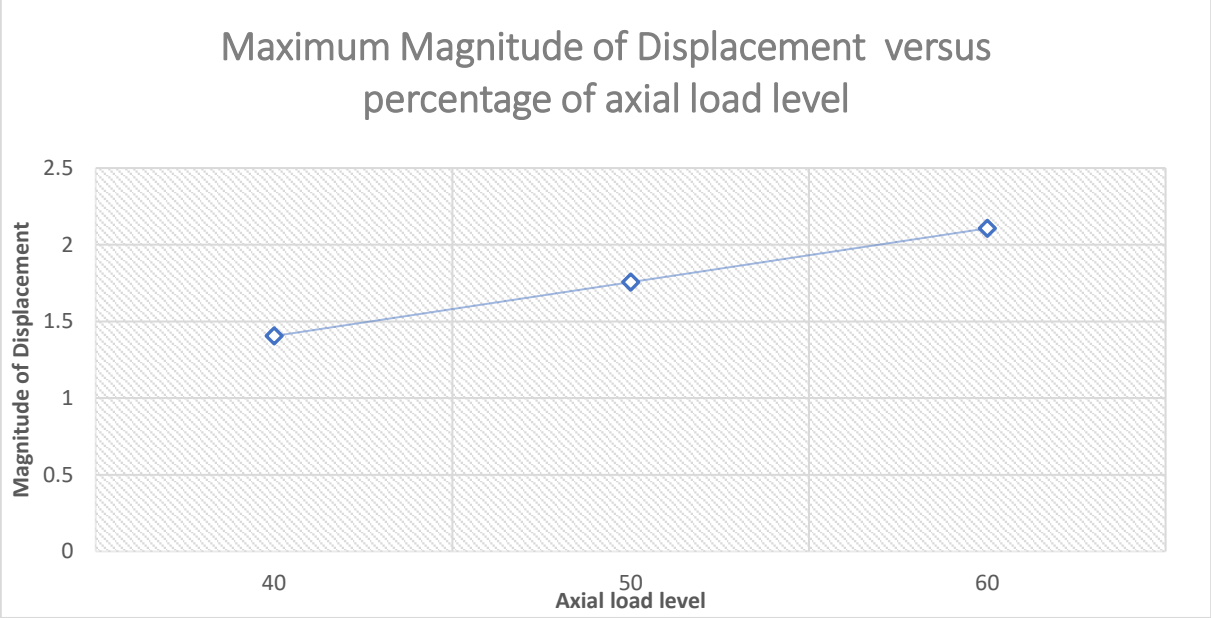

Figure 5.8: Summary of maximum Stress and displacement magnitude under different level of axial load of CCC with reinforcement bars

It was summarized that, When Concentrated load of 40%P, 50%P and 60%P (where P=6275.1KN is axial load capacity of circular composite column) applied on circular composite column, As it discussed before, maximum stress of Composite column section is 87.8, 109.8, and 131.7MPa as axial load of 2502.84KN, 3128.55KN and 3754.26KN respectively and maximum magnitude of displacement also increased 1.405mm, 1.756mm and 2.107mm respectively.. which is summarized in Figure 5.8 above. The stress distribution of concrete is high on the outside of the concrete section where it has contact with steel and it lower at the center of steel core but the stress distribution of in steel is higher than the concrete material.

5.2.3 CCC with embedded steel profile subjected to axial load

a. Circular composite column subjected to Axial Load at 40% [2502.84KN] of load-bearing capacity, P[6257.1KN].

According to the result from Abaqus software as in Figure 5.9 (a) shows Von Mises stress distribution, which is used to predict yielding of materials under loading from the results of axial load. This figure showed in four patterns of elements of composite column results of stress distribution from Abaqus software. The First part is indicating the stress distribution in the circular steel tube. As it can be seen from diagram stress distributed by a colorful rainbow with different values between 68.7MPa and 76.1MPa. at the edge support, it shows less stress and maximal stress around edge support, while the entire elements are distributed as a medium in green colors. The second part of Figure 5.9 (a) indicating the stress distribution in the concrete core element. As can be seen from this figure, stress distributed by a colorful rainbow with different values between 7.6MPa and 11.6MPa. at the edge support, it shows less stress, while the entire elements are distributed as the moderate medium. The third part of Figure 5.9 (a), Shows a steel profile embedded in concrete fill core stress distribution is close to stress distribution in steel tube, which between 54.5Mpa and 73.3MPa. The fourth part indicates, all parts of the composite column when sticking together. In this case from this result, it clearly understood the Mises stress magnitude is between 7.61Mpa and 76.1Mpa, which is the lower magnitude stress distributed in concrete and higher value in a steel tube element.

The magnitude of displacement distribution in members is shown in Figure 5.9 (b). This figure has two parts. The first part indicates the magnitude of Displacement distribution (U-magnitude) of the composite column in deformed state plot only. The second part indicates the magnitude of the Displacement distribution (U-magnitude) of the composite column in the deformed state from the undeformed state plot. From Figure 5.9 (b), it is observed that the member is more displaced around section close to points of load application or at the top edge of the column. Here is the maximum magnitude of displacement under 40% of axial load that has occurred at the top which is 1.218mm.

Member displacement gradually decreases from top to bottom and negligible at the bottom end of the column which is fully fixed support.

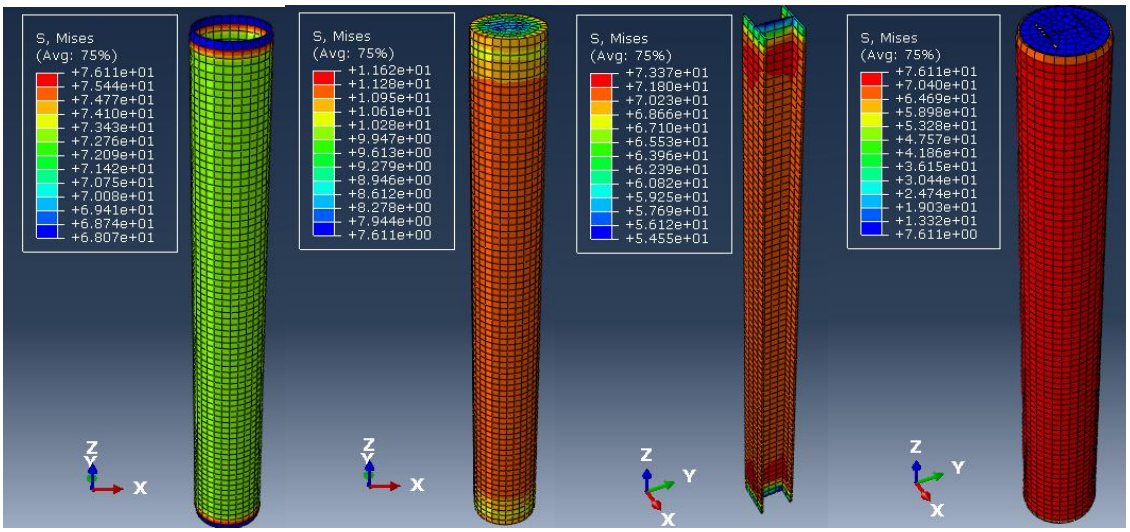

(a)

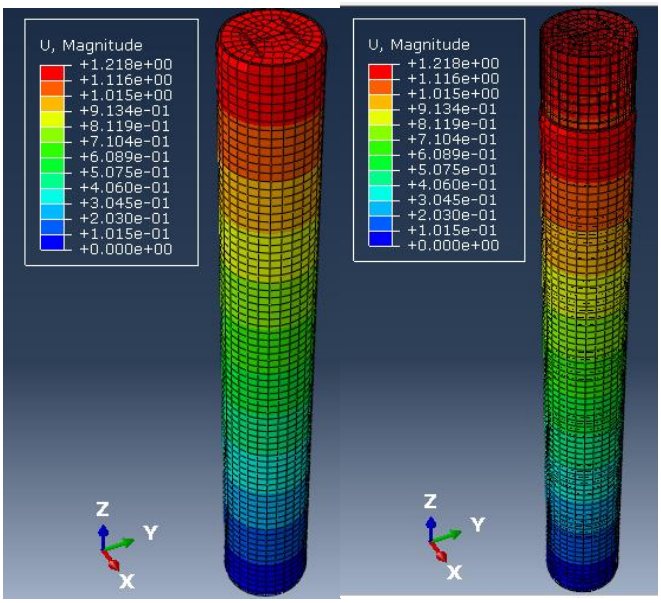

(b)

Figure 5.9: Stress and Magnitude of Displacement distribution in CCC with embedded steel profile at40% of P.

b. Circular composite column subjected to Axial Load at 50% [3128.55KN] of load-bearing capacity, P[6257.1KN].

The stress and magnitude of displacement distributions discussed for figures is the same condition as prescribed figures before. But the magnitudes are different. As can be seen in Figure 5.10, The stress magnitude in the steel tube varies between 85.09MPa and 95.14MPa. Stress distributed in the concrete section between 9.513MPa and 14.52MPa. Steel profile embedded in concrete fill core stress distribution is close to stress distribution in steel tube, which between 68.19Mpa and 91.71MPa. From the result it can be seen, the

Mises stress magnitude is between 9.513Mpa and 95.14Mpa, which is the lower magnitude stress distributed in concrete and higher value in a steel tube element.

The magnitude of displacement distribution from Figure 5.10 (b), it is observed that the member is more displaced around section close to points of load application or at the top edge of the column. Here is the maximum magnitude of displacement under 50% of the axial load that has occurred at the top which is 1.522mm. Member displacement gradually decreases from top to bottom and negligible at the bottom end of the column which is fully fixed support.

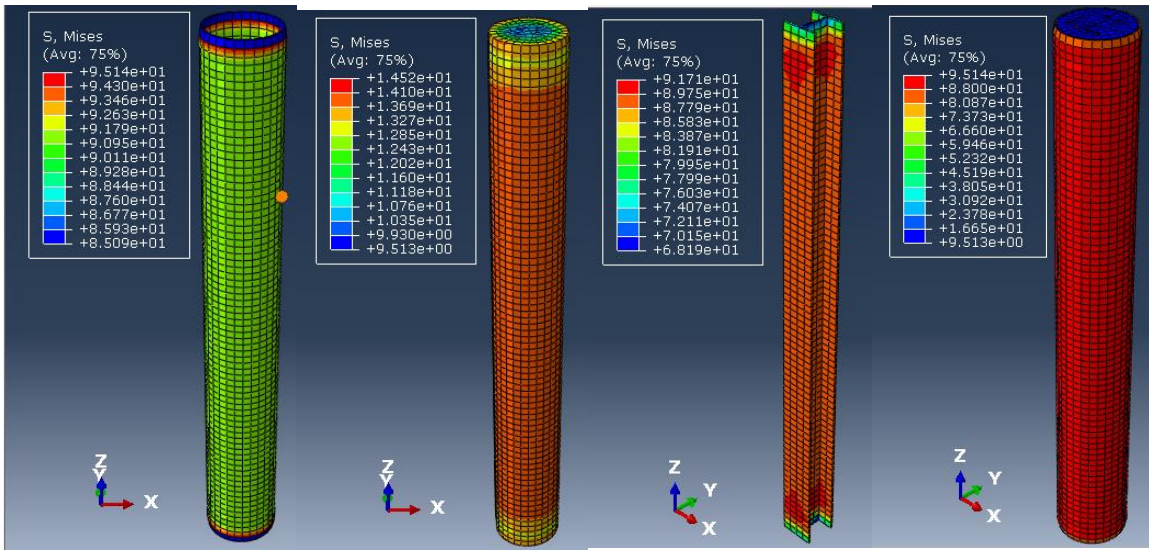

(a)

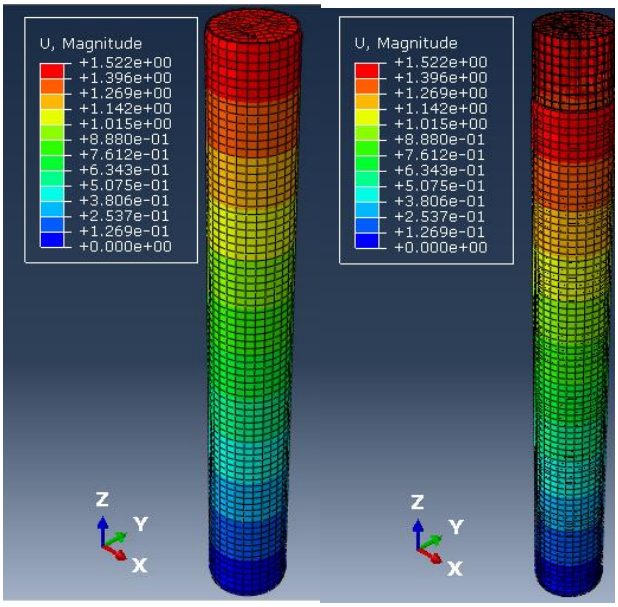

(b)

Figure 5.10: Stress and magnitude of displacement distribution in CCC with embedded steel profile at 50% of P.

c. Circular composite column subjected to Axial Load at 60% [3754.26KN] of load-bearing capacity, P[6257.1KN].

The stress and magnitude of displacement distribution discussed for figures is the same condition as prescribed figures before. But the magnitudes are different. As can be seen in Figure 5.11, The stress magnitude in the steel tube varies between 102.1MPa and 114.2MPa. Stress distributed in the concrete section between 11.42MPa and 17.42MPa. Steel profile embedded in concrete fill core stress distribution is close to stress distribution in steel tube, which between 81.82Mpa and 110.1MPa. From the result it can be seen, the Mises stress magnitude is between 11.42Mpa and 114.2Mpa, which is the lower magnitude stress distributed in concrete and higher value in a steel tube element.

The magnitude of displacement distribution from Figure 5.11 (b), it is observed that the member is more displaced around section close to points of load application or at the top edge of the column. Here is the maximum magnitude of displacement under 60% of the axial load that has occurred at the top which is 1.827mm. Member displacement gradually decreases from top to bottom and negligible at the bottom end of the column which is fully fixed support.

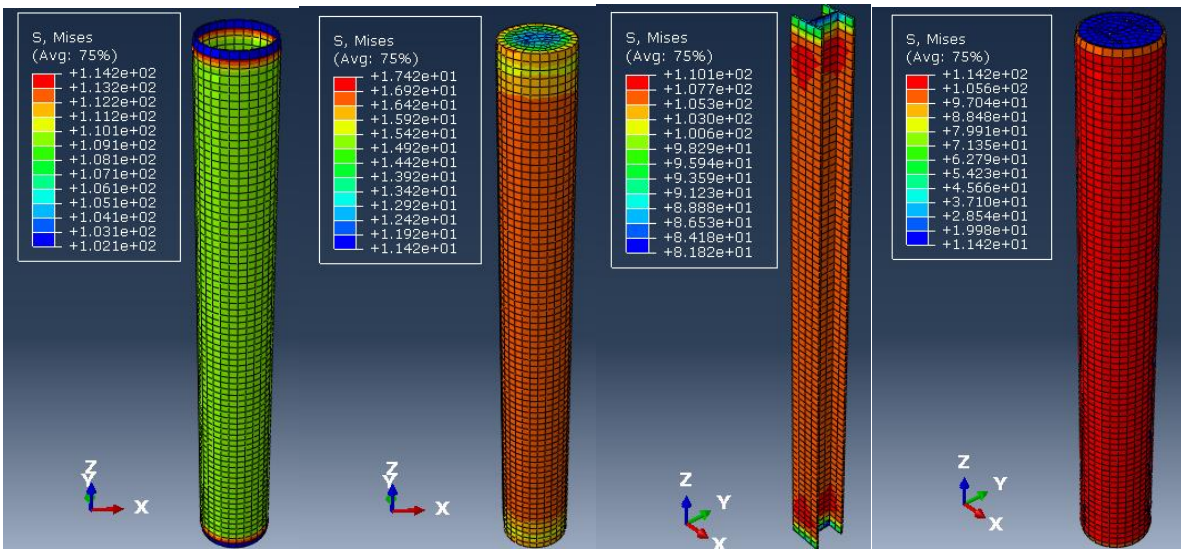

(a)

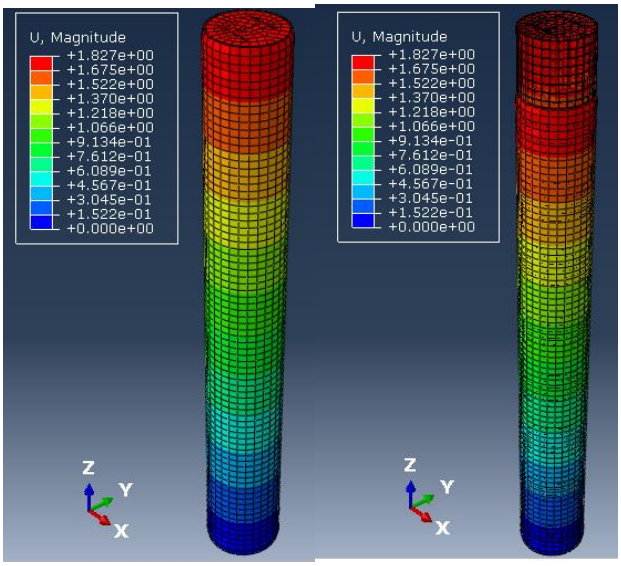

(b)

Figure 5.11: Stress and Magnitude of Displacement distribution in CCC with embedded steel profile at 60% of P.

It was summarized that, When Concentrated load of 40%P, 50%P and 60%P (where P=6275.1KN is axial load capacity of circular composite column) applied on circular composite column, As it discussed before, maximum stress of Composite column section is 76.11, 95.14 and 1114.2MPa as axial load of 2502.84KN, 3128.55KN and 3754.26KN respectively and maximum magnitude of displacement also increased 1.218mm, 1.522mm and 1.827mm respectively, which is summarized in Figure 5.12 below. The stress distribution of concrete is high on the outside of the concrete section where it has contact with steel and it lower at the center of steel core but the stress distribution of in steel is higher than the concrete material.

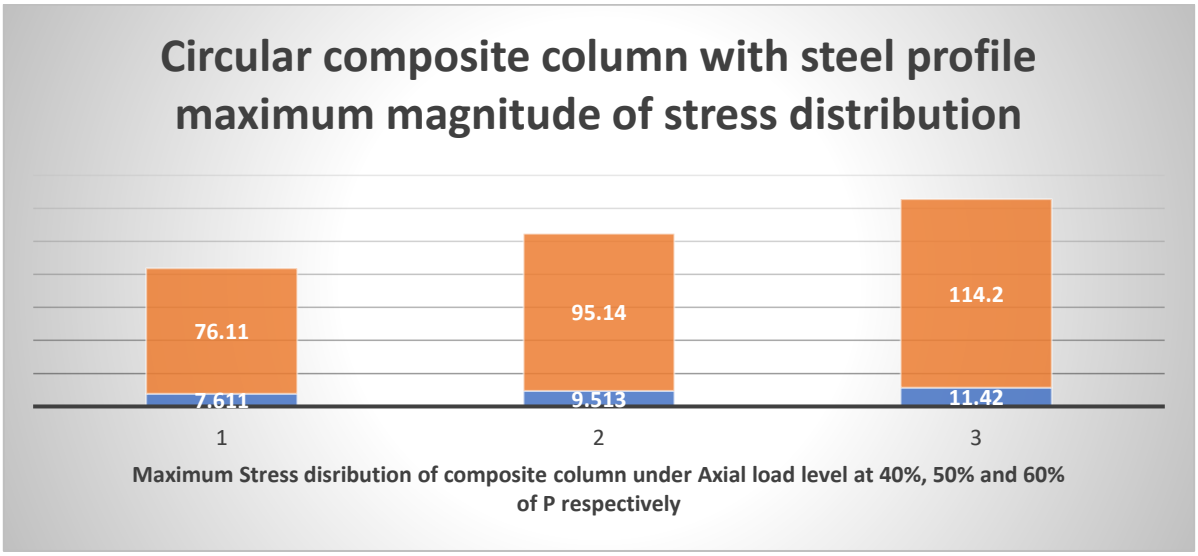

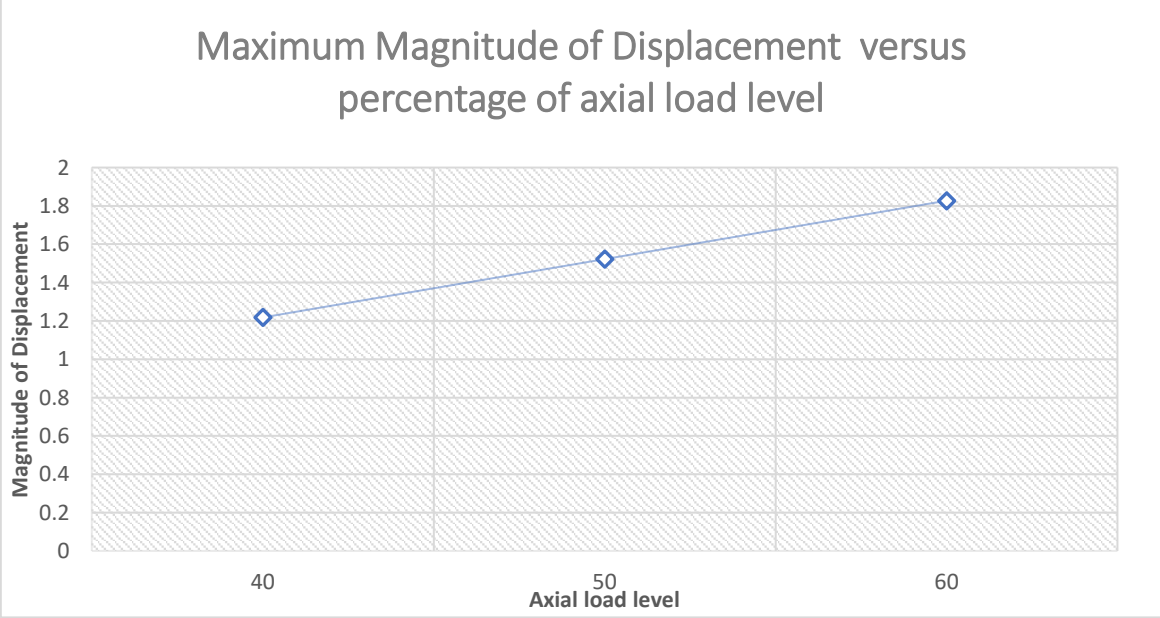

Figure 5.12: Summary of maximum Stress and displacement magnitude under different levels of axial load for CCC with steel profile.

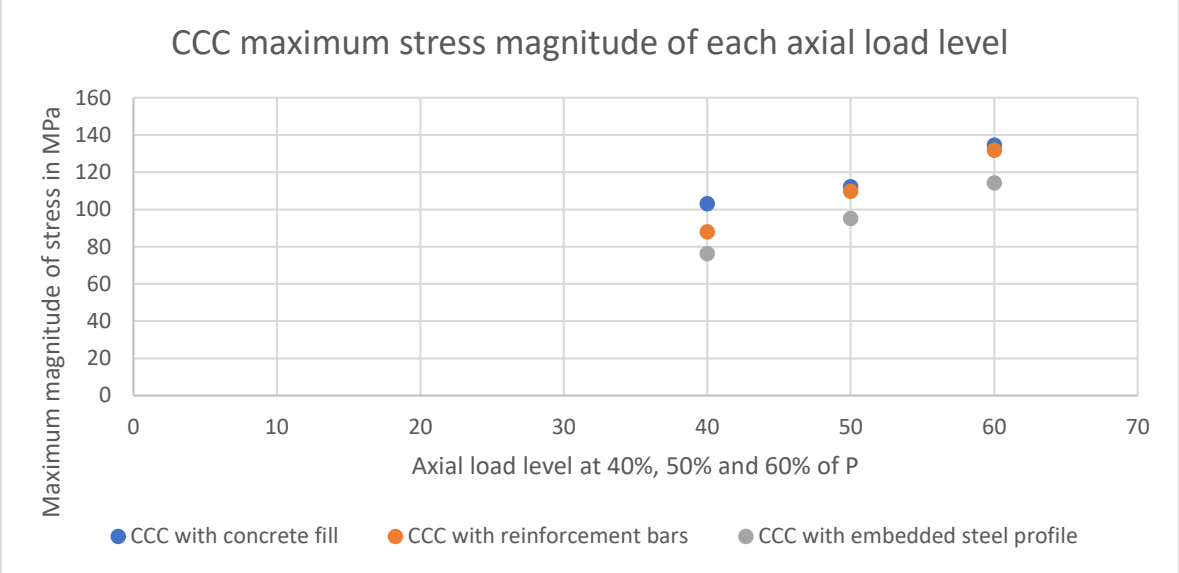

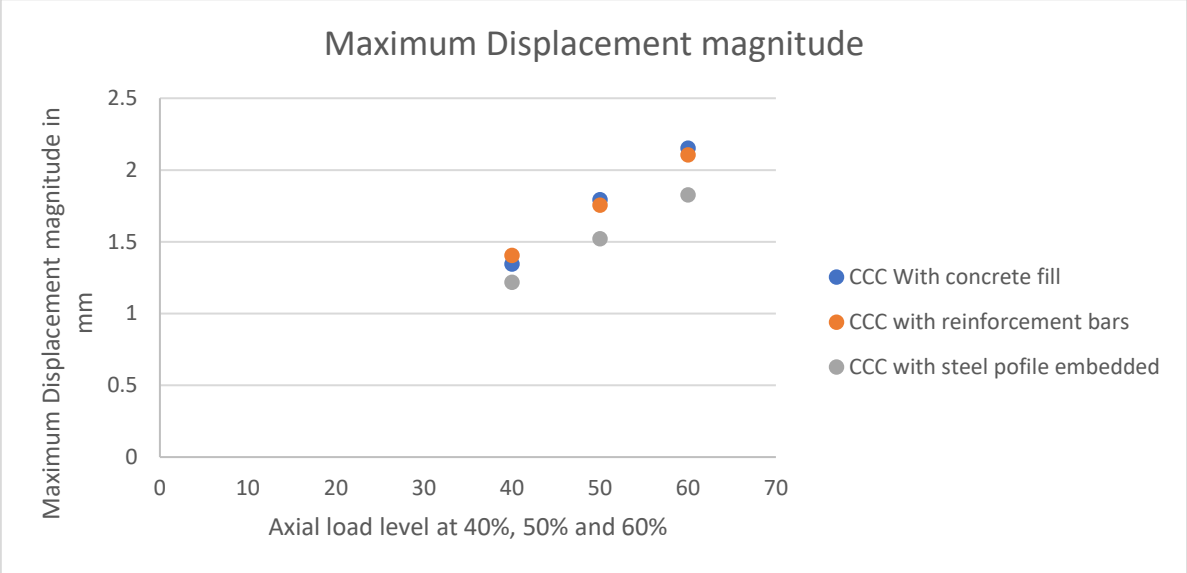

Figure 5.13: The Summary result of the CCC under axial load only

From Figure 5.13, it's observed that the stress distribution magnitudes are less in CCC with steel profile embedded and it shows minimum displacement(U) under axial load only relatively.

5.2.4 Square concrete-filled composite column section

a. Square composite column subjected to Axial Load at 40% [2598.08KN] of load-bearing capacity, P[6495.4KN].

The stress and magnitude of displacement distribution discussed for figures arrangements is the same condition as prescribed for figures before. but the magnitudes are different. As can be seen in Figure 5.14, The stress magnitude in the steel tube varies between 71.72MPa and 89.03MPa. Stress distributed in the concrete section between 9.683MPa and 13.63MPa.

From the result it can be seen, the Mises stress magnitude of composite member part is between 9.683Mpa and 89.03Mpa, which is the lower magnitude stress distributed in concrete and higher value in a steel tube element.

The magnitude of displacement distribution from Figure 5.14 (b), it is observed that the member is more displaced around section close to points of load application or at the top edge of the column. Here is the maximum magnitude of displacement under 40% of axial load that has occurred at the top which is 1.436mm. Member displacement gradually decreases from top to bottom and negligible at the bottom end of the column which is fully fixed support.

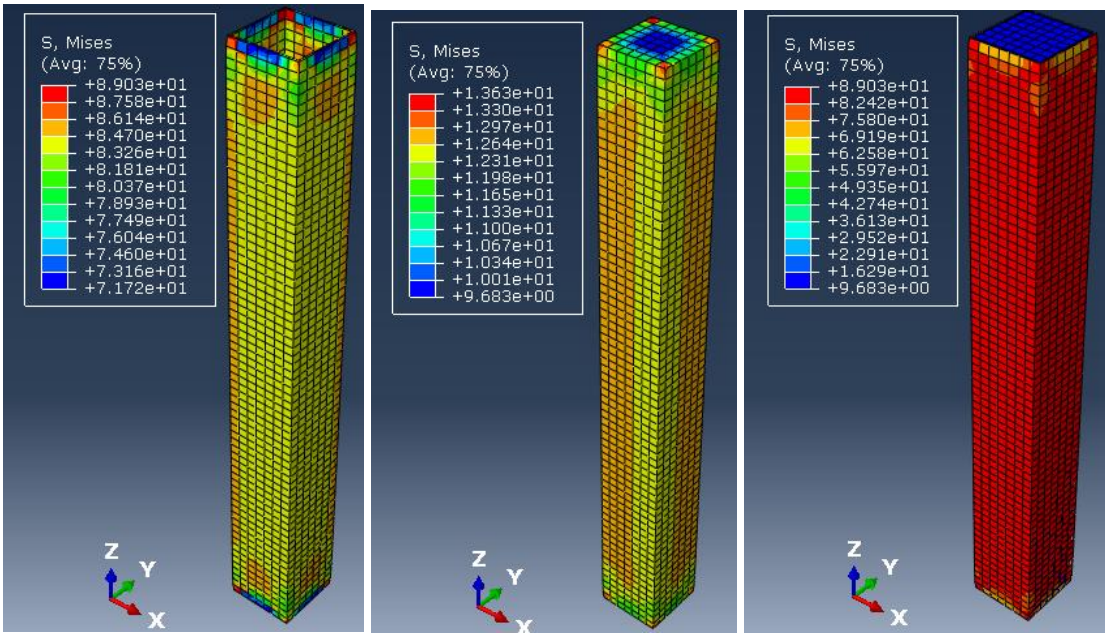

(a)

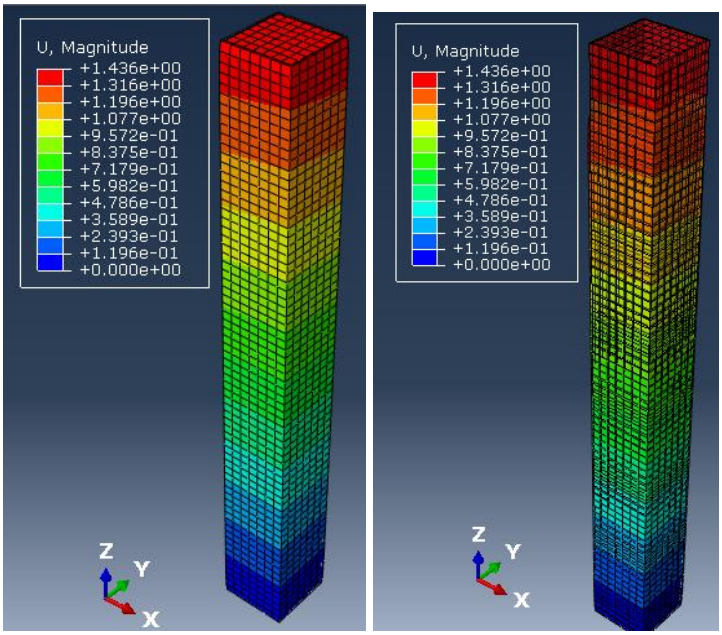

(b)

Figure 5.14: Square composite column with concrete fill at 40% of P.

b. Square composite column subjected to Axial Load at 50% [3247.60KN] of load-bearing capacity, P[6495.4KN].

The stress and magnitude of displacement distribution discussed for figures arrangements is the same condition as prescribed for figures before. but the magnitudes are different. As can be seen in Figure 5.15 (a), The stress magnitude in the steel tube varies between 86.95MPa and 111.3MPa. Stress distributed in the concrete section between 12.1MPa and 17.09MPa. From the result it can be seen, the Mises stress magnitude of composite member part is between 12.1Mpa and 111.3Mpa, which is the lower magnitude stress distributed in concrete and higher value in a steel tube element.

The magnitude of displacement distribution from Figure 5.15 (b), it is observed that the member is more displaced around section close to points of load application or at the top edge of the column. Here is the maximum magnitude of displacement under 50% of the axial load has occurred at the top which is 1.795mm. Member displacement gradually decreases from top to bottom and negligible at the bottom end of the column which is fully fixed support.

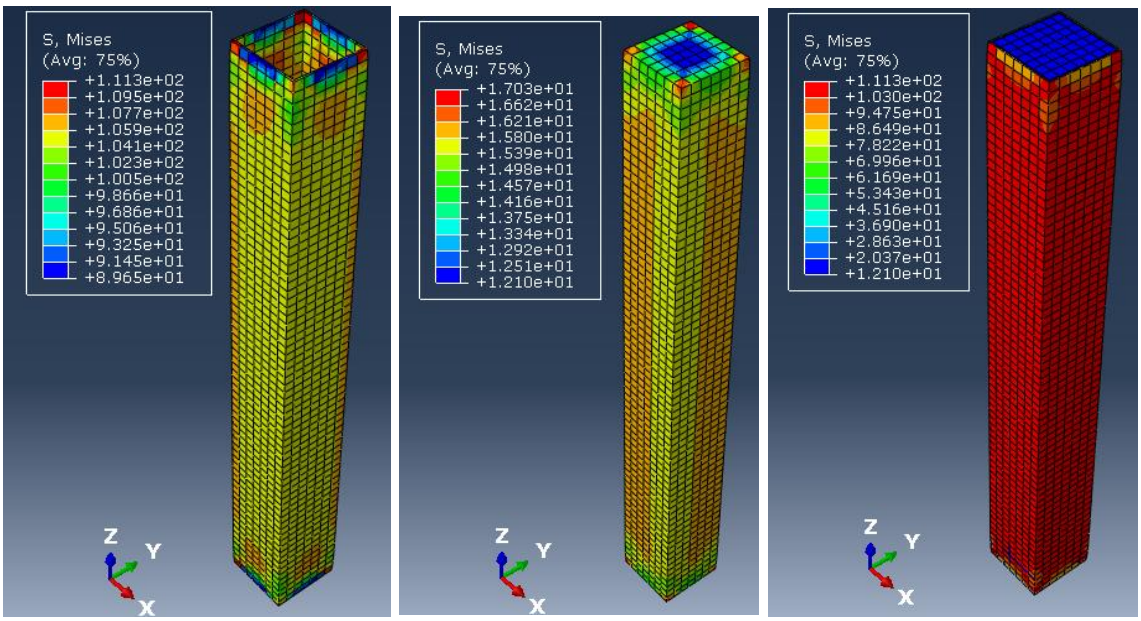

(a)

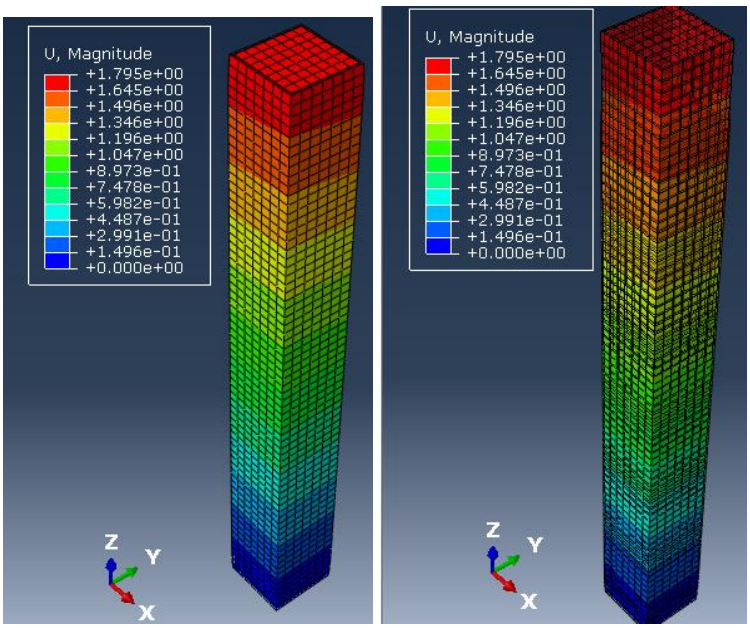

(b)

Figure 5.15: Square composite column with concrete fill at 50% of P

c. Square composite column subjected to Axial Load at 60% [3897.12KN] of load bearing capacity, P[6495.4KN].

The stress and magnitude of displacement distribution discussed for figures arrangements is the same condition as prescribed for figures before. but the magnitudes are different. As can be seen in Figure 5.16 (a), The stress magnitude in the steel tube varies between 107.6MPa and 133.5MPa. Stress distributed in the concrete section between 14.52MPa and 20.44MPa. From the result it can be seen, the Mises stress magnitude of composite member part is between 14.52Mpa and 133.5Mpa, which is the lower magnitude stress distributed in concrete and higher value in a steel tube element.

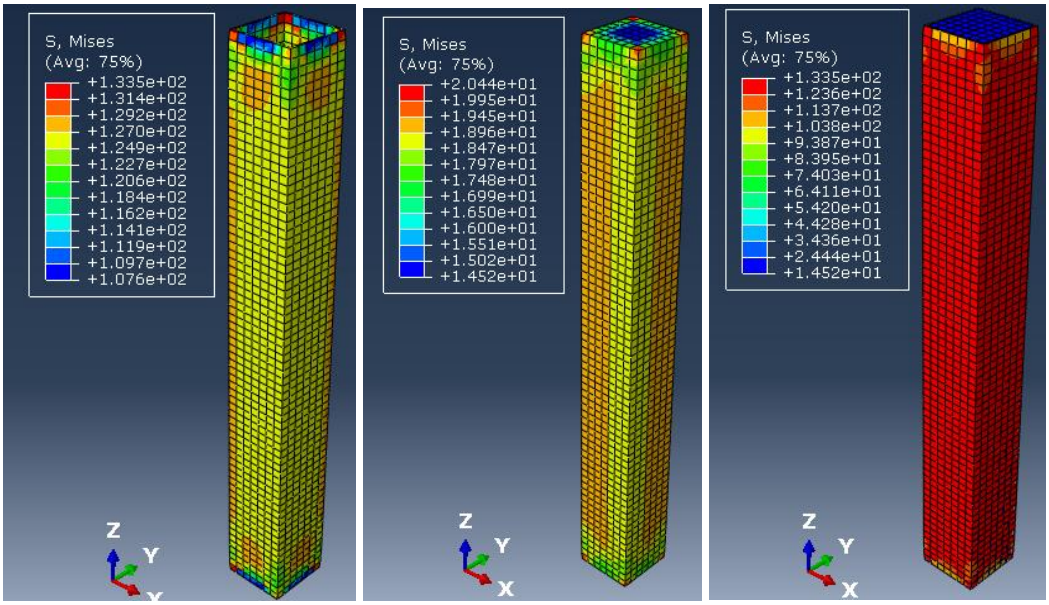

(a)

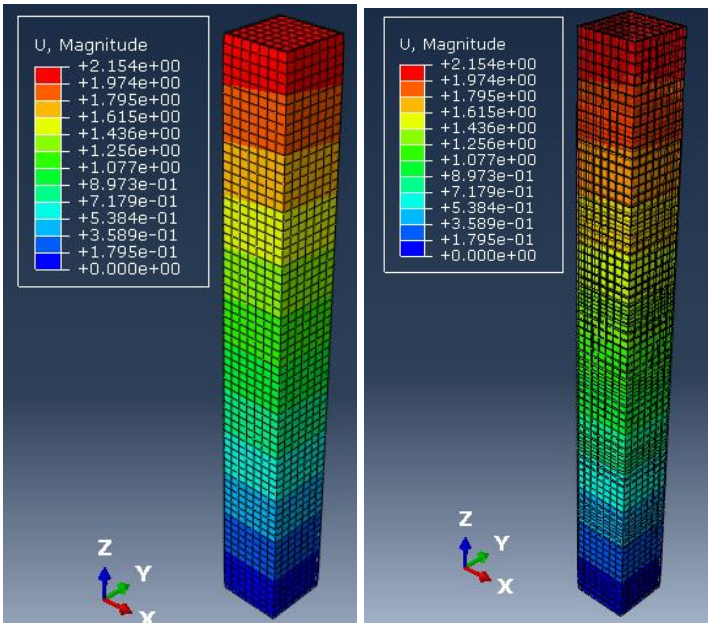

(b)

Figure 5.16: Square composite column with concrete fill at 60% of P

The magnitude of displacement distribution from Figure 5.16 (b), it is observed that the member is more displaced around section close to points of load application or at the top edge of the column. Here is the maximum magnitude of displacement under 60% of the axial load that has occurred at the top which is 2.154mm. Member displacement gradually decreases from top to bottom and negligible at the bottom end of column which is fully fixed support

5.2.5 SCC with reinforcement embedded in the concrete-filled section

a. Square composite column subjected to Axial Load at 40% [2598.08KN] of load-bearing capacity, P[6495.4KN].

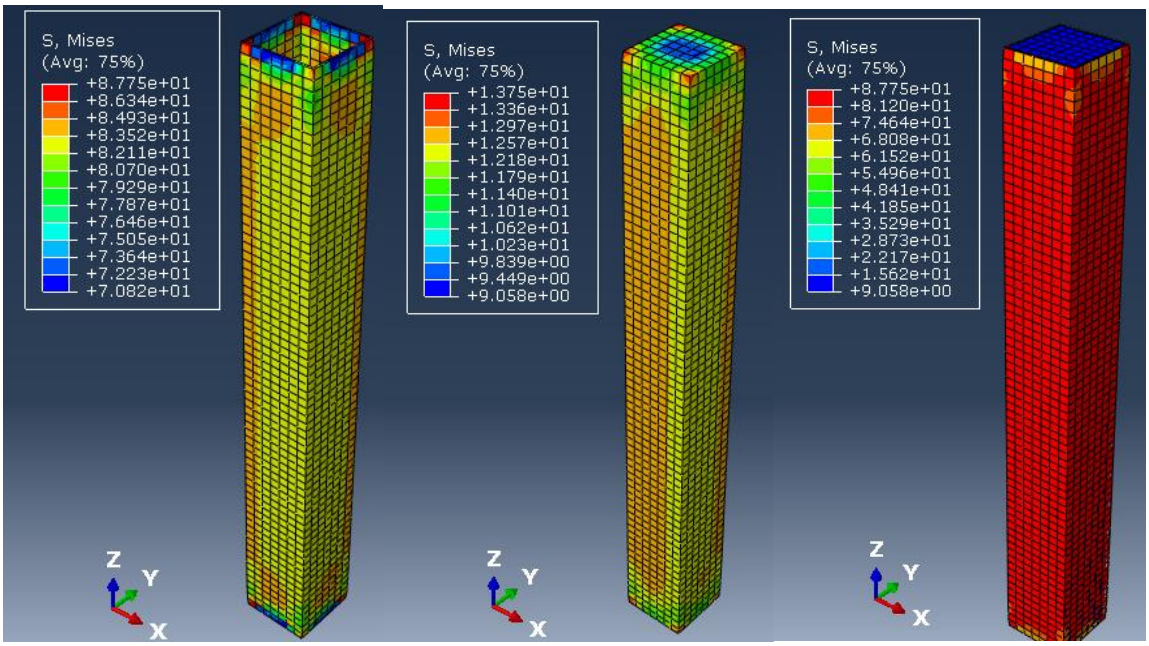

(a)

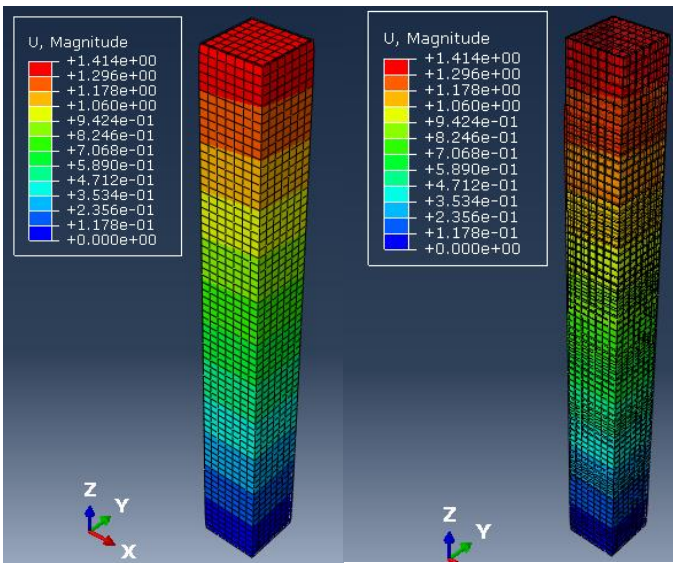

(b)

Figure 5.17: Square composite column with reinforcement bars at 40% of P

The stress and displacement magnitude of distribution discussed for figures arrangements are the same conditions as prescribed for figures before. but the magnitudes and parts are different. The same logical pattern of stress distribution is here, as it is discussed in detail for the circular composite column with reinforcement embedded. The stress distribution in bars is not taken as the picture from software since from previous results, it was observed that stress distribution in bars is close to steel bars stress magnitudes. But less than stress in steel tubes at all. As can be seen in Figure 5.17 (a) above, the stress magnitude in the steel tube varies between 70.82MPa and 87.75MPa. Stress distributed in the concrete section between 9.058MPa and 13.75MPa. From the result it can be seen, the Mises stress magnitude of composite member part is between 9.058Mpa and 87.75Mpa, which is the lower magnitude stress distributed in concrete and higher value in a steel tube element.

The magnitude of displacement distribution from Figure 5.17 (b), it is observed that the member is more displaced around section close to points of load application or at the top edge of the column. Here is the maximum magnitude of displacement under 40% of axial load that has occurred at the top which is 1.414mm. Member displacement gradually decreases from top to bottom and negligible at the bottom end of column which is fully fixed support

b. Square composite column subjected to Axial Load at 50% [3247.60KN] of load-bearing capacity, P[6495.4KN].

The stress and displacement magnitude of distribution discussed for figures arrangements are the same conditions as prescribed for figures before. but the magnitudes and parts are different. The same logical pattern of stress distribution is here, as it is discussed in detail for the circular composite column with reinforcement embedded. The stress distribution in bars is not taken as a picture from software since from previous results, it was observed that stress distribution in bars is close to steel bars stress magnitudes. But less than stress in steel tubes at all. As can be seen in Figure 5.18 (a) below, the stress magnitude in the steel tube varies between 88.52MPa and 109.7MPa. Stress distributed in the concrete section between 11.32MPa and 17.18MPa. From the result it can be seen, the Mises stress magnitude of

composite member part is between 11.32Mpa and 109.7Mpa, which is the lower magnitude stress distributed in concrete and higher value in a steel tube element.

The magnitude of displacement distribution from Figure 5.18 (b), it is observed that the member is more displaced around section close to points of load application or at the top edge of the column. Here is the maximum magnitude of displacement under 50% of the axial load has occurred at the top which is 1.766mm. Member displacement gradually decreases from top to bottom and negligible at the bottom end of column which is fully fixed support

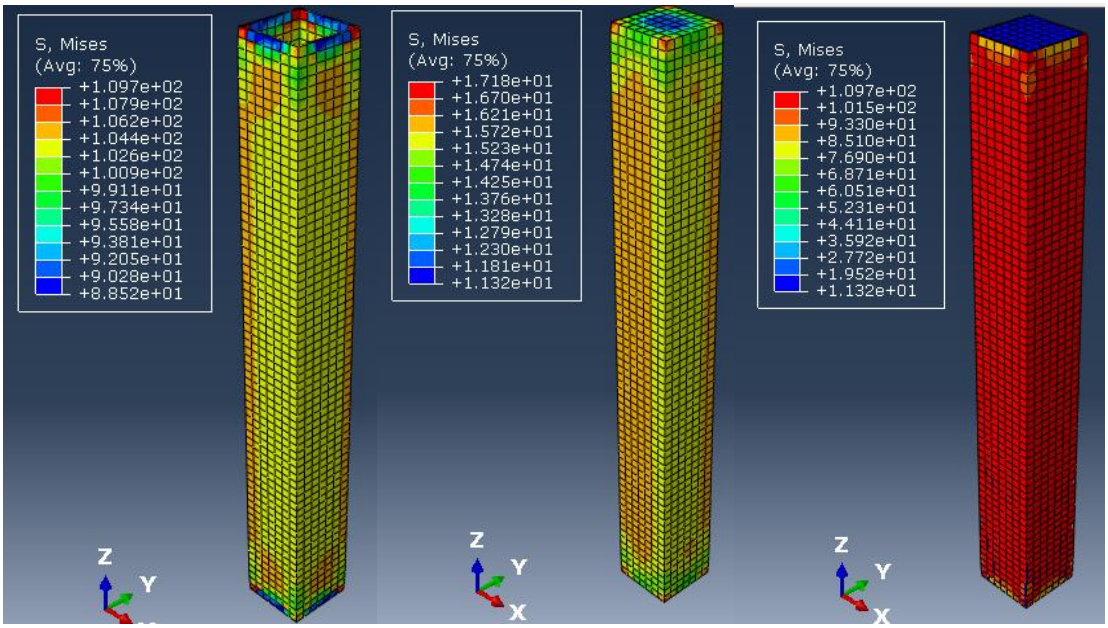

(a)

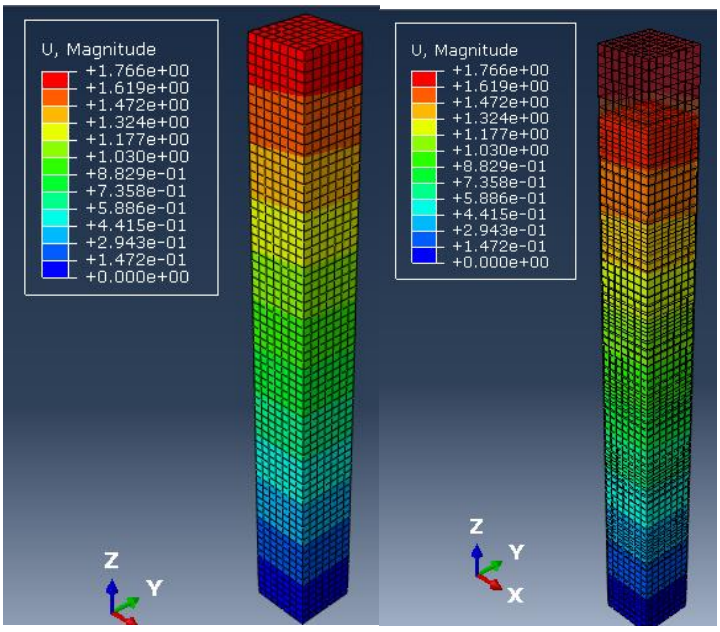

(b)

Figure 5.18: Square composite column with reinforcement bars at 50% of P

c. Square composite column subjected to Axial Load at 60% [3897.12KN] of load-bearing capacity, P[6495.4KN].

The stress and displacement magnitude of distribution discussed for figures arrangements are the same conditions as prescribed for figures before. but the magnitudes and parts are different. The same logical pattern of stress distribution is here, as it is discussed in detail for the circular composite column with reinforcement embedded. The stress distribution in bars is not taken as a picture from software since from previous results, it was observed that stress distribution in bars is close to steel bars stress magnitudes. But less than stress in steel tubes at all. As can be seen in Figure 5.19 (a) below, the stress magnitude in the steel tube varies between 106.2MPa and 131.6MPa. Stress distributed in the concrete section between 13.59MPa and 20.62MPa. From the result it can be seen, the Mises stress magnitude of composite member part is between 13.59Mpa and 131.6Mpa, which is the lower magnitude stress distributed in concrete and higher value in a steel tube element.

The magnitude of displacement distribution from Figure 5.19 (b), it is observed that the member is more displaced around section close to points of load application or at the top edge of the column. Here is the maximum magnitude of displacement under 60% of the axial load that has occurred at the top which is 2.119mm. Member displacement gradually decreases from top to bottom and negligible at the bottom end of column which is fully fixed support

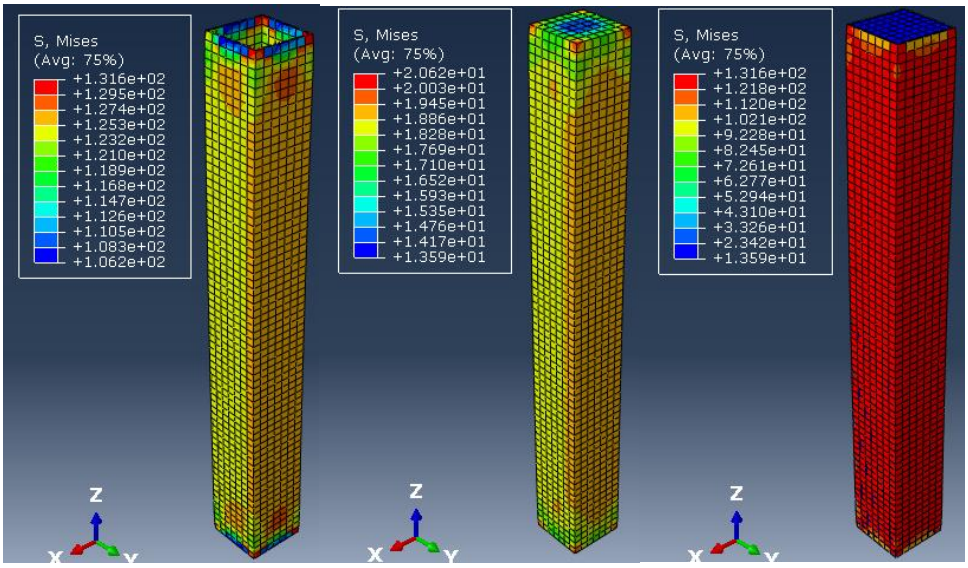

(a)

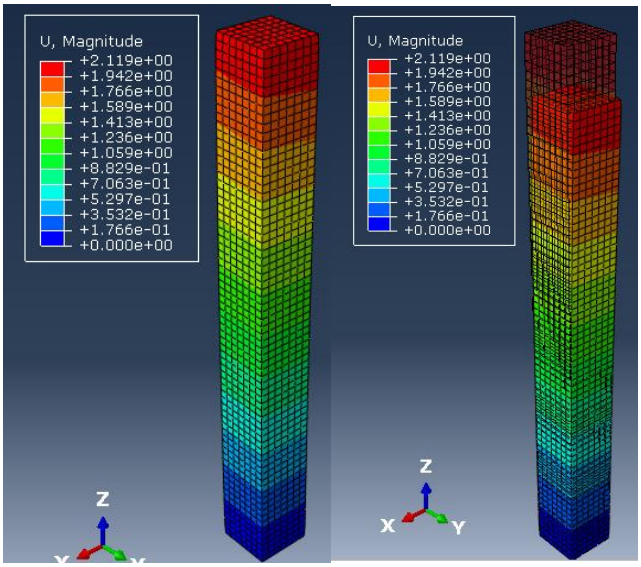

(b)

Figure 5.19: Square composite column with reinforcement bars at 60% of P

5.2.6 SCC with embedded steel profile in concrete-filled section

a. A square composite column with embedded steel profile subjected to Axial Load at 40% [2598.08KN] of load-bearing capacity, P[6495.4KN].

According to the result from Abaqus software as in Figure 5.20 (a) shows Von Mises stress distribution, which is used to predict yielding of materials under loading from the results of axial load. This figure showed in four patterns of elements of composite column results of stress distribution from Abaqus software. The First part is indicating the stress distribution in the circular steel tube. As it can be seen from diagram stress distributed by a colorful rainbow with different values between 61.33MPa and 76MPa. at the edge support, it shows less stress and maximal stress around edge support, while the entire elements are distributed as the medium in green colors. The second part of Figure 5.20 (a) indicating the stress distribution in the concrete core element. As can be seen from this figure, stress distributed by a colorful rainbow with different values between 7.884MPa and 11.9MPa. at the edge support, it shows less stress, while the entire elements are distributed as a moderate medium. The third part of Figure 5.20 (a), Shows a steel profile embedded in concrete fill core stress distribution is close to stress distribution in steel tube, which between 51.4Mpa and 71.6MPa. The fourth part indicates, all parts of the composite column when sticking together. In this case from this result, it clearly understood the Mises stress magnitude of the composite part is between 7.844Mpa and 76Mpa, which is the lower magnitude stress distributed in concrete and higher value in a steel tube element.

The magnitude of displacement distribution in members is shown in Figure 5.20 (b). This figure has two parts. The first part indicates the magnitude of Displacement distribution (U-magnitude) of the composite column in deformed state plot only. The second part indicates the magnitude of the Displacement distribution (U-magnitude) of the composite column in

the deformed state from the undeformed state plot. From Figure 5.20 (b), it is observed that the member is more displaced around section close to points of load application or at the top edge of the column. Here is the maximum magnitude of displacement under 40% of axial load that has occurred at the top which is 1.224mm. Member displacement gradually decreases from top to bottom and negligible at the bottom end of the column which is fully fixed support.

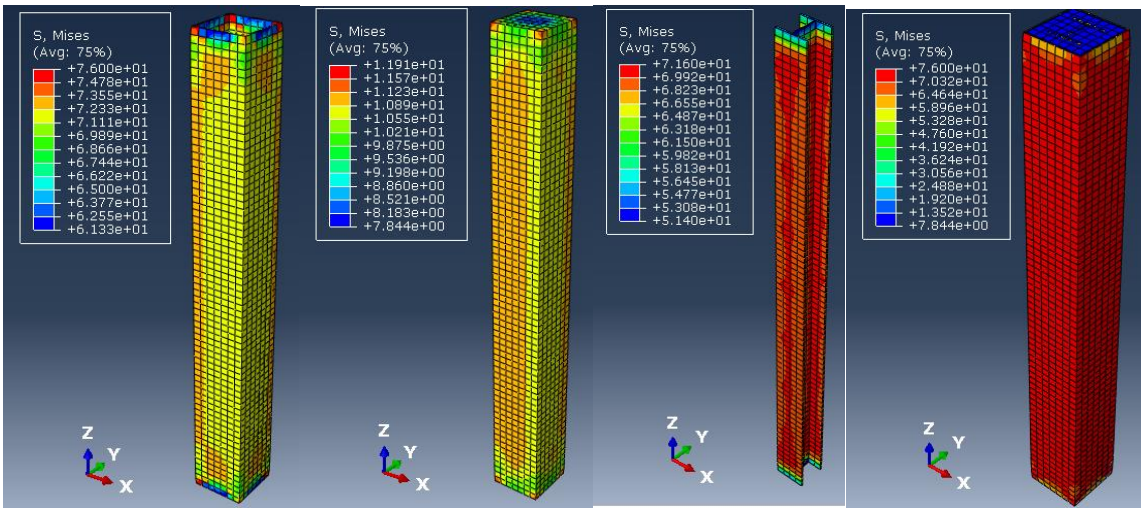

(a)

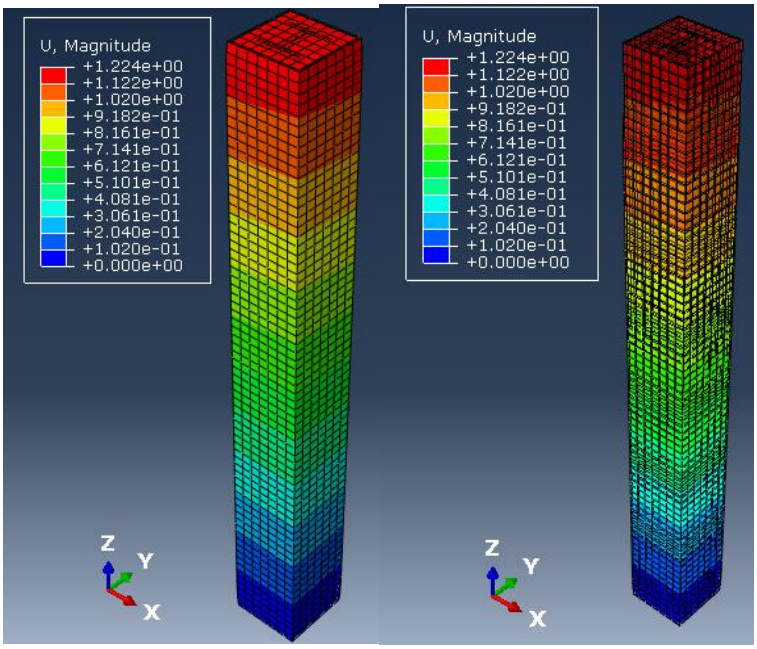

(b)

Figure 5.20: Square composite column with embedded steel profile at 40% of P

b. Square composite column subjected to Axial Load at 50% [3247.60KN] of load-bearing capacity, P[6495.4KN].

The stress and displacement magnitude of distribution discussed for figures arrangements are the same conditions as prescribed for figures above. but the magnitudes are different. The same logical pattern of stress distribution is here, as it is discussed in detail for the

circular composite column with reinforcement embedded. As can be seen in Figure 5.21 (a) below, the stress magnitude in the steel tube varies between 76.66MPa and 95MPa. Stress distributed in the concrete section between 9.805MPa and 14MPa. The stress magnitude in the steel profile varies between 64.25MPa and 89.5MPa. From the result it can be seen, the Mises stress magnitude of composite member part is between 9.805Mpa and 95Mpa, which is the lower magnitude stress distributed in concrete and higher value in a steel tube element.

The magnitude of displacement distribution from Figure 5.21 (b), it is observed that the member is more displaced around section close to points of load application or at the top edge of the column. Here is the maximum magnitude of displacement under 50% of the axial load has occurred at the top which is 1.53mm. Member displacement gradually decreases from top to bottom and negligible at the bottom end of column which is fully fixed support

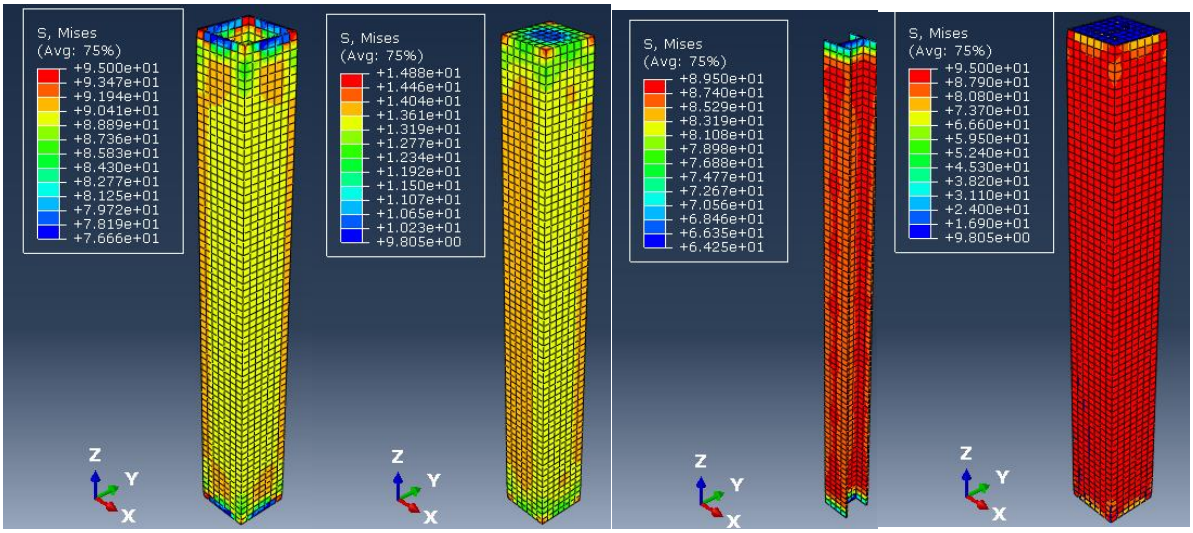

(a)

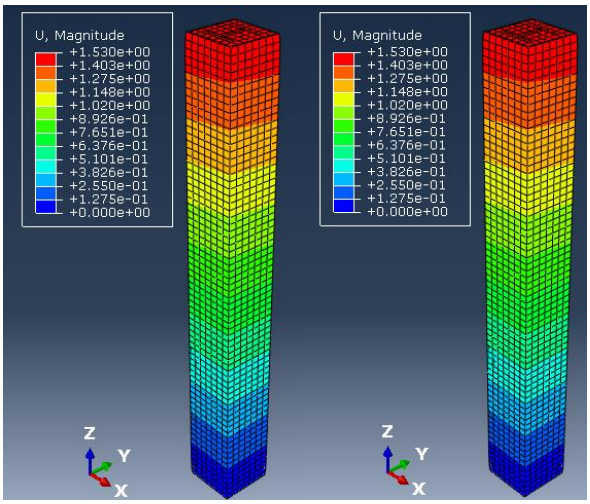

(b)

Figure 5.21: Square composite column with embedded steel profile at 50% of P

c. Square composite column subjected to Axial Load at 50% [3897.12KN] of load-bearing capacity, P[6495.4KN].

The stress and displacement magnitude of distribution discussed for figures arrangements are the same conditions as prescribed for figures above. but the magnitudes are different. The same logical pattern of stress distribution is here, as it is discussed in detail for the circular composite column with reinforcement embedded. As can be seen in Figure 5.22 (a) below, the stress magnitude in the steel tube varies between 91.99MPa and 114MPa. Stress distributed in the concrete section between 11.77MPa and 17.88MPa. The stress magnitude in steel profile varies between 77.1MPa and 107.4MPa. From the result it can be seen, the Mises stress magnitude of composite member part is between 11.77Mpa and 114Mpa, which is the lower magnitude stress distributed in concrete and higher value in a steel tube element.

The magnitude of displacement distribution from Figure 5.22 (b), it is observed that the member is more displaced around section close to points of load application or at the top edge of the column. Here is the maximum magnitude of displacement under 60% of the axial load that has occurred at the top which is 1.836mm. Member displacement gradually decreases from top to bottom and negligible at the bottom end of column which is fully fixed support

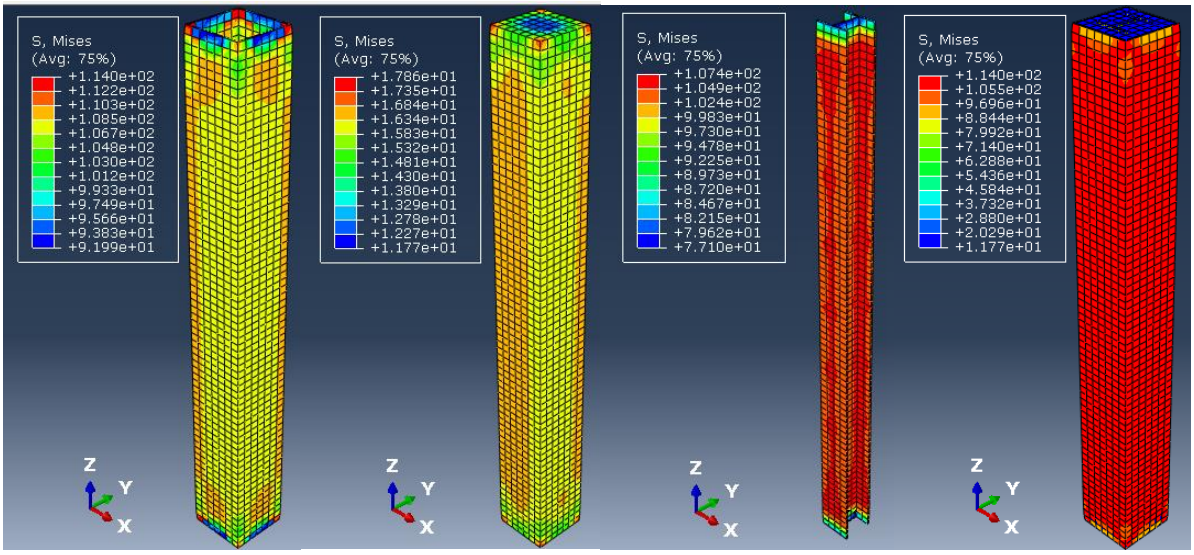

(a)

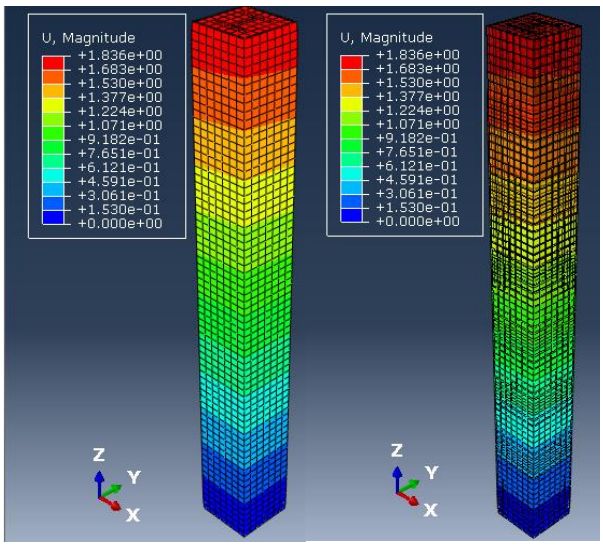

(b)

Figure 5.22: Square composite column with embedded steel profile at 60% of P

From Figure 5.23 below, it's observed that the stress distribution magnitudes are less in SCC with steel profile embedded and it shows minimum displacement(U) under axial load rather than a square composite column with concrete fill and reinforcement bars too.

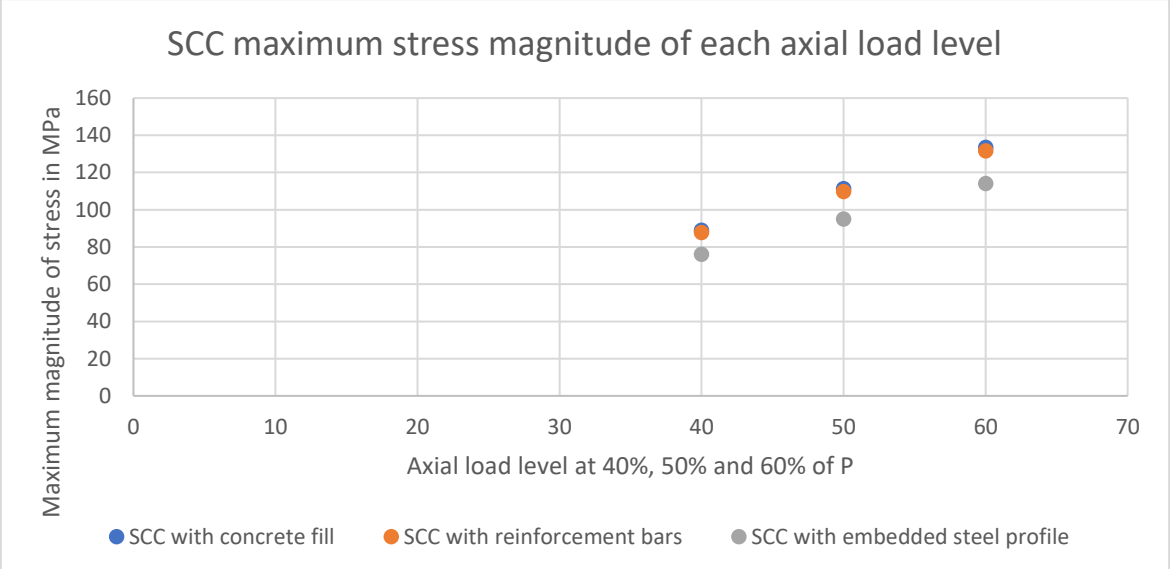

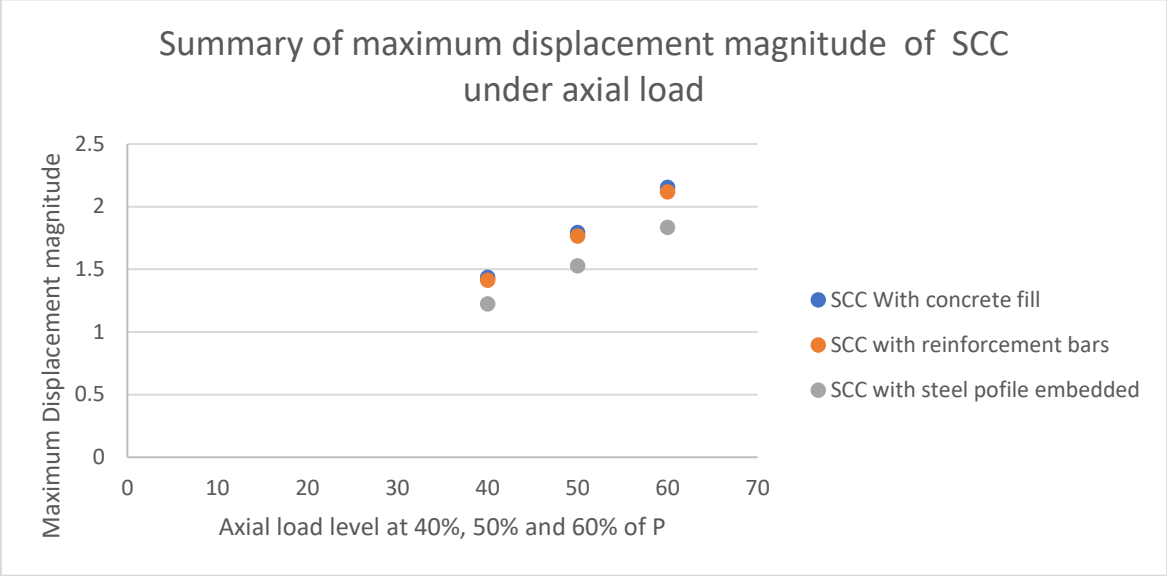

Figure 5.23: Summary result of the square composite column (SCC) under axial load only

5.3 Effect of combined action of Axial and Torsion loads

The effect of the combined action of axial and torsion load on the composite column is analyzed based on the behavior of column analysis under axial load and adding torsion moment to the respective axial load. The circular and square section of the composite column with the circular or square section of the steel tube is analyzed and the effect of torsion on the column is studied by using Abaqus software. The effect of the combined action of axial load and Torsion is identified in terms of evaluating the rotation, compression, and distribution of stress. Based on this the following results obtained and discussed in detail.

5.3.1 CCC with concrete-filled which subjected to both axial and torsional loads

a. Circular composite column subjected to Axial load at 40% [2502.84KN] of load-bearing capacity, P[6257.1KN] and 60KNm constant torsional Load

When columns subjected to axial load(compression effect) and torsional load, displacement under both axial and torsional loads with twisting deformation will have occurred. In Figure below shows Von Mises stress distribution, which is used to predict yielding of materials under loading from the results of the axial and torsional load. Figure 5.24 (a) showed in three patterns of elements of composite column results of stress distribution from Abaqus software. The First part is indicating the stress distribution in the circular steel tube. As can be seen from the diagram, stress distributed by a colorful rainbow with different values between 84.24MPa and 93.33MPa. at the edge support, it shows less stress and maximal stress around edge support, while the entire elements are distributed as a medium in green colors. The second part of Figure 5.24 (a) indicating the stress distribution in the concrete core element. As can be seen from this figure, stress distributed by a colorful rainbow with different values between 9.752MPa and 13.58MPa. at the edge support, it shows less stress, while the entire elements are distributed as a moderate medium. The third part shows the stress distribution of all parts of the composite column when stick together. In this case from

this result, it clearly understood the Mises stress magnitude is between 9.752Mpa and 93.33Mpa, which is the lower magnitude stress distributed in concrete and higher value in a steel tube element. From this figure, it concluded that stress distribute in concrete is less by 85.45 % than stress distributed in steel tube.

The magnitude of displacement distribution in members is shown in Figure 5.24 (b). This figure has two parts. The first part indicates the magnitude of Displacement distribution (U-magnitude) of the composite column is deformed and twisted state plot only. The second part indicates the magnitude of Displacement distribution (U-magnitude) of the composite column is deformed and twisted state from undeformed state plot. additionally, it was observed that the member is more displaced around section close to points of load application or at the top edge of the column. Here is the maximum magnitude of displacement under 40% of axial load that has occurred at the top which is 1.582mm. Member displacement gradually decreases from top to bottom and negligible at the bottom end of the column which is fully fixed support.

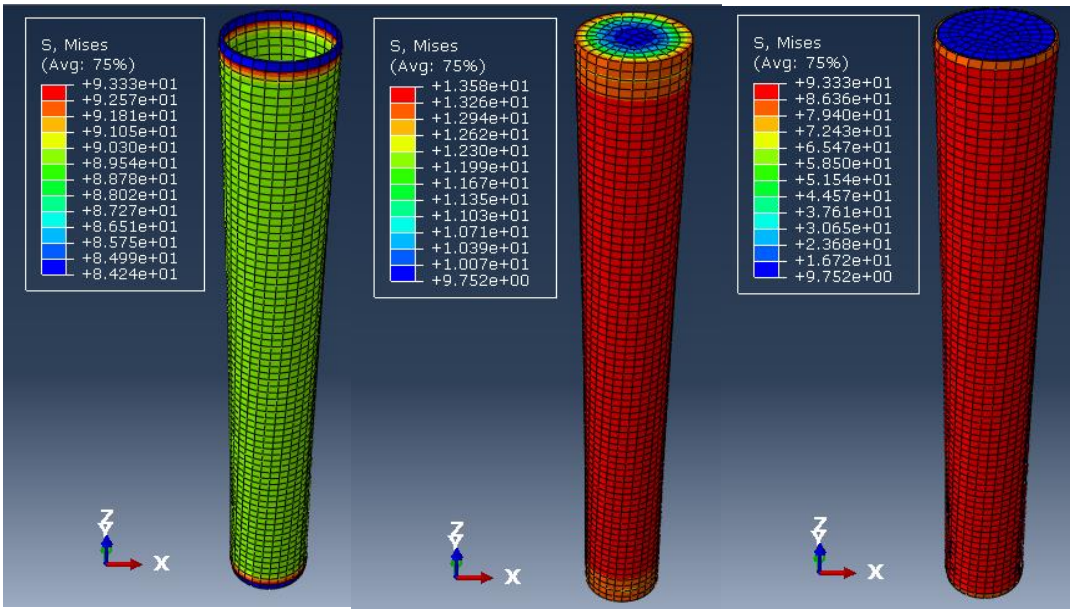

(a)

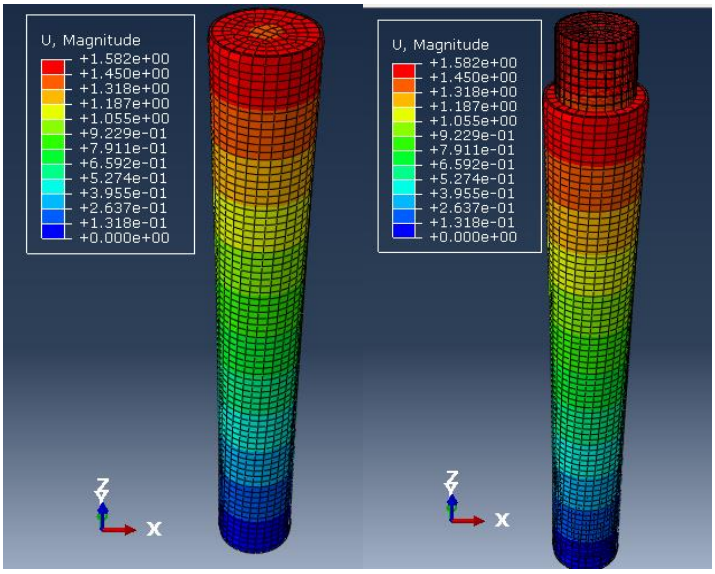

(b)

Figure 5.24: CCC with concrete fill subjected to axial load at 40% of P and torsional load

b. Circular composite column subjected to Axial load at 50% [3128.55KN] of load-bearing capacity, P[6257.1KN] and 60KNm constant torsional Load

When columns subjected to axial load(compression effect) and torsional load, displacement under both axial and torsional loads with twisting deformation will have occurred. In Figure below shows Von Mises stress distribution, which is used to predict yielding of materials under loading from the results of the axial and torsional load. Figure 5.25 (a) showed in three patterns of elements of composite column results of stress distribution from Abaqus software. The First part is indicating the stress distribution in the circular steel tube. As can be seen from the diagram, stress distributed by a colorful rainbow with different values between 103.5MPa and 115MPa. at the edge support, it shows less stress and maximal stress around edge support, while the entire elements are distributed as a medium in green colors. The second part of Figure 5.25 (a) indicating the stress distribution in the concrete core element. As can be seen from this figure, stress distributed by a colorful rainbow with different values between 12.5MPa and 16.82MPa. at the edge support, it shows less stress, while the entire elements are distributed as a moderate medium. The third part shows the stress distribution of all parts of the composite column when stick together. In this case from this result, it clearly understood the Mises stress magnitude is between 12.5Mpa and 115Mpa, which is the lower magnitude stress distributed in concrete and higher value in a steel tube element. From this figure, it concluded that stress distribute in concrete is less by 85.37 % than stress distributed in steel tube.

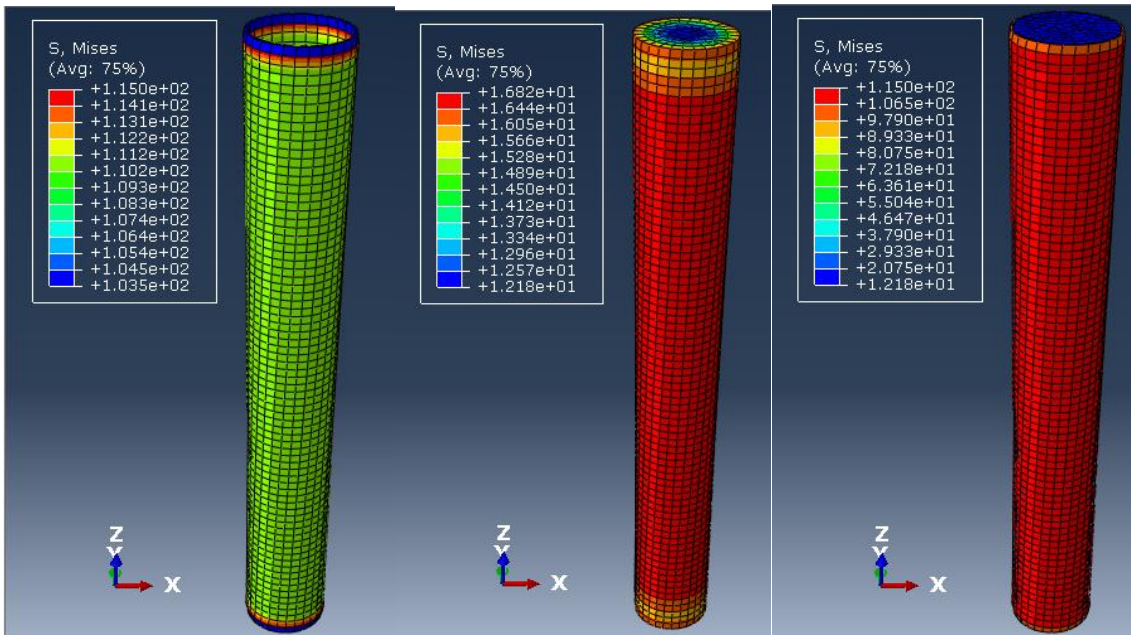

(a)

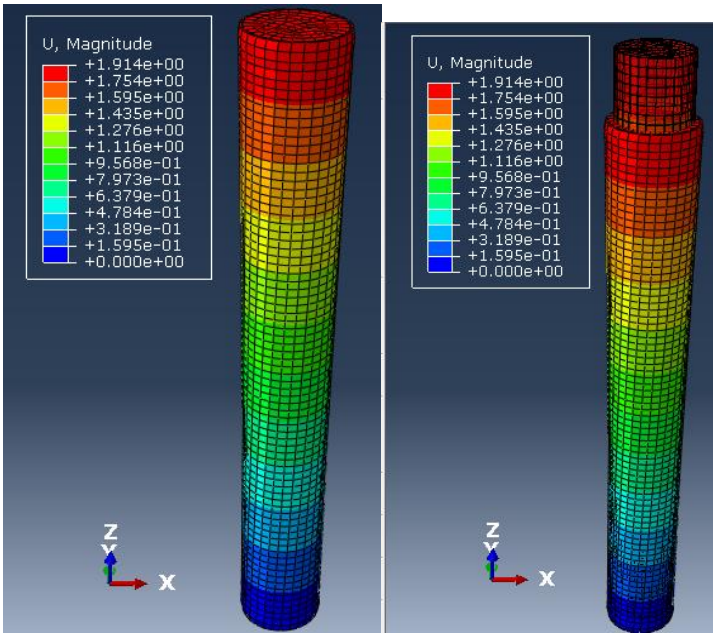

(b)

Figure 5.25: CCC with concrete fill subjected to axial load at 50% of P and torsional load

The magnitude of displacement distribution in member is showed in Figure 5.25 (b). This figure has two parts. The first part indicates the magnitude of Displacement distribution (U-magnitude) of the composite column is deformed and twisted state plot only. The second part indicates the magnitude of Displacement distribution (U-magnitude) of the composite column is deformed and twisted state from undeformed state plot. additionally, it was observed that the member is more displaced around section close to points of load application or at the top edge of the column. Here is the maximum magnitude of displacement under 50% of the axial load has occurred at the top which is 1.914mm. Member displacement gradually decreases from top to bottom and negligible at the bottom end of column which is fully fixed support

c. Circular composite column subjected to Axial load at 60% [3754.26KN] of load-bearing capacity, P[6257.1KN]and 60 KNm constant torsional Load

When columns subjected to axial load(compression effect) and torsional load, displacement under both axial and torsional loads with twisting deformation will have occurred. In Figure below shows Von Mises stress distribution, which is used to predict yielding of materials under loading from the results of the axial and torsional load. Figure 5.26 (a) showed in three patterns of elements of composite column results of stress distribution from Abaqus software. The First part is indicating the stress distribution in the circular steel tube. As can be seen from the diagram, stress distributed by a colorful rainbow with different values between 123MPa and 137MPa. at the edge support, it shows less stress and maximal stress around edge support, while the entire elements are distributed as the medium in green colors. The second part of Figure 5.26 (a) indicating the stress distribution in the concrete core element. As can be seen from this figure, stress distributed by a colorful rainbow with different values between 14.61MPa and 20.09MPa. at the edge support, it shows less stress, while the entire elements are distributed as a moderate medium. The third part shows the stress distribution of all parts of the composite column when stick together. In this case from this result, it clearly understood the Mises stress magnitude is between 14.61Mpa and 137Mpa, which is the lower magnitude stress distributed in concrete and higher value in a steel tube element. From this figure, it concluded that stress distribute in concrete is less by 85.34 % than stress distributed in steel tube.

The magnitude of displacement distribution in members is shown in Figure 5.26 (b). This figure has two parts. The first part indicates the magnitude of Displacement distribution (U-magnitude) of the composite column is deformed and twisted state plot only. The second part indicates the magnitude of Displacement distribution (U-magnitude) of the composite column is deformed and twisted state from undeformed state plot. additionally, it was observed that the member is more displaced around section close to points of load application or at the top edge of the column. Here is the maximum magnitude of displacement under 60% of the axial load that has occurred at the top which is 2.253mm. Member displacement gradually decreases from top to bottom and negligible at the bottom end of column which is fully fixed support

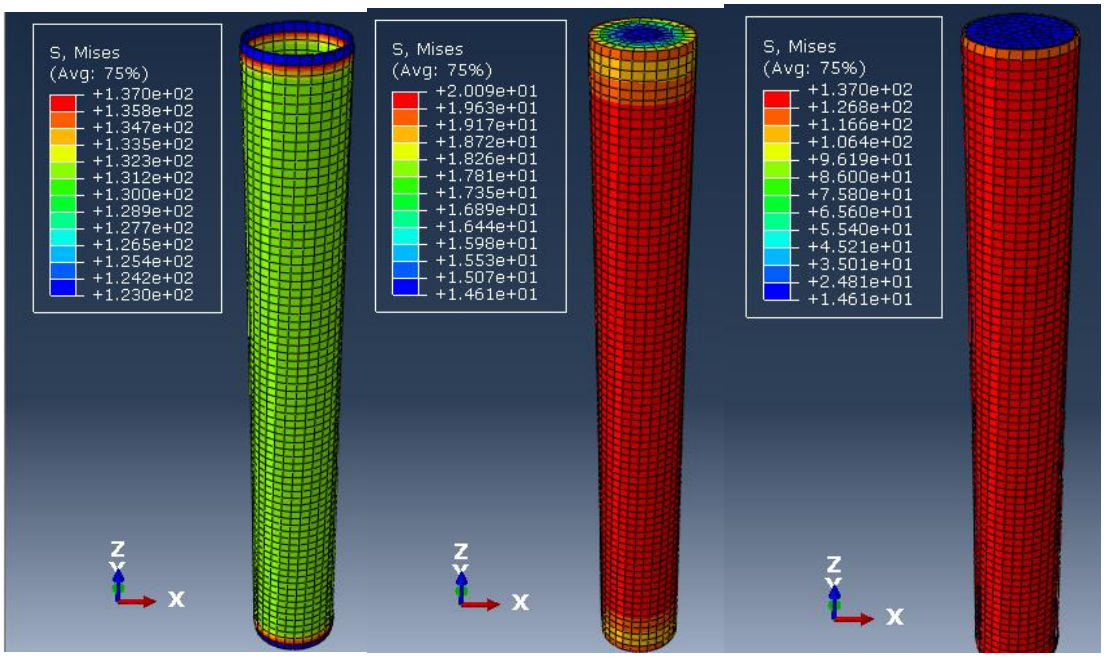

(a)

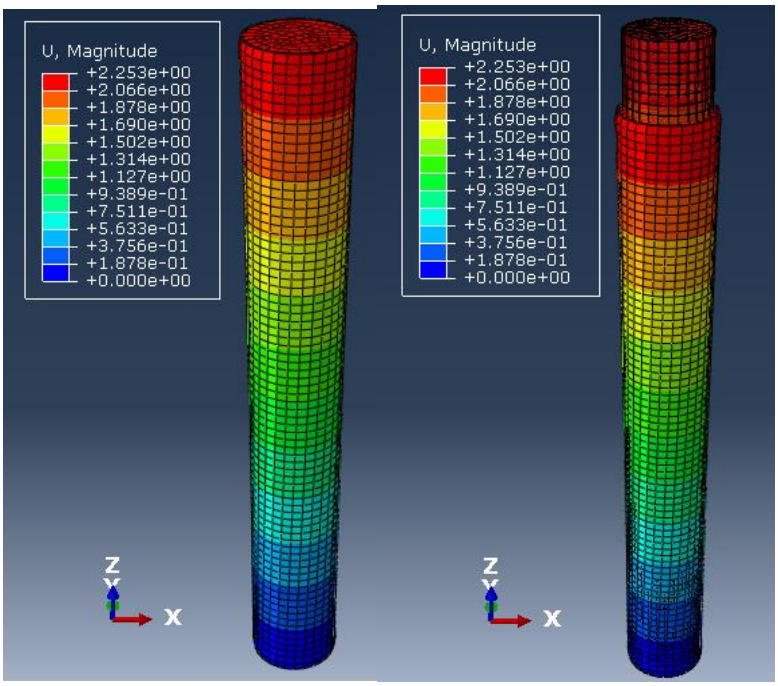

(b)

Figure 5.26: CCC with concrete fill subjected to axial load at 60% of P and torsional load

5.3.2 CCC with reinforcement bars subjected to both axial and torsional loads

a. Circular composite column subjected to Axial load at 40% [2502.84KN] of load-bearing capacity, P[6257.1KN] and 60KNm constant torsional Load

The stress and displacement magnitude of distribution discussed for figures arrangements are the same conditions as prescribed for figures above. but the magnitudes and parts are different. The same logical pattern of stress distribution is here, as it is discussed in detail

for the circular composite column with reinforcement embedded. As can be seen in Figure 5.27 (a) below, the stress magnitude in the steel tube varies between 82.63MPa and 91.52MPa. Stress distributed in the concrete section between 9.558MPa and 13.28MPa. The magnitude of stress in longitudinal reinforcement it varied widely between 6.511Mpa and 86.52Mpa. From the result it can be seen, the Mises stress magnitude of composite member part is between 6.511Mpa and 86.52Mpa, which is the lower magnitude stress distributed in bars and higher value in a steel tube element.

The magnitude of displacement distribution from Figure 5.27 (b), it is observed that the member is more displaced around section close to points of load application or at the top edge of the column. Here is the maximum magnitude of displacement under 40% of axial load that has occurred at the top which is 1.555mm. Member displacement gradually decreases from top to bottom and negligible at the bottom end of column which is fully fixed support

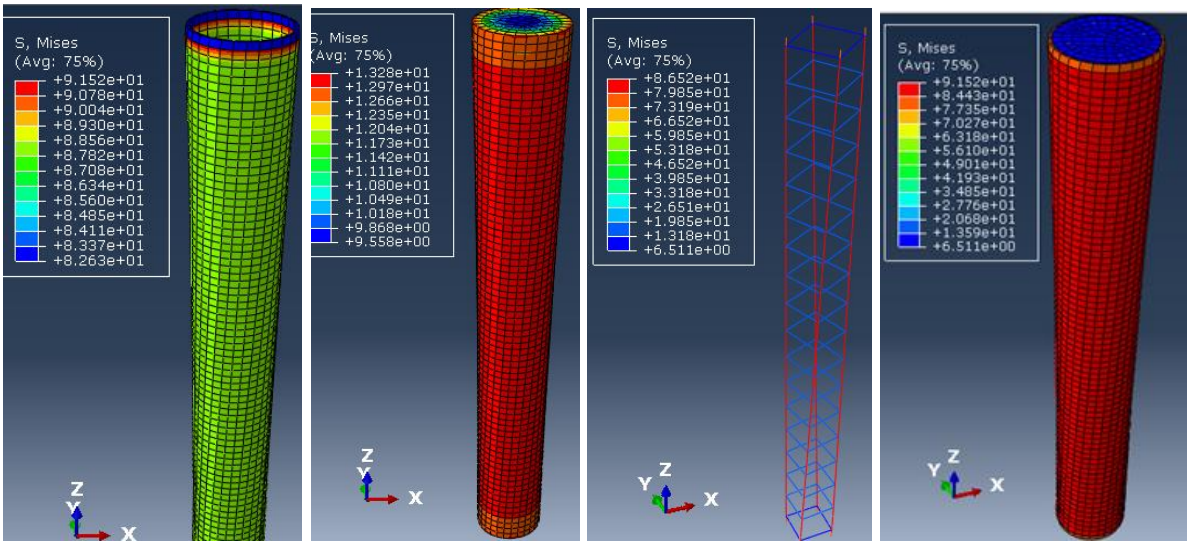

(a)

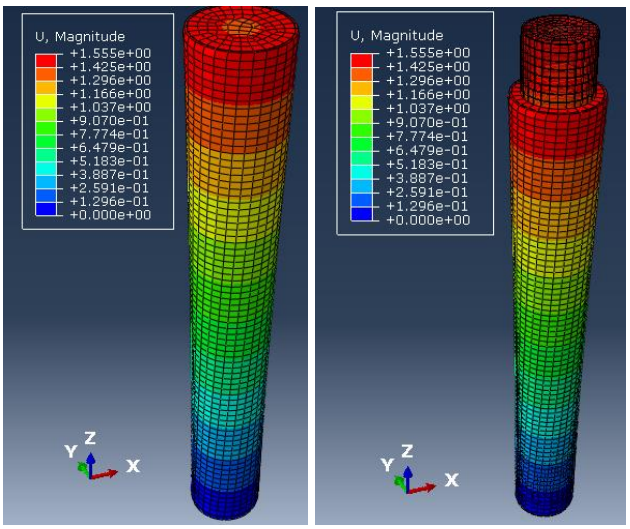

(b)

Figure 5.27: CCC with embedded reinforcement bars under axial load at 40% of P and torsional load

b. Circular composite column subjected to Axial load at 50% [3128.55KN] of load-bearing capacity, P[6257.1KN] and 60KNm constant torsional Load

The stress and displacement magnitude of distribution discussed for figures arrangements are the same conditions as prescribed for figures above. but the magnitudes and parts are different. The same logical pattern of stress distribution is here, as it is discussed in detail for the circular composite column with reinforcement embedded. As can be seen in Figure 5.28 (a) below, the stress magnitude in the steel tube varies between 101.5MPa and 112.7MPa. Stress distributed in the concrete section between 11.9MPa and 16.4MPa. The magnitude of stress in longitudinal reinforcement it varied widely between 8.139Mpa and 108.2Mpa.

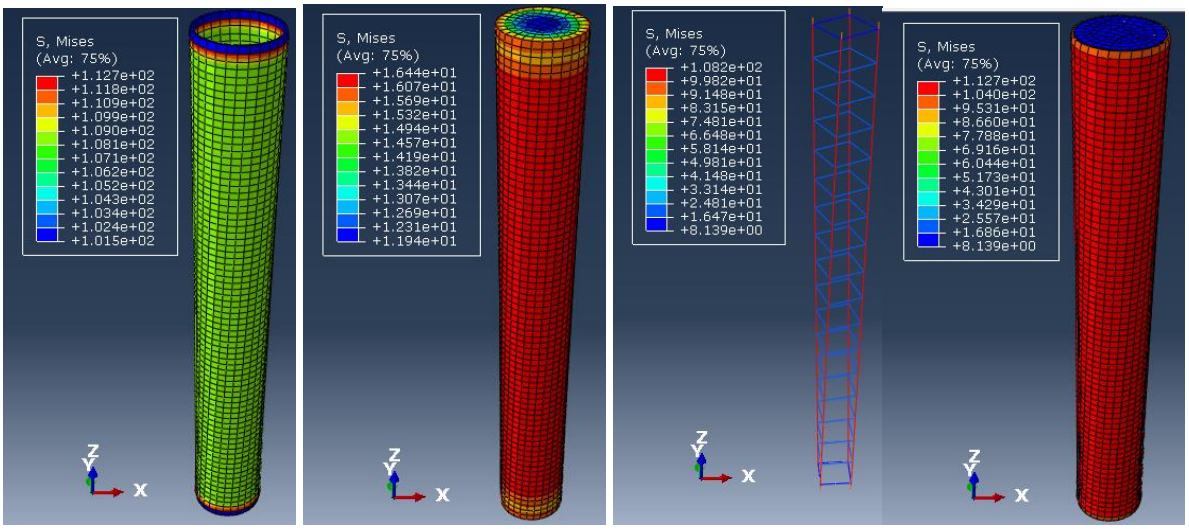

(a)

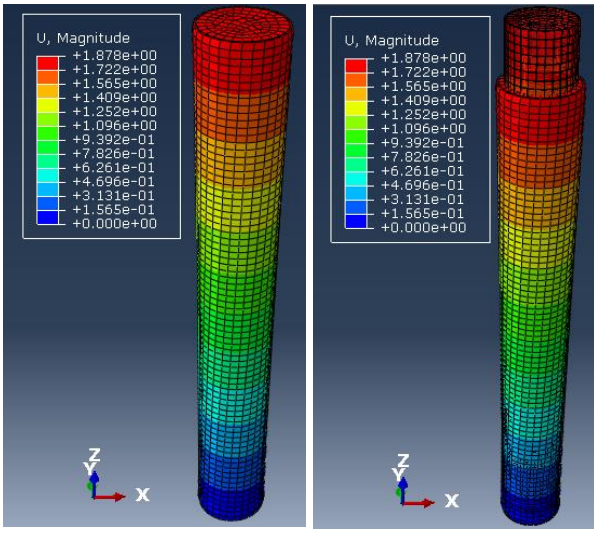

(b)

Figure 5.28: CCC with embedded reinforcement bars under axial load at 50% of P and torsional load

From the result it can be seen, the Mises stress magnitude of composite member part is between 8.139Mpa and 112.7Mpa, which is the lower magnitude stress distributed in bars and higher value in a steel tube element.

The magnitude of displacement distribution from Figure 5.28 (b), it is observed that the member is more displaced around section close to points of load application or at the top edge of the column. Here is the maximum magnitude of displacement under 50% of the axial load that has occurred at the top which is 1.878mm. Member displacement gradually decreases from top to bottom and negligible at the bottom end of the column which is fully fixed support**.**

c. Circular composite column subjected to Axial load at 60% [3754.26KN] of load-bearing capacity, P[6257.1KN]and 60 KNm constant torsional Load

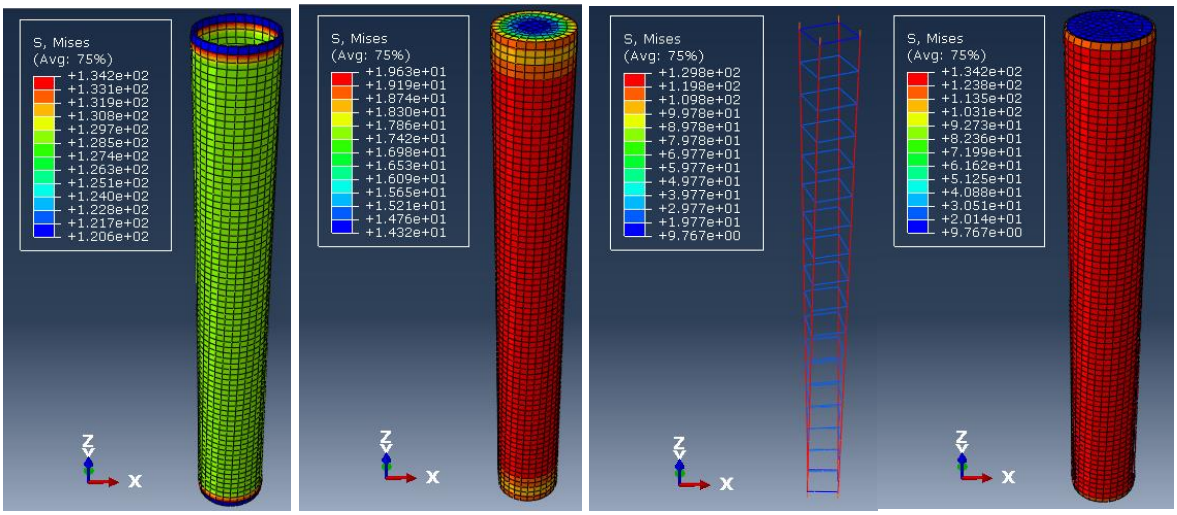

(a)

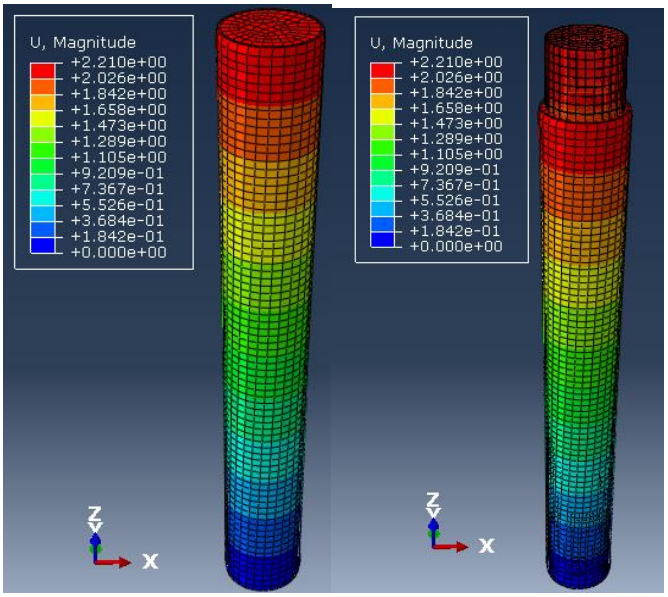

(b)

Figure 5.29: CCC with embedded reinforcement bars under axial load at 60% of P and torsional load

The stress and displacement magnitude of distribution discussed for figures arrangements are the same conditions as prescribed for figures above. but the magnitudes and parts are different. The same logical pattern of stress distribution is here, as it is discussed in detail for the circular composite column with reinforcement embedded. As can be seen in Figure 5.29 (a) above, the stress magnitude in the steel tube varies between 120.6MPa and 134.2MPa. Stress distributed in the concrete section between 14.32MPa and 19.63MPa. The magnitude of stress in longitudinal reinforcement it varied widely between 9.767Mpa and 129.8Mpa. From the result it can be seen, the Mises stress magnitude of composite member part is between 9.767Mpa and 134.2Mpa, which is the lower magnitude stress distributed in bars and higher value in a steel tube element.

The magnitude of displacement distribution from Figure 5.29 (b), it is observed that the member is more displaced around section close to points of load application or at the top edge of the column. Here is the maximum magnitude of displacement under 60% of the axial load that has occurred at the top which is 2.21mm. Member displacement gradually decreases from top to bottom and negligible at the bottom end of the column which is fully fixed support**.**

5.3.3 CCC column with embedded steel profile under axial and torsional loads

a. **Circular composite column subjected to Axial load at 40% [2502.84KN] of load-bearing capacity, P[6257.1KN] and 60KNm constant torsional Load**

The stress and displacement magnitude of distribution discussed for figures arrangements are the same conditions as prescribed for figures above. but the magnitudes and parts are different. The same logical pattern of stress distribution is here, as it is discussed in detail for the circular composite column with reinforcement embedded. As can be seen in Figure 5.30 (a) below, the stress magnitude in the steel tube varies between 72.3MPa and 80.05MPa. Stress distributed in the concrete section between 7.459MPa and 12MPa. The magnitude of stress in the embedded steel profile varied close to stress distribution in steel tube, between 54.3Mpa and 73.59Mpa. From the result it can be seen, the Mises stress magnitude of composite member part is between 7.459Mpa and 80.05Mpa, which is the lower magnitude stress distributed in concrete and higher value in a steel tube element.

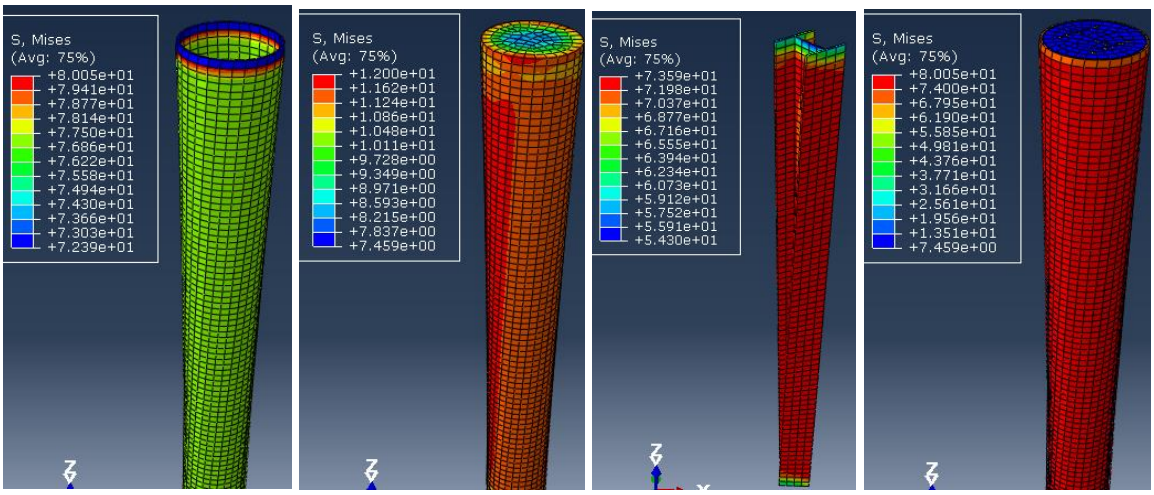

(a)

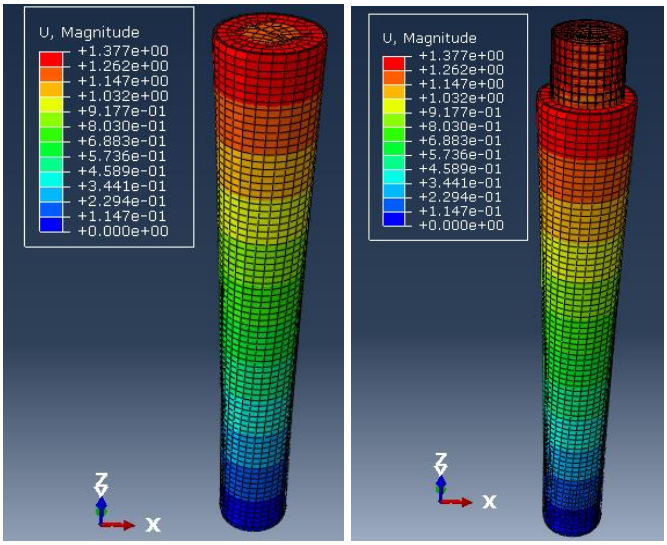

(b)

Figure 5.30: CCC with embedded steel profile under axial load at 40% of P and torsional load

The magnitude of displacement distribution from Figure 5.30 (b) above, it is observed that the member is more displaced around section close to points of load application or at the top edge of the column. Here is the maximum magnitude of displacement under 40% of axial load that has occurred at the top which is 1.377mm. Member displacement gradually decreases from top to bottom and negligible at the bottom end of column which is fully fixed support

b. **Circular composite column subjected to Axial load at 50% [3128.55KN] of load-bearing capacity, P[6257.1KN] and 60KNm constant torsional Load**

The stress and displacement magnitude of distribution discussed for figures arrangements are the same conditions as prescribed for figures above. but the magnitudes and parts are different. The same logical pattern of stress distribution is here, as it is discussed in detail for the circular composite column with reinforcement embedded. As it can be seen in Figure 5.31 (a) below, the stress magnitude in the steel tube varies between 88.57MPa and 98.32MPa. Stress distributed in the concrete section between 9.353MPa and 14.88MPa. The magnitude of stress in the embedded steel profile varied close to stress distribution in steel tube, between 67.03Mpa and 91.83Mpa. From the result it can be seen, the Mises stress magnitude of composite member part is between 9.353Mpa and 98.32Mpa, which is the lower magnitude stress distributed in concrete and higher value in a steel tube element.

The magnitude of displacement distribution from Figure 5.31 (b) below, it is observed that the member is more displaced around section close to points of load application or at the top edge of the column. Here is the maximum magnitude of displacement under 50% of the axial load has occurred at the top which is 1.652mm. Member displacement gradually decreases from top to bottom and negligible at the bottom end of column which is fully fixed support

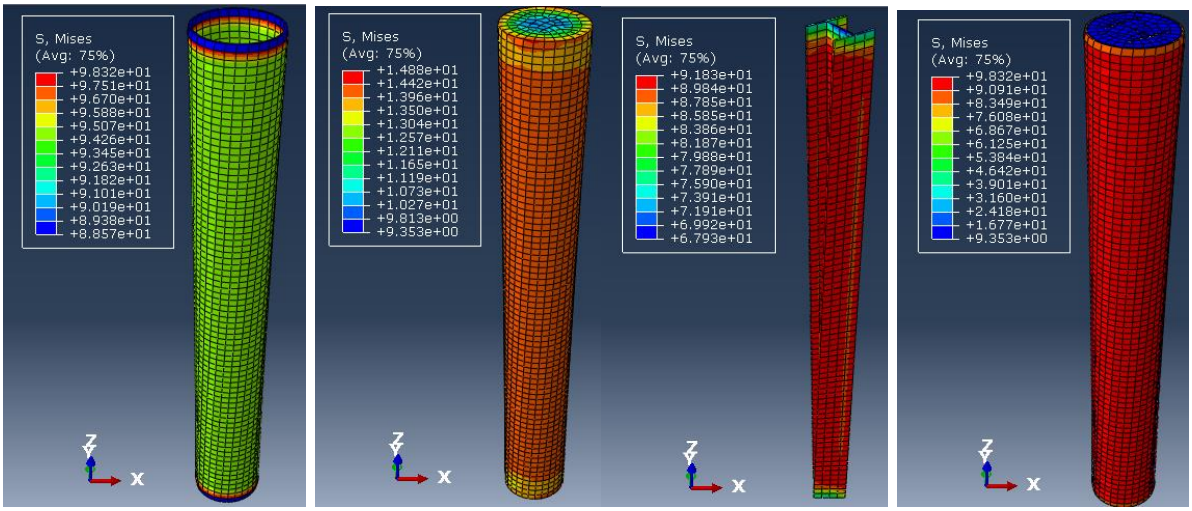

(a)

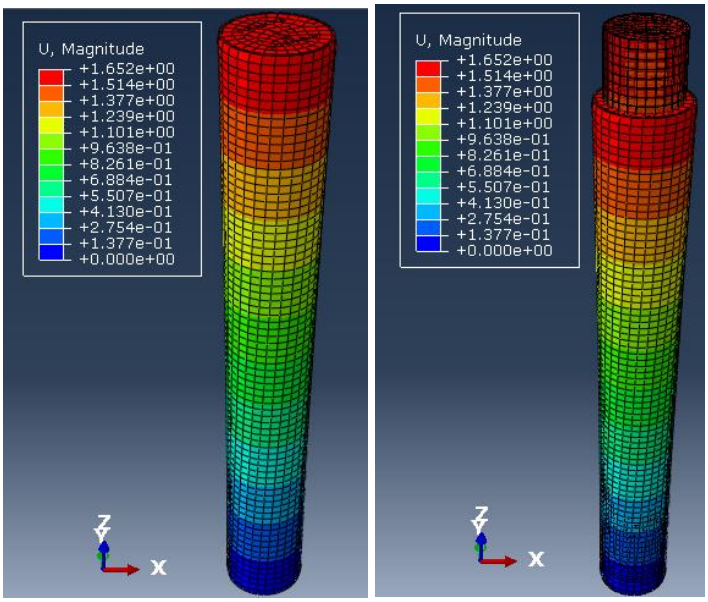

(b)

Figure 5.31: CCC with embedded steel profile under axial load at 50% of P and torsional load

c. **Circular composite column subjected to Axial load at 60% [3754.26KN] of load-bearing capacity, P[6257.1KN] and 60KNm constant torsional Load**

The stress and displacement magnitude of distribution discussed for figures arrangements are the same conditions as prescribed for figures above. but the magnitudes and parts are different. The same logical pattern of stress distribution is here, as it is discussed in detail for the circular composite column with reinforcement embedded. As it can be seen in Figure 5.32 (a) below, the stress magnitude in the steel tube varies between 105MPa and 116.8MPa. Stress distributed in the concrete section between 11.26MPa and 17.76MPa. The magnitude of stress in the embedded steel profile varied close to stress distribution in steel tube, between 81.57Mpa and 110.1Mpa. From the result it can be seen, the Mises stress magnitude of composite member part is between 11.26Mpa and 116.8Mpa, which is the lower magnitude stress distributed in concrete and higher value in a steel tube element.

The magnitude of displacement distribution from Figure 5.32 (b) below, it is observed that the member is more displaced around section close to points of load application or at the top edge of the column. Here is the maximum magnitude of displacement under 60% of the axial load that has occurred at the top which is 1.936mm. Member displacement gradually decreases from top to bottom and negligible at the bottom end of the column which is fully fixed support.

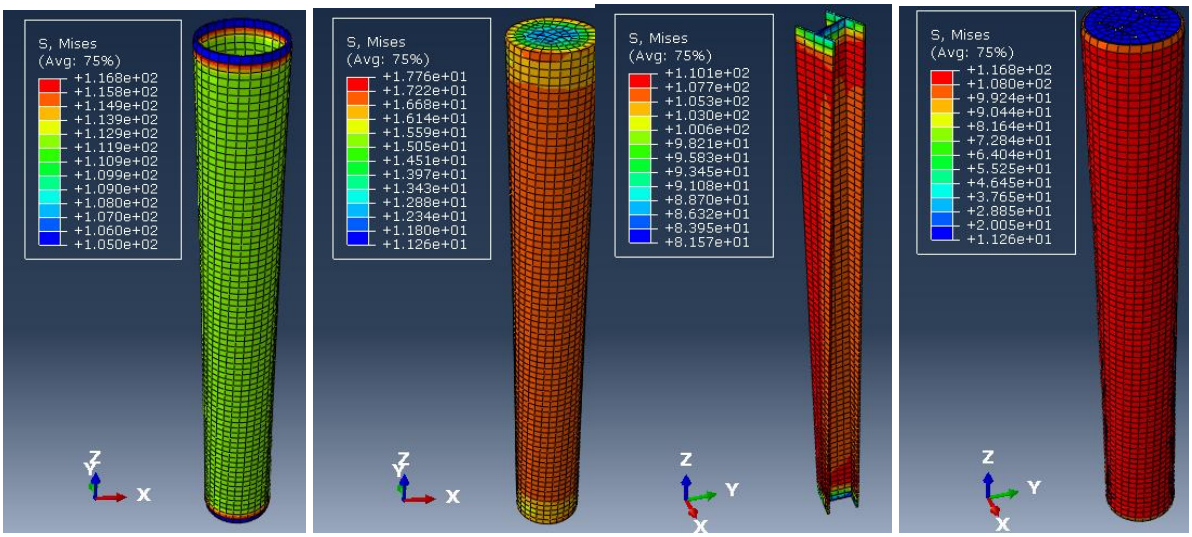

(a)

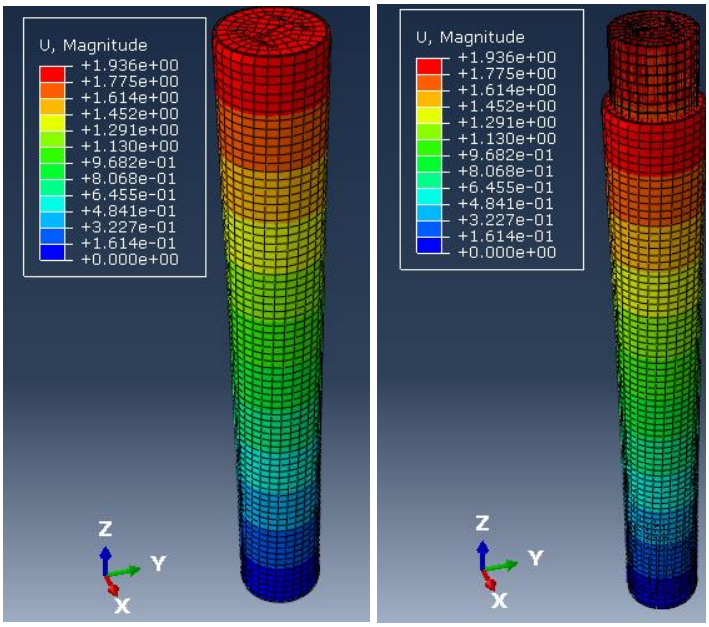

(b)

Figure 5.32: CCC with embedded steel profile under axial load at 60% of P and torsional load

To summarize, it's observed that from Figure 5.33 below the stress distribution magnitudes are less in CCC with steel profile embedded and it shows minimum displacement(U) under both axial and torsional load rather than a circular composite column with concrete fill and reinforcement bars. The stress distribution of concrete is high on the outside of the concrete

section where it has contact with steel and it lower at the center of steel core but the stress distribution of in steel is higher than the concrete material.

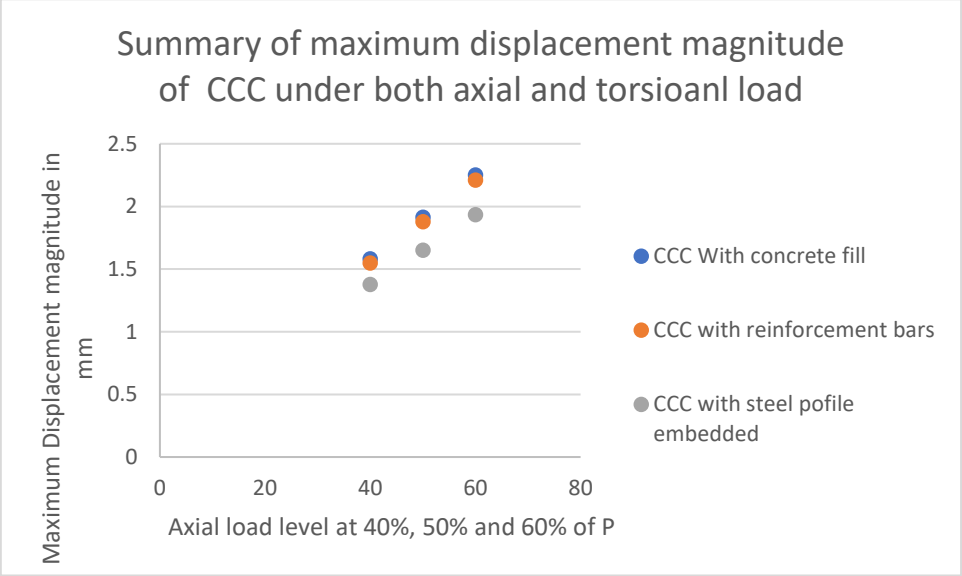

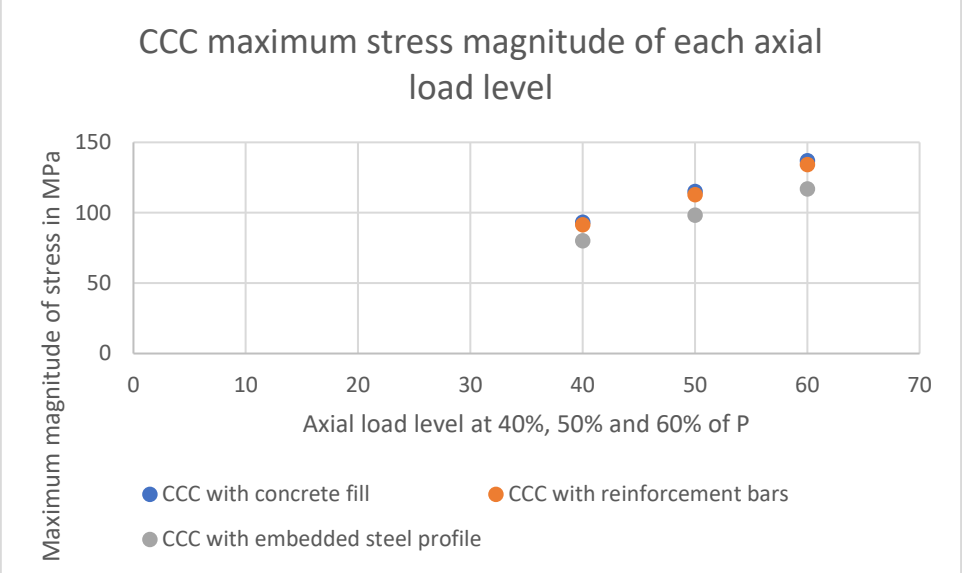

Figure 5.33: The Summary result of CCC under both axial and torsional load

5.3.4 SCC with concrete fill which subjected to both axial and torsional loads

a. Square composite column subjected to Axial Load at 40% [2598.08KN] of load-bearing capacity, P[6495.4KN].

The stress and magnitude of displacement distribution discussed for figures arrangements is the same condition as prescribed for figures above. but the magnitudes are different. As can be seen in Figure 5.34 (a), The stress magnitude in the steel tube varies between 73.56MPa and 92.56MPa. Stress distributed in the concrete section between 9.747MPa and 13.86MPa. From the result it can be seen, the Mises stress magnitude of composite member part is

between 9.747Mpa and 92.56Mpa, which is the lower magnitude stress distributed in concrete and higher value in a steel tube element.

The magnitude of displacement distribution from Figure 5.34 (b), it is observed that the member is more displaced around section close to points of load application or at the top edge of the column. Here is the maximum magnitude of displacement under 40% of axial load that has occurred at the top which is 1.77mm. Member displacement gradually decreases from top to bottom and negligible at the bottom end of the column which is fully fixed support.

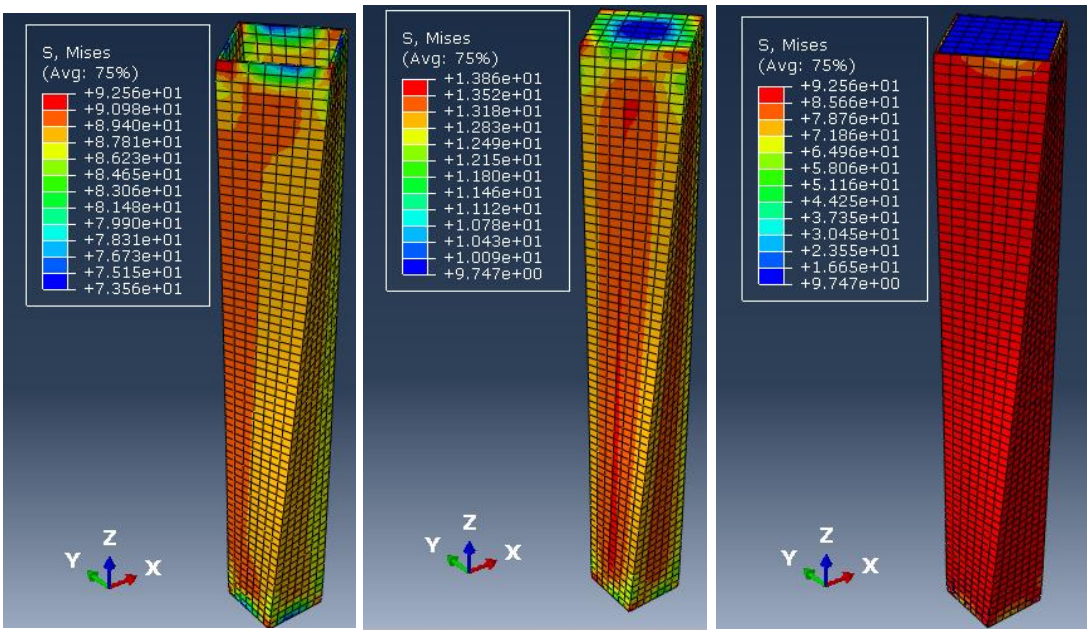

(a)

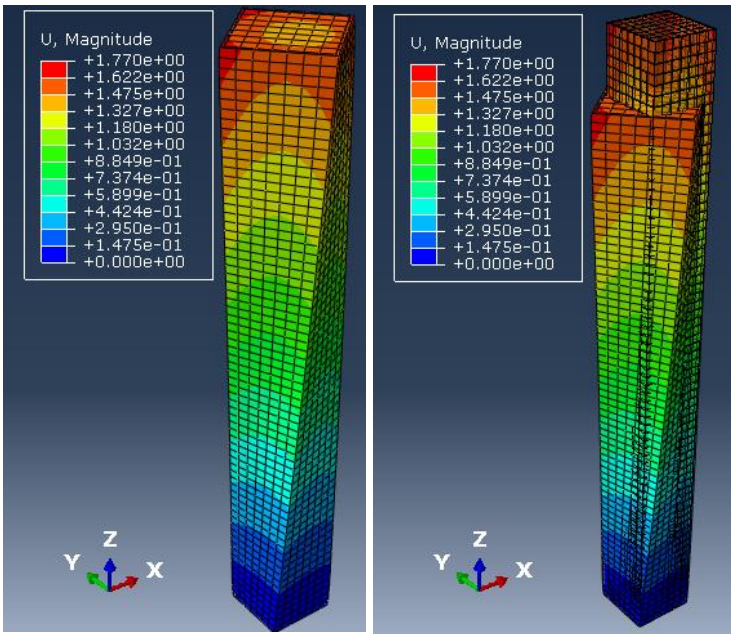

(b)

Figure 5.34: SCC with concrete fill under axial load at 40% of P and torsional load

b. Square composite column subjected to Axial Load at 50% [3247.60KN] of load-bearing capacity, P[6495.4KN].

The stress and magnitude of displacement distribution discussed for figures arrangements is the same condition as prescribed for figures above. but the magnitudes are different. As can be seen in Figure 5.35 (a), The stress magnitude in the steel tube varies between 90.95MPa and 114.1MPa. Stress distributed in the concrete section between 12.15MPa and 17.22MPa. From the result it can be seen, the Mises stress magnitude of composite member part is between 12.15Mpa and 92.56Mpa, which is the lower magnitude stress distributed in concrete and higher value in a steel tube element.

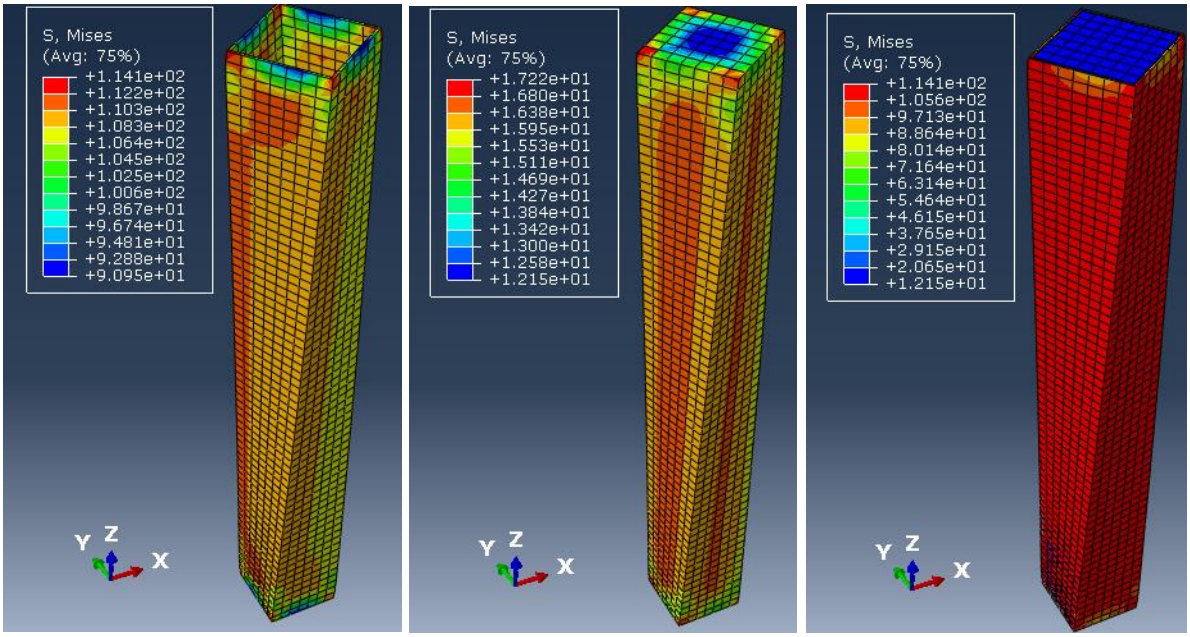

(a)

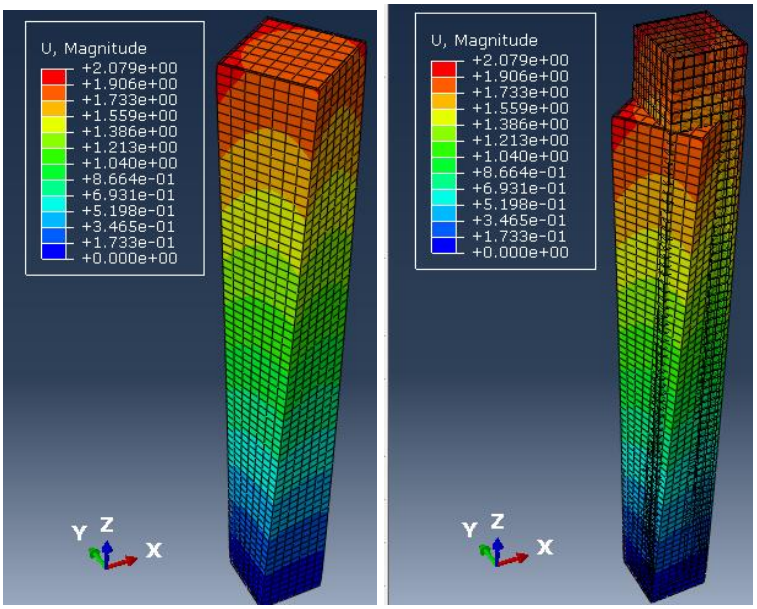

(b)

Figure 5.35: SCC with concrete fill under axial load at 50% of P and torsional load

The magnitude of displacement distribution from Figure 5.35 (b), it is observed that the member is more displaced around section close to points of load application or at the top edge of the column. Here is the maximum magnitude of displacement under 50% of the axial load that has occurred at the top which is 2.079mm. Member displacement gradually decreases from top to bottom and negligible at the bottom end of the column which is fully fixed support.

c. Square composite column subjected to Axial Load at 60% [3897.12KN] of load-bearing capacity, P[6495.4KN].

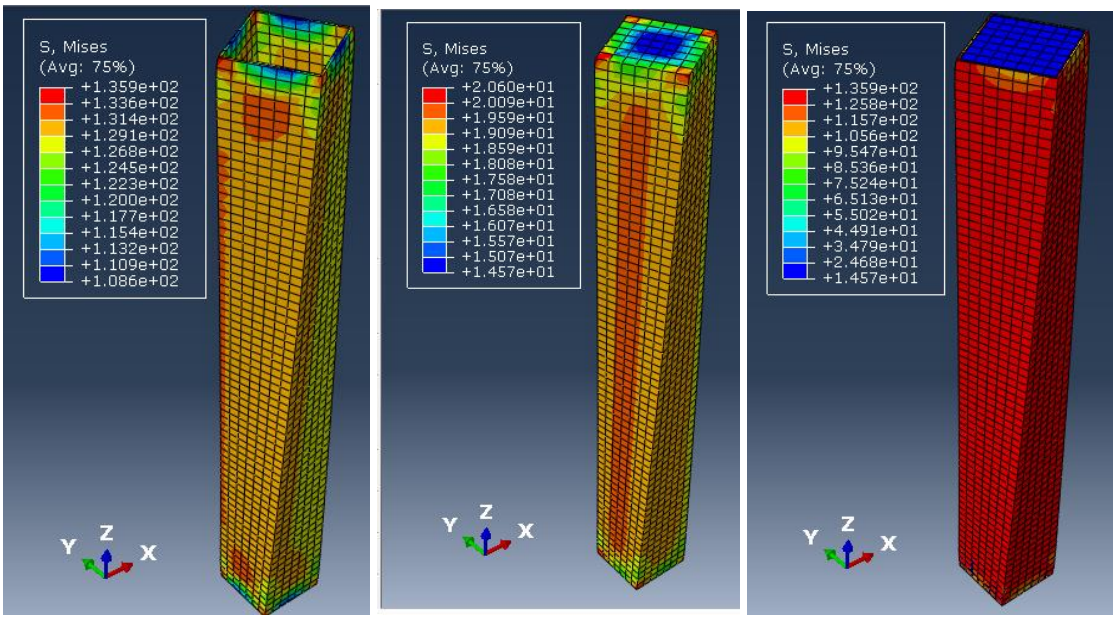

(a)

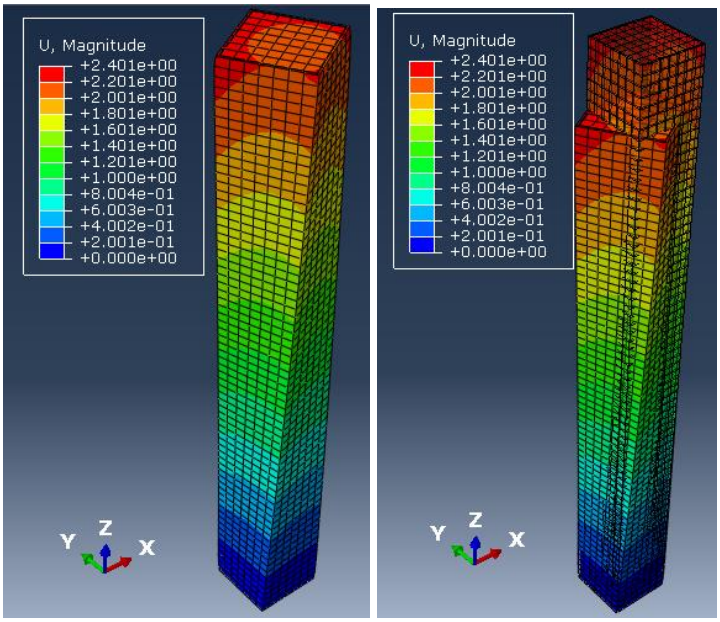

(b)

Figure 5.36: SCC with concrete fill under axial load at 60% of P and torsional load

The stress and magnitude of displacement distribution discussed for figures arrangements is the same condition as prescribed for figures above. but the magnitudes are different. As can be seen in Figure 5.36 (a), The stress magnitude in the steel tube varies between 108.6MPa and 135.9MPa. Stress distributed in the concrete section between 14.57MPa and 20.6MPa. From the result it can be seen, the Mises stress magnitude of composite member part is between 14.57Mpa and 135.9Mpa, which is the lower magnitude stress distributed in concrete and higher value in a steel tube element.

The magnitude of displacement distribution from Figure 5.36 (b), it is observed that the member is more displaced around section close to points of load application or at the top edge of the column. Here is the maximum magnitude of displacement under 60% of the axial load that has occurred at the top which is 2.401mm. Member displacement gradually decreases from top to bottom and negligible at the bottom end of the column which is fully fixed support.

5.3.5 SCC with embedded reinforcement bars under both axial and torsional loads

a. Square composite column subjected to Axial Load at 40% [2598.08KN] of load-bearing capacity, P[6495.4KN].

The stress and magnitude of displacement distribution discussed for figures arrangements is the same condition as prescribed for figures above. but the magnitudes and parts are different. As can be seen in Figure 5.37 (a), The stress magnitude in the steel tube varies between 72.51MPa and 91.03MPa. Stress distributed in the concrete section between 8.748MPa and 14.17MPa. From the result it can be seen, the Mises stress magnitude of composite member part is between 8.748Mpa and 91.03Mpa, which is the lower magnitude stress distributed in concrete and higher value in a steel tube element.

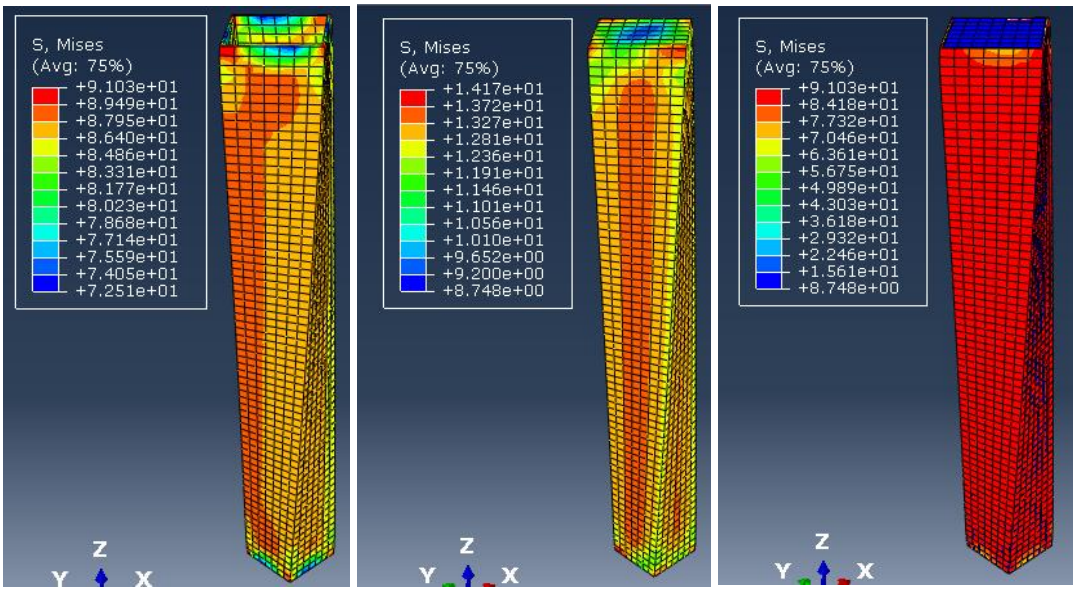

(a)

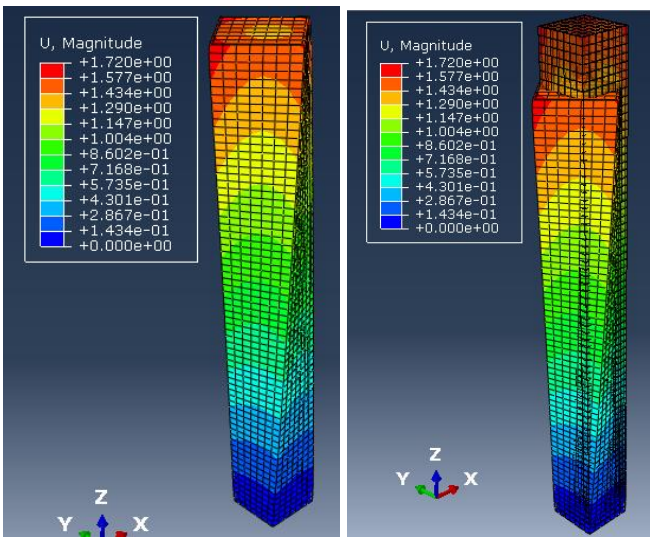

(b)

Figure 5.37: SCC with embedded reinforcement bars under axial load at 40% of P and torsional load

The magnitude of displacement distribution from Figure 5.37 (b) above, it is observed that the member is more displaced around section close to points of load application or at the top edge of the column. Here is the maximum magnitude of displacement under 40% of axial load that has occurred at the top which is 1.72mm. Member displacement gradually decreases from top to bottom and negligible at the bottom end of the column which is fully fixed support.

b. Square composite column subjected to Axial Load at 50% [3247.6KN] of load-bearing capacity, P[6495.4KN].

The stress and magnitude of displacement distribution discussed for figures arrangements is the same condition as prescribed for figures above. but the magnitudes and parts are different. As can be seen in Figure 5.38 (a), The stress magnitude in the steel tube varies between 89.73MPa and 112.3MPa. Stress distributed in the concrete section between 10.98MPa and 17.57MPa. From the result it can be seen, the Mises stress magnitude of composite member part is between 10.98Mpa and 112.33Mpa, which is the lower magnitude stress distributed in concrete and higher value in a steel tube element.

The magnitude of displacement distribution from Figure 5.38 (b), it is observed that the member is more displaced around section close to points of load application or at the top edge of the column. Here is the maximum magnitude of displacement under 50% of the axial load that has occurred at the top which is 2.027mm. Member displacement gradually decreases from top to bottom and negligible at the bottom end of the column which is fully fixed support.

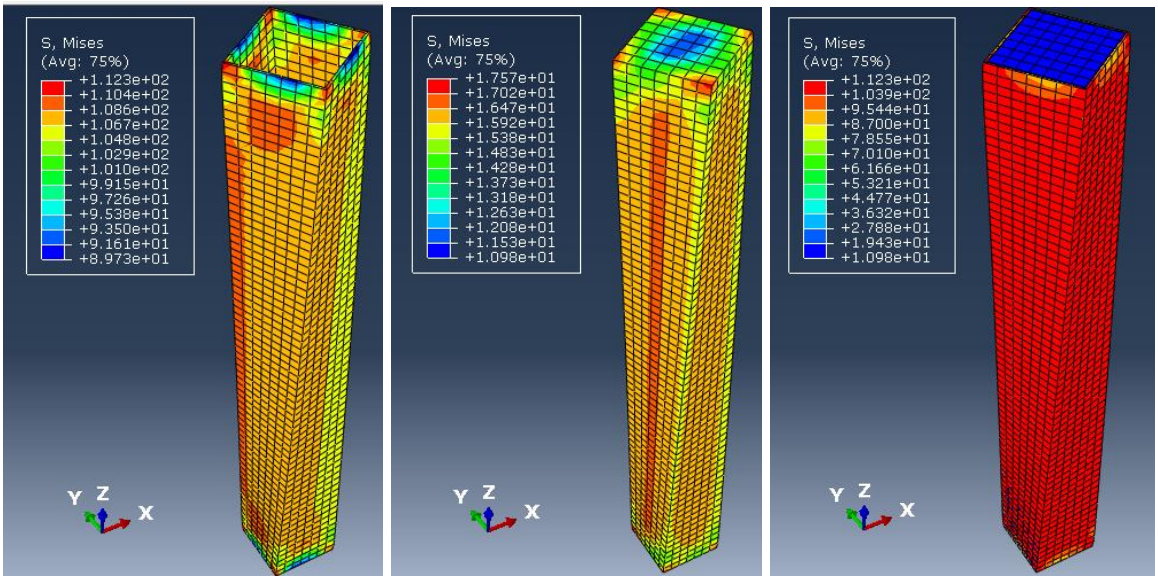

(a)

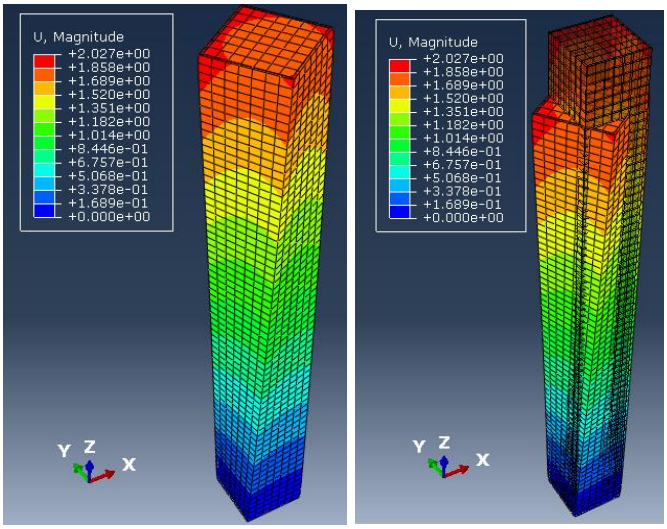

(b)

Figure 5.38: SCC with embedded reinforcement bars under axial load at 50% of P and torsional load

c. Square composite column subjected to Axial Load at 60% [3897.12KN] of load-bearing capacity, P[6495.4KN].

The stress and magnitude of displacement distribution discussed for figures arrangements is the same condition as prescribed for figures above. but the magnitudes and parts are different. As can be seen in Figure 5.39 (a), The stress magnitude in the steel tube varies between 107.2MPa and 133.8MPa. Stress distributed in the concrete section between 13.23MPa and 20.98MPa. From the result it can be seen, the Mises stress magnitude of composite member part is between 13.23Mpa and 133.8Mpa, which is the lower magnitude stress distributed in concrete and higher value in a steel tube element.

The magnitude of displacement distribution from Figure 5.39 (b), it is observed that the member is more displaced around section close to points of load application or at the top edge of the column. Here is the maximum magnitude of displacement under 60% of the

axial load that has occurred at the top which is 2.346mm. Member displacement gradually decreases from top to bottom and negligible at the bottom end of the column which is fully fixed support.

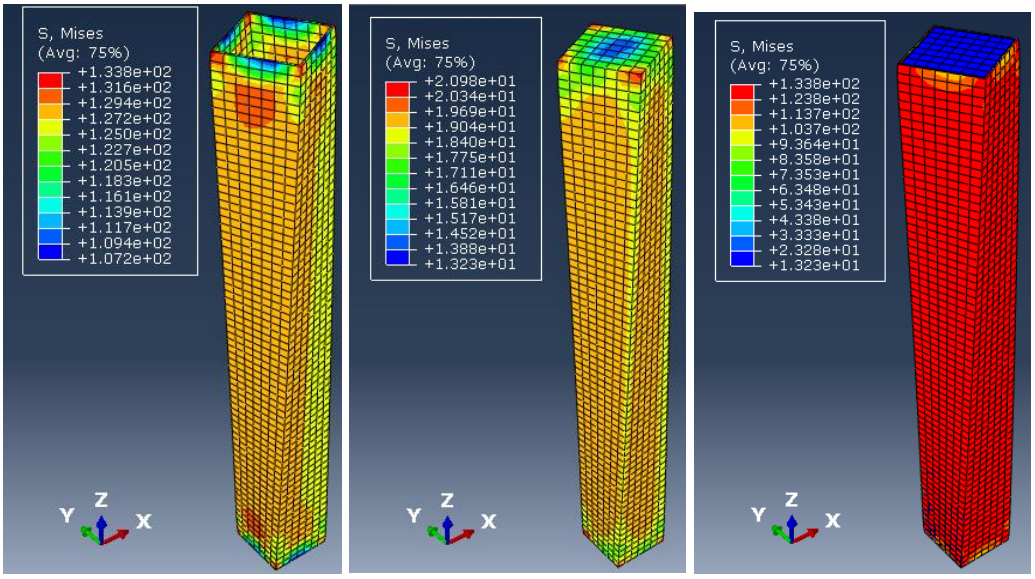

(a)

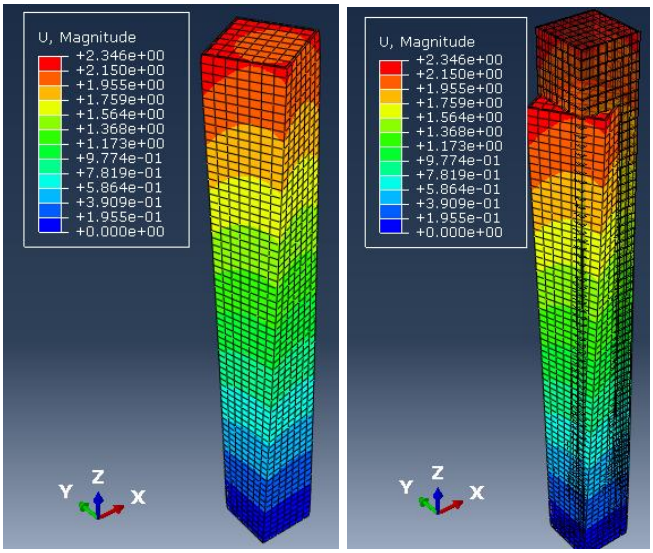

(b)

Figure 5.39: SCC with embedded reinforcement bars under axial load at 60% of P and torsional load

5.3.6 SCC with embedded steel profile under both axial and torsional loads

a. Square composite column subjected to Axial Load at 40% [2598.08KN] of load-bearing capacity, P[6495.4KN].

The stress and magnitude of displacement distribution discussed for figures arrangements is the same condition as prescribed for figures above. but the magnitudes and parts are

different. As can be seen in Figure 5.40 (a), There are three parts in this composite column such as steel tube, concrete core, and embedded H- steel profile. The stress magnitude in the steel tube varies between 63.46MPa and 79.77MPa. Stress distributed in the concrete section between 7.55MPa and 12.35MPa. The magnitude of Von Mises stress distributed in steel profile between 51.44Mpa and 72.046Mpa. From the result it can be seen, the Mises stress magnitude of composite member part is between 7.55Mpa and 79.77Mpa, which is the lower magnitude stress distributed in concrete and higher value in a steel tube element.

The magnitude of displacement distribution from Figure 5.40 (b), it is observed that the member is more displaced around section close to points of load application or at the top edge of the column. Here is the maximum magnitude of displacement under 40% of axial load that has occurred at the top which is 1.563mm. Member displacement gradually decreases from top to bottom and negligible at the bottom end of the column which is fully fixed support.

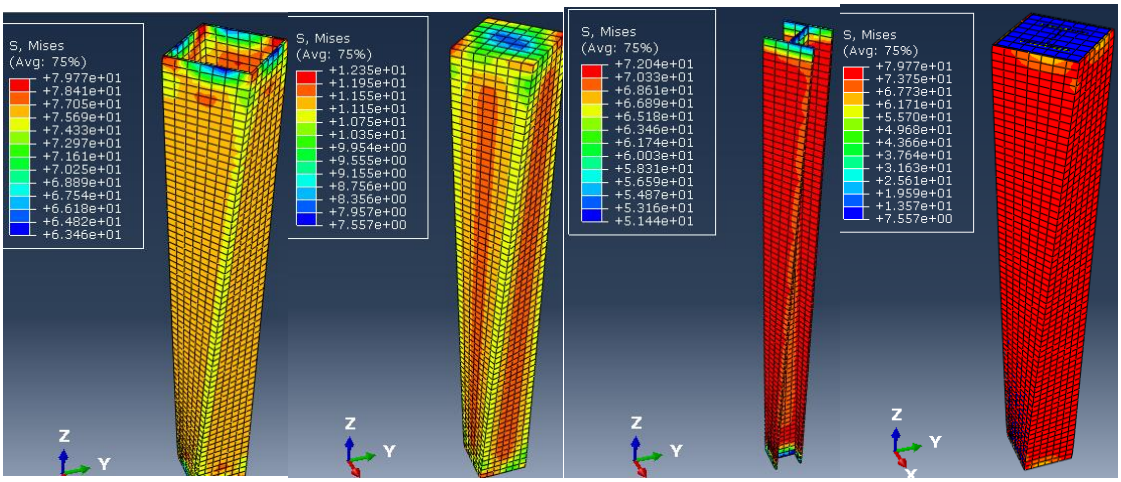

(a)

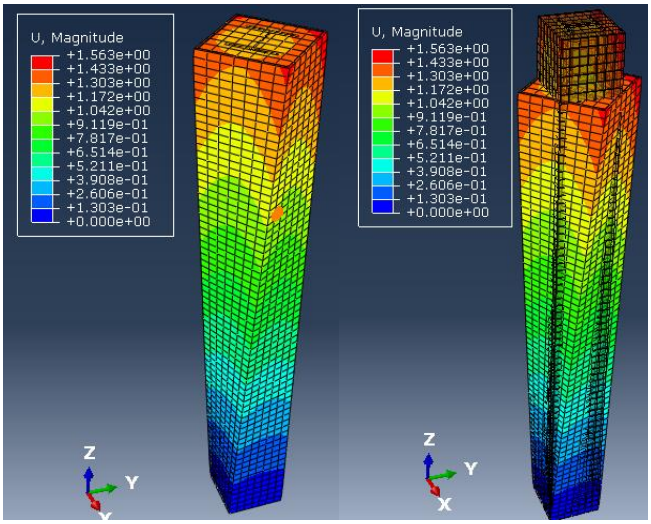

(b)

Figure 5.40: SCC with embedded steel profile under axial load at 40% of P and torsional load

b. Square composite column subjected to Axial Load at 50% [3247.6KN] of load-bearing capacity, P[6495.4KN].

The stress and magnitude of displacement distribution discussed for figures arrangements is the same condition as prescribed for figures above. but the magnitudes and parts are different. As can be seen in Figure 5.41 (a), There are three parts in this composite column such as steel tube, concrete core, and embedded H- steel profile. The stress magnitude in the steel tube varies between 78.15MPa and 98.03MPa. Stress distributed in the concrete section between 9.485MPa and 15.29MPa. The magnitude of Von Mises stress distributed in steel profile between 64.28Mpa and 89.871Mpa. From the result it can be seen, the Mises stress magnitude of composite member part is between 9.489Mpa and 98.03Mpa, which is the lower magnitude stress distributed in concrete and higher value in a steel tube element.

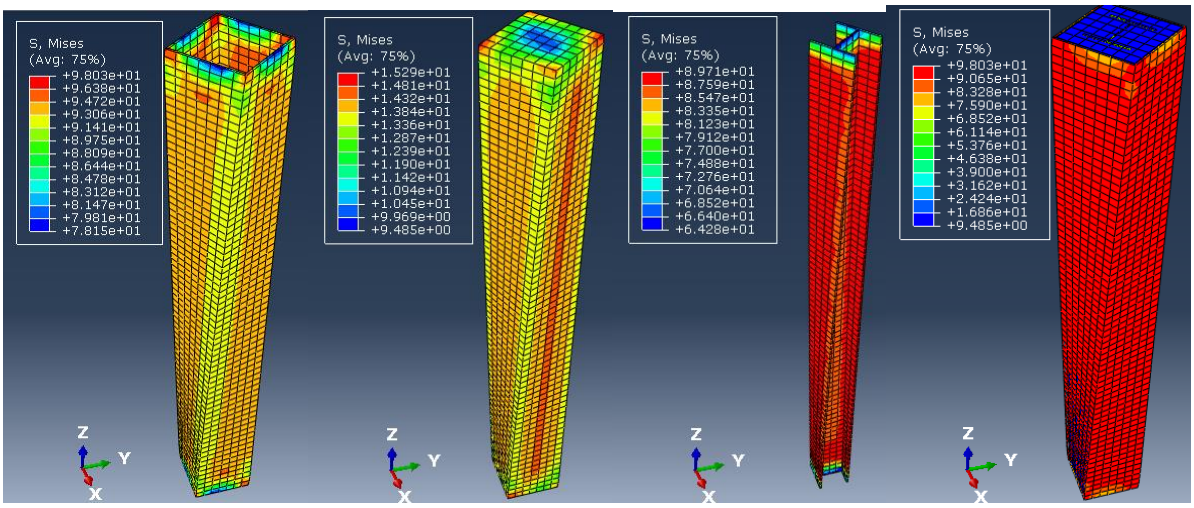

(a)

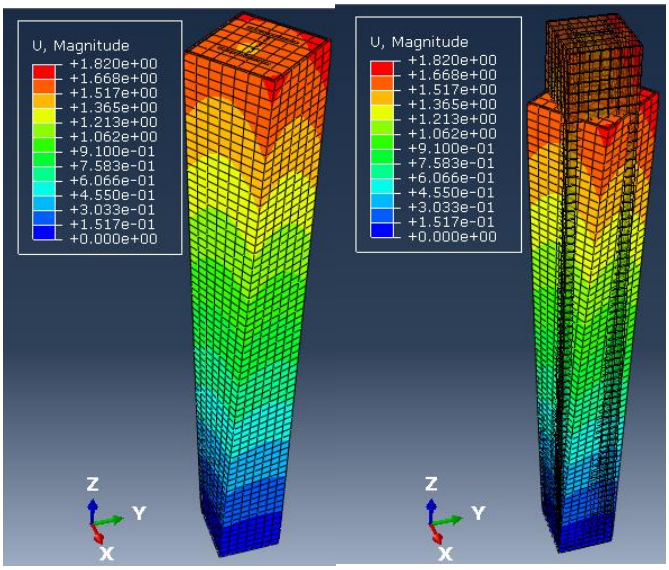

(b)

Figure 5.41: SCC with embedded steel profile under axial load at 50% of P and torsional load

The magnitude of displacement distribution from Figure 5.41 (b), it is observed that the member is more displaced around section close to points of load application or at the top edge of the column. Here is the maximum magnitude of displacement under 50% of the axial load that has occurred at the top which is 1.82mm. Member displacement gradually decreases from top to bottom and negligible at the bottom end of the column which is fully fixed support.

c. Square composite column subjected to Axial Load at 60% [3897.12KN] of load-bearing capacity, P[6495.4KN].

The stress and magnitude of displacement distribution discussed for figures arrangements is the same condition as prescribed for figures above. but the magnitudes and parts are different. As can be seen in Figure 5.42 (a), There are three parts in this composite column such as steel tube, concrete core, and embedded H- steel profile. The stress magnitude in the steel tube varies between 93.14MPa and 116.5MPa. Stress distributed in the concrete section between 11.42MPa and 18.24MPa. The magnitude of Von Mises stress distributed in steel profile between 77.13Mpa and 107.4Mpa.

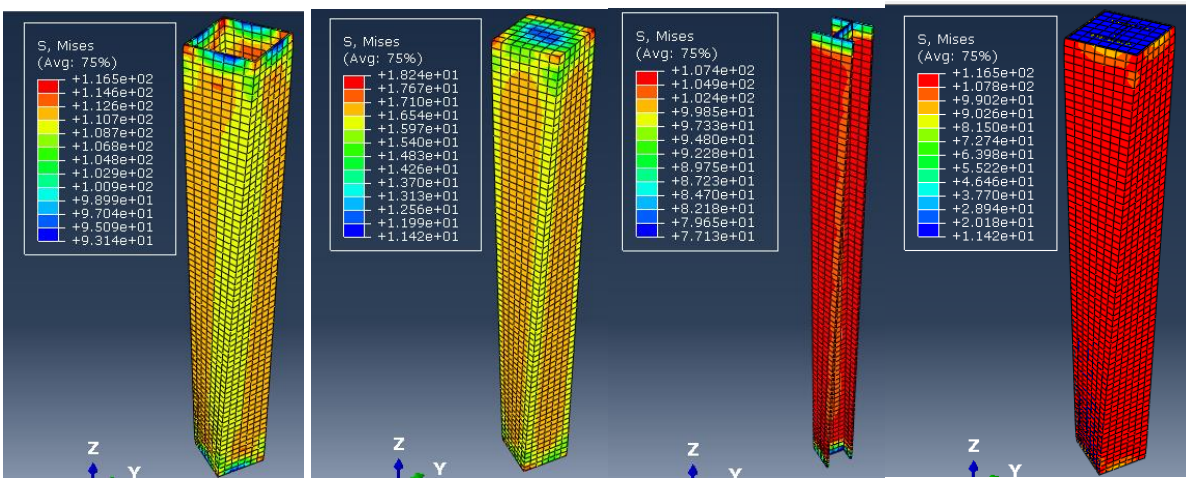

(a)

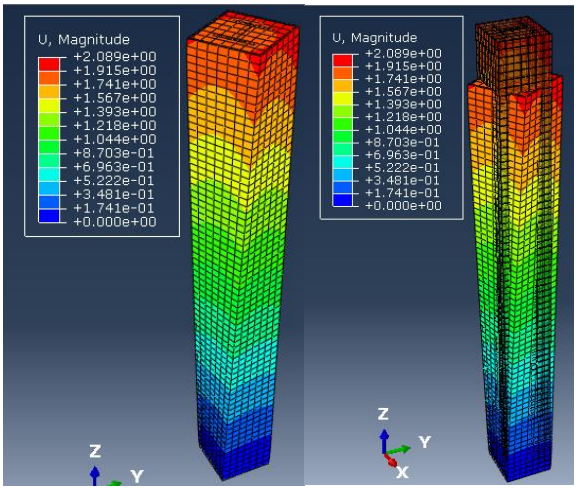

(b)

Figure 5.42: SCC with embedded steel profile subjected to axial load at 60% of P and torsional load

From the result it can be seen, the Mises stress magnitude of composite member part is between 11.42Mpa and 116.5Mpa, which is the lower magnitude stress distributed in concrete and higher value in a steel tube element.

The magnitude of displacement distribution from Figure 5.42 (b) above, it is observed that the member is more displaced around section close to points of load application or at the top edge of the column. Here is the maximum magnitude of displacement under 60% of the axial load that has occurred at the top which is 2.089mm. Member displacement gradually decreases from top to bottom and negligible at the bottom end of the column which is fully fixed support.

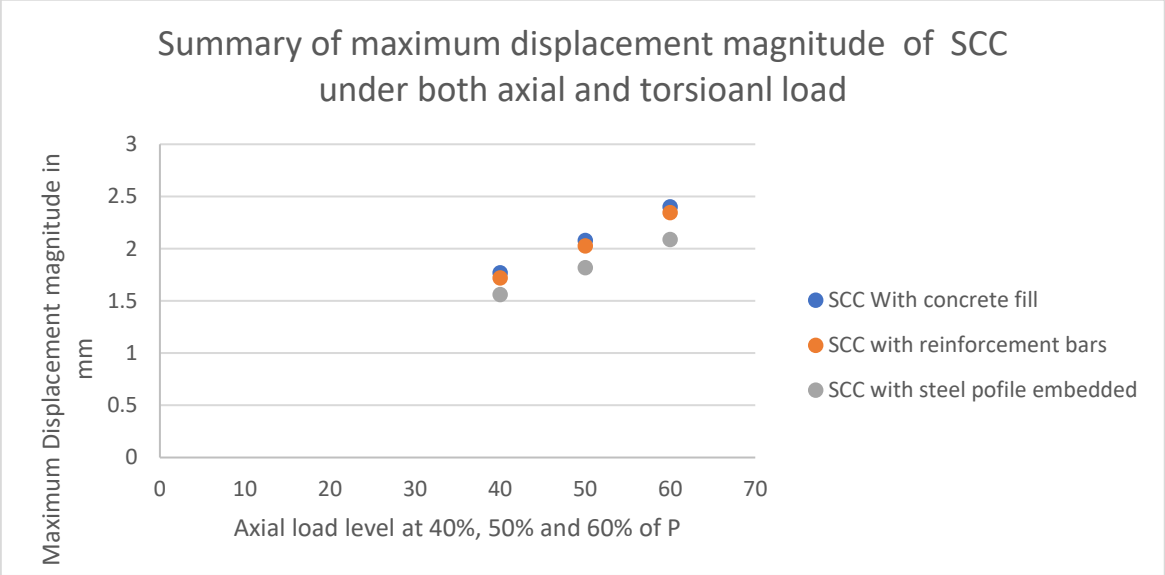

(a)

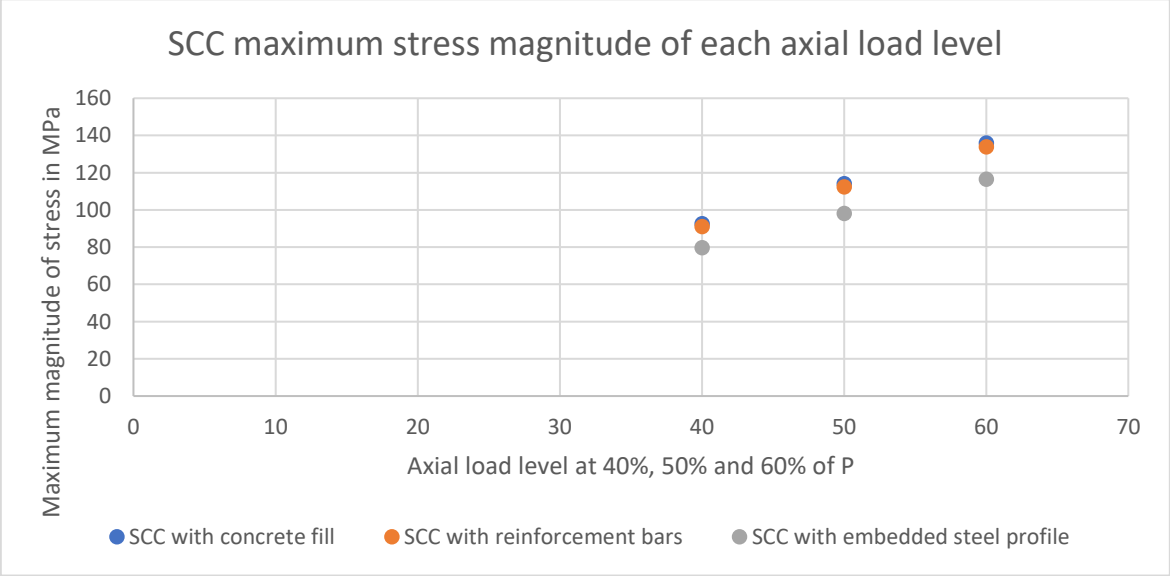

(b)

Figure 5.43: The Summary result of SCC under both axial and torsional load

From Figure 5.43 (a), it is observed that the square composite column (SCC) shows less magnitude of displacement than others. SCC with reinforcement bars relatively close to SCC with concrete fill in the magnitude of displacement. However, from this figure, it shows better with little difference in U-magnitude of displacement under both axial and torsional loads. For all SCC subjected to both axial and torsional load, as axial load increases by 10% the magnitude of displacement also increase for all condition with no constant difference of U. It is observed from Figure 5.43 (b), The stress distribution in SCC with concrete fill shows greater maximum values of Von Mises stress, where SCC with steel profile embedded shows lest value than others. This stress distribution is depending mainly on concrete infilled, steel profile and reinforcement bars where steel tube is considered constant for all specimens in this paper. Among of all steel profile section shows better stress sharing capacity than all other next to steel tube.

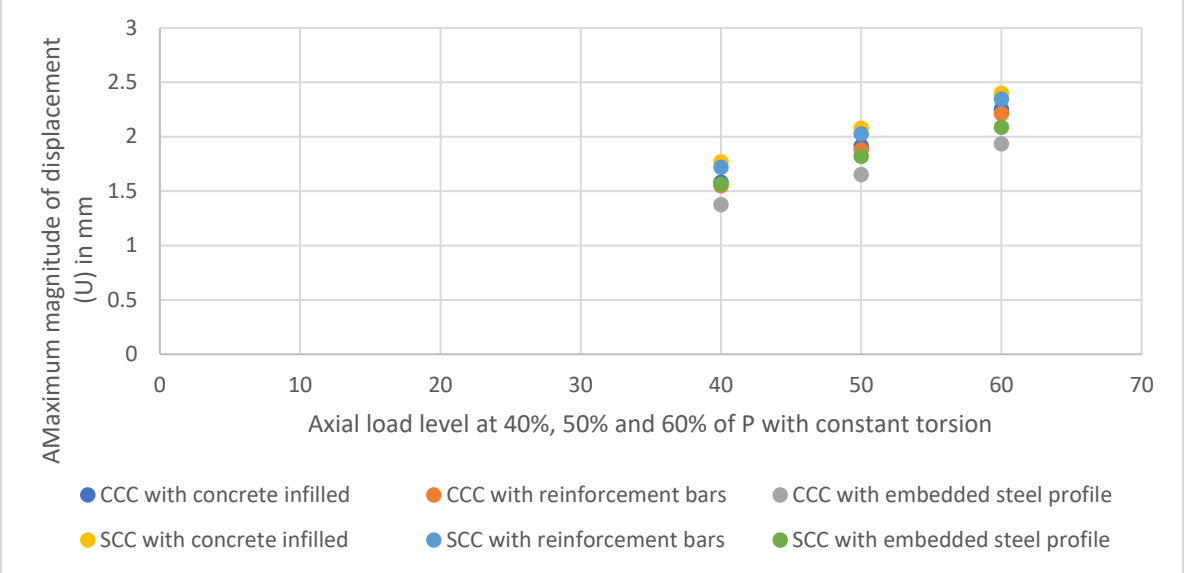

(a)

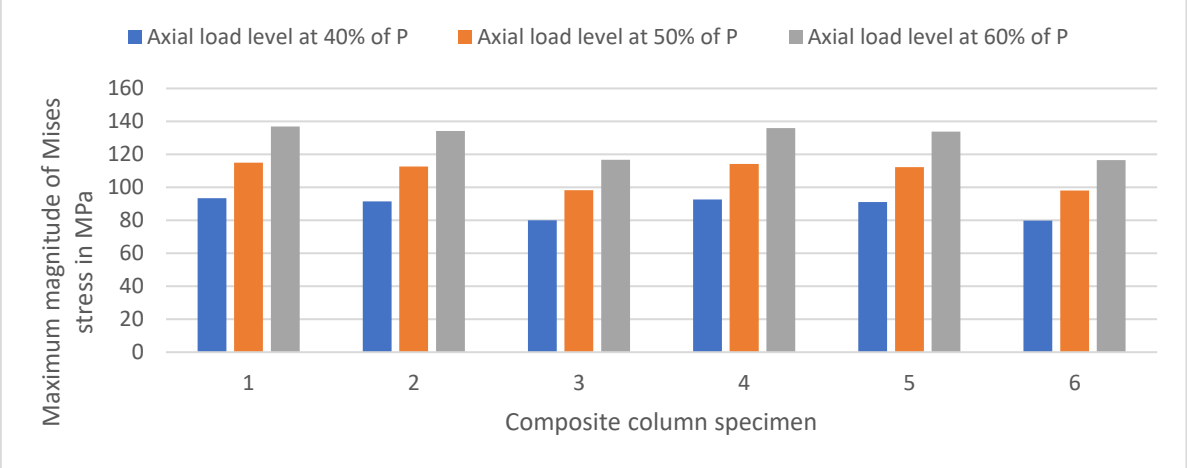

(b)

Figure 5.44: The summary of CCC and SCC displacement and stress result under both axial and torsional loads

Figure 5.44 shows the results of maximum magnitude displacement and stresses of composite column specimens those subjected to both axial and torsional loads. These are:

1. CCC with concrete-filled subjected to axial and torsional loads.
2. CCC with reinforcement bars subjected to axial and torsional loads.
3. CCC with embedded steel profile subjected to axial and torsional loads.
4. SCC with concrete-filled subjected to axial and torsional loads.
5. SCC with reinforcement bars subjected to axial and torsional loads.
6. SCC with embedded steel profile subjected to axial and torsional loads.

From this figure, it's observed that the circular cross-section shows less displacement under all axial load level and square composite column with concrete-filled shows maximum U-displacement under all axial load level with the constant torsional load. As a general for all level of axial load with constant torsion circular section CC shapes shows less displacement than square section CC shapes with very close stress distribution. From the circular composite column, the CCC with embedded steel profile shows better performance under compression and twisting effect from this result.

This paper presented twelve specimens of the composite column under different conditions. These are:

1. Circular composite column (CCC) with concrete-filled subjected to axial load only.
2. CCC with reinforcement bars subjected to axial load only.
3. CCC with embedded steel profile subjected axial load only
4. Square composite column (SCC) with concrete-filled subjected axial load only.
5. SCC with reinforcement bars subjected to axial load only.
6. SCC with embedded steel profile subjected axial load only.
7. CCC with concrete-filled subjected to axial and torsional loads.
8. CCC with reinforcement bars subjected to axial and torsional loads.
9. CCC with embedded steel profile subjected to axial and torsional loads.
10. SCC with concrete-filled subjected to axial and torsional loads.
11. SCC with reinforcement bars subjected to axial and torsional loads.
12. SCC with embedded steel profile subjected to axial and torsional loads.

For all specimens in Figure 5.45, the results of the maximum magnitude of displacement and Von Mises stress were recorded and presented from Abaqus software by specifying the level of axial load. Figure 5.45(a), shows the magnitudes of displacement (U) for all specimens. From this, it is observed that specimen number-3 and 6 or CCC with embedded steel profile and SCC with embedded steel profile subjected to compression-only are less than others specimen relatively. Specimen from 1-6 shows a composite column subjected to compression only. While specimen 7-12 stands for the composite column under the effect of both compression and twisting. In general, when the member is subjected to both compression and twisting affect the magnitude of cross-section increases than the cross-section that subjected compression effect only.

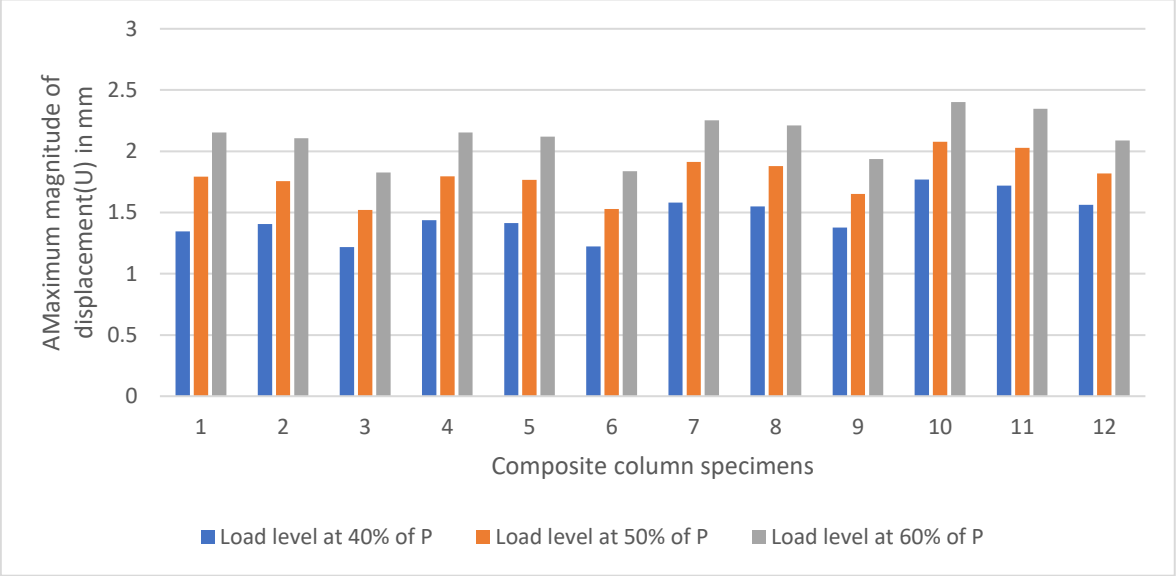

(a)

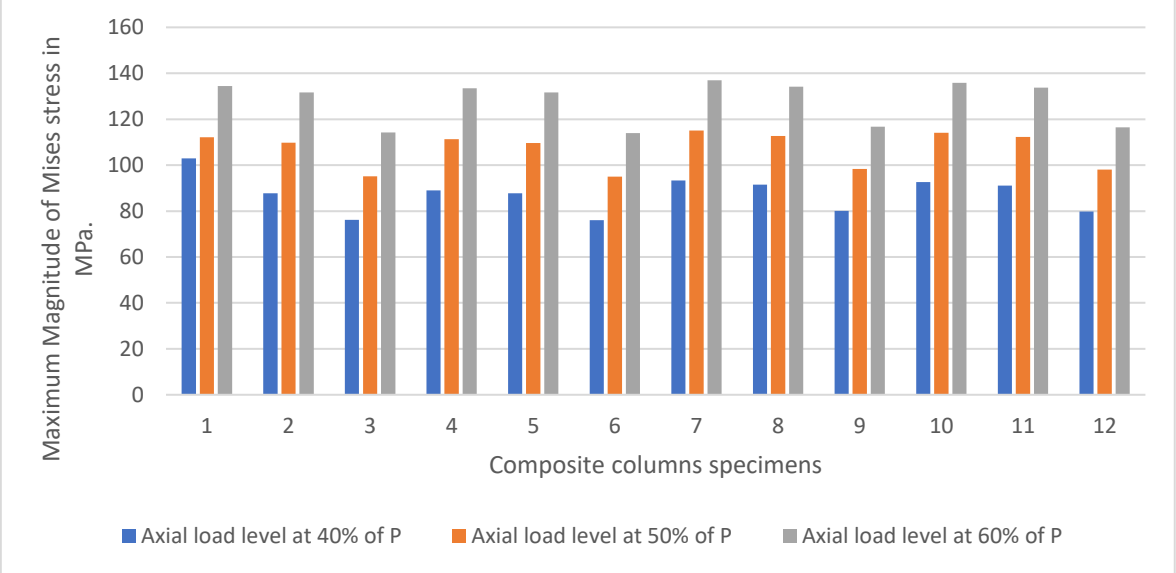

(b)

Figure 5.45: Summary of all composite column maximum magnitude of displacement and stress result

6 CONCLUSIONS

This paper investigated the behavior of the circular composite column and square composite column under compression-only and combined compression with torsion separately. Based on the software results by referencing experimental results for the validation of software results. For all specimens, it was compared to the effects of different levels of axial loads at 40%, 50% and 60% of the load-bearing capacity of section applied alone first. Then for all cross-section, constant torsion 60KNm was applied under all levels of axial load keeping this torsion as constant. Based on the discussed result, the following conclusions can be drawn within the scope of the current study:

- As axial load level increases the magnitudes of displacement (U) also increased for all studied composite columns.
- The circular cross-section composite column shows better stress and distribution than square cross-section and fewer displacement magnitudes in most cases as observed from software results. The use of high strength concrete results in an increment in the ultimate load and in the concrete contribution ratio of the CFST columns. As regards to the shape effect, the configuration with circular steel tubes provides to be the most efficient, contrarily to the square sections, which presents the poorest ultimate load and indexes values. [15] [16] [17]
- The experiment program result shows that a circular concrete-filled composite column is better to be used for unsymmetrical buildings in areas where an earthquake may happen and when there is a cantilever beam on the column. [17] [21] From numerical analysis it is observed that circular section shows better performance under twisting effect than the square cross-sections.
- The composite cross-section with reinforcement and embedded steel profile decreases the magnitude of displacement under the effect of compression and twisting. The provision of longitudinal reinforcement and steel profile increases the resistance of the composite column under compression and torsion [15].
- The twisting of the column under constant Torsion decreases as the axial load increases. [22]
- Under the action of axial load, CCC and SCC columns, as load level increased by 10% the stress distribution also increased by averagely less than 4%.
- In all specimens, is observed embedded steel profile has much effect on stress distribution than other parts.
- In case of composite column with reinforcement bars, the Mises stress distribution is varied widely than steel tube and concrete section as observed from numerical results.
- The provision of longitudinal reinforcement increases the resistance of the composite column under compression and torsion.
- The behavior of composite column subjected to axial and torsional loads as prescribed under the experimental program-1 [15] is can be concluded in a similar manner based on Abaqus software package result in generally.
- Von Mises Stress distribution magnitudes are less in concrete material sections other than the steel material section.
- When a member of the composite column subjected to both compression and twisting, the magnitude of displacement is increased than the member subjected to the compression effect only.

7 ACKNOWLEDGMENTS

I would like to express my sincere appreciation to my Advisor Dr. Kovács Nauzika for the support, guidance, encouragement, and insights that provided me throughout the study. She has been devoting her precious time and providing all necessary relevant information to carry out this TDK research paper.

8 REFERENCES

[1] Hajjar, J.F. (2000), "concrete-filled Steel Tube Columns under Earthquake Loads," Progress in Structural Engineering and Materials, Vol. 2, No. 1

[2] AISC 1999, 'Load and Resistance Factor Design Specification for Structural Steel Buildings'.

[3] SSRC (1979), "A Specification for the Design of Steel-Concrete Composite Columns," Structural Stability Research Council Task Group 20 (SSRC TG20), Engineering Journal, AISC, Vol. 16, No. 4.

[4] Leon, R.T. and Aho, M.F. (2002), "Toward New Design Provisions for Composite Columns," Composite Construction in Steel and Concrete IV, Hajjar, J.F., Hosain, M., Easterling, W.S., and Shahrooz, B.M. (eds.), American Society of Civil Engineers, Reston, VA, pp. 518–527

[5] Eurocode, 4. (2004). BS EN 1994-1-1, Eurocode 4: Design of Composite Steel and Concrete Structure Part 1-1: General Rules and Rules for Buildings. London: British Standard Institution

[6] H-L. HsuC-L. Wang, 'Flexural–torsional behavior of steel-reinforced concrete members subjected to repeated loading', May 2000Earthquake Engineering & Structural Dynamics 29(5):667 – 682.

[7] Xiao-Ling Zhao, Lin-Hai Han, Hui Lu, ' Concrete-filled Tubular Members and Connections'.

[8] ACI 318-11, ' ACI Committee 318Building Code Requirements for Structural Concrete (ACI 318-11)', An ACI Standard and Commentary.

[9] Jun-Qing Xue, Bruno Briseghella and Bao-Chun Chen, 'Effects of debonding on circular CFST stub columns', February 2012, Journal of Constructional Steel Research 69(1)

[10] Ellobody, E., & Young, B. (2006), 'Nonlinear analysis of concrete-filled steel SHS and RHS columns. Thin-Walled Structures', 919–930

[11] Han, L.H. and Zhong, S.T. (1995), 'The studies of pure torsion problem for concrete-filled steel tube'. Industrial Construction 92:5, 562-573

[12] M.A. Dabaon, M.H. El-Boghdadi, and M.F. Hassanein. Experimental investigation on concrete-filled stainless steel stiffened tubular stub columns. Engineering Structures, 31:300-307, 2009

[13] Buick Davison, G. W. (2012). Steel Designer's Manual. Wiley- Blackwell.

[14] G. Hanswille: Eurocode 4 composite columns

[15] Qing-Xin Ren, Lin-Hai Han, Chao Hou, Zhong Tao, Shuai L, 'Concrete-encased CFST columns under combined compression and torsion: Experimental investigation', Journal of Constructional Steel Research 138 (2017) 729–741

[16] David Hernández-Figueirido, Carmen Ibañez, Ana Piquer and Óscar Martínez-Ramos, 'Experimental study of cross-section shape and infill influence on CFST stub columns subjected to axial load', or https://doi.org/10.1002/cepa.268.

[17] Stephen P. Schneider, 'AXIALLY LOADED CONCRETE-FILLED STEEL TUBES', Journal of Structural Engineering, Vol. 124, Issue 10 (October 1998).

[18] Giakoumelis, G., and Lam, D. (2004). The axial capacity of circular concrete-filled tube columns, Journal of Constructional Steel Research, 60:7, 1049-1068

[19] American Institute of Steel Construction, 'Specification for Structural Steel Buildings', ANSI /AISC 360-16, 2016.

[20] Abaqus/CAE analysis user's manual version 6.13

[21] Denavit, M. D., Hajjar, J. F., & Leon, R. T. (2011). Seismic Behavior of Steel Reinforced Concrete Beam-Columns and Frames. Structures Congress, 2852-2861

[22] Chen, Y.W. (2003). Research on torsion behavior of concrete-filled steel tube. Taiwan: Central University.